國立臺灣大學生命科學院生化科學研究所

博士論文

Graduate Institute of Biochemical Sciences
College of Life Science
National Taiwan University
Doctoral Dissertation

多形性神經膠母細胞瘤及其腫瘤幹細胞表面醣分子之探討

Investigation of Surface Glycans on Glioblastoma multiforme and Its Stem Cells

羅翊偉

Yi-Wei Lou

指導教授：翁啟惠 博士

Advisor: Chi-Huey Wong, Ph.D.

中華民國 103 年 1 月

January, 2014

誌謝

漫長的博士班在口試結束後算是告一段落了，而心中多年的大石頭總算是可以放下，準備往人生的下一階段邁進。在這段求學過程中，我最想感謝的是指導教授翁啟惠老師，當我在博士班最低潮的時候，翁老師提供我一個無後顧之憂且得以自由發揮的研究環境，讓我可以享有今天的成果。與翁老師的討論總是讓我受益匪淺，而翁老師對研究的熱誠與態度，更是我學習的榜樣。還要感謝學姐徐翠玲博士，她的時常叮嚀讓我在人生與求學的道路上保持正確的方向。

本論文的實驗工作完成得感謝蕭宏昇老師、邱繼輝老師、吳宗益老師的大力幫忙，因為有各位老師的專業協助，才讓實驗有著順利的進展。另外，感謝林國儀老師、楊文光老師、沈家寧老師、邱士華老師、杜邦憲老師、神奈木玲兒老師在口試過程中提供學生寶貴的建議以及對論文的修改，讓我在博士班的最後一堂課獲益良多，對往後的實驗方向增添許多靈感與信心。

感謝身邊曾經共事過的同仁，在這段博士班生涯中，陪伴我成長。生化所的銘佛、淑芳、鈞鴻、威霖、李函、怡芬、青文；從基因體畢業的秉青、建邦、詩芬、柏樟、鼎鈞；一同持續在基因體奮戰的子文、俊結、士齊、寶源、博凱、子豪、慧慈、容慈、政越、衍龍、俊宇；雖然相處的時間不一，但是與你們的相處充滿著樂趣，讓實驗生活添加許多色彩。也要感謝台大生化所秘書麗芬與講師佳幸在一些事務上的幫忙。

最後，感謝家人的支持，尤其是我的母親，謝謝你們長久對我的體諒與信賴，包容我自私地選擇這條路。感謝鶴芸一路來的照顧，願意攜手共度一生。你們的肯定是我心靈上最大的支柱。謹以此篇論文獻給我最愛的你們。

羅翊偉

2014 年 1 月中研院基因體

摘要

多形性神經膠母細胞瘤被世界衛生組織定義為第四級的星狀細胞瘤，是最常見也是最惡性的成人腦瘤。根據統計，即使接受過手術切除、放射線治療和化學治療，病人的中位存活時間仍只有 14.6 個月，癒後情況相當差。因此，針對此腫瘤發展一個新的治療方式是相當重要的。我們在 17 株多型性神經膠母細胞瘤細胞株上利用流式細胞技術分析其表面醣分子之表現，結果顯示其中 12 株具有階段特異性胚胎抗原-4(SSEA-4)之表現。而高效能薄層層析免疫染色與基質輔助雷射脫附游離質譜分析結果確定了 SSEA-4 分子的存在與結構。我們利用免疫組織化學染色法分析病人檢體顯示著有百分之六十九的病人其腦癌細胞具有 SSEA-4 的表現。相比之下，正常人類大腦組織則鮮少有 SSEA-4 的表現。此外，免疫組織化學染色結果指出 SSEA-4 的表現與星狀細胞瘤惡化程度有著成正比的關係。接著，我們利用 SSEA-4 的單株抗體(MC813-70)可以在體外誘發補體依賴型細胞毒殺作用在多型性神經膠母細胞瘤細胞上而引發細胞死亡。並且在實驗老鼠動物上，SSEA-4 的單株抗體能有效的抑制腫瘤的生長。進一步的實驗指出 SSEA-4 不僅表現在多型性神經膠母細胞瘤，我們甚至觀察到 SSEA-4 表現在許多不同癌症的細胞株上，因此我們認為針對 SSEA-4 發展治療抗體與疫苗是一個有潛力的方向。而在另一方面，我們成功地產生一群具有較高幹細胞特性的癌細胞群。而為了去找尋多形性神經膠母細胞瘤幹細胞上是否具有特定分子的表現，我們利用抗體染色去進行多種醣類的比較，這包括了醣蛋白和醣脂質。在這些被偵測的醣分子中，我們發現一神經節苷脂 GD2 大量表現在多形性神經膠母細胞瘤幹細胞上，更多的實驗將會闡明 GD2 與多形性神經膠母細胞瘤幹細胞的關係。

關鍵詞：多形性神經膠母細胞瘤、階段特異性胚胎抗原-4、單株抗體、醣脂、腫瘤幹細胞、神經節苷脂、標靶治療、腫瘤相關抗原

Abstract

Glioblastoma multiforme (GBM), the grade IV astrocytoma, is the most common and aggressive brain tumor in adults. Despite advances in medical managements, the survival rate of GBM patients remains poor, suggesting that identification of GBM-specific targets for therapeutic development is urgently needed. Analysis of several glycan antigens on GBM cell lines revealed that 12 out of 17 GBM cell lines were positive for stage-specific embryonic antigen-4 (SSEA-4), and the identity of SSEA-4 was confirmed by high performance thin-layer chromatography immunostaining and mass spectrometry. Immunohistochemical staining confirmed that 38/55 (69%) of human GBM specimens, but not normal brain tissue, were SSEA-4-positive, and correlated with high-grade astrocytoma. MC813-70, an SSEA-4 specific monoclonal antibody, was found to induce complement-dependent cytotoxicity against SSEA-4^{hi} GBM cell lines *in vitro*, and suppressed GBM tumor growth in mice. Since SSEA-4 is expressed on GBM and many other types of cancers, but not on normal cells, it could be a target for development of therapeutic antibodies and vaccines. On the other hand, we successfully generated a population of GBM cells with higher stemness and tumorigenicity. In order to discover the specific markers expressed on GBM stem cells, we utilized a panel of glycan-related antibodies to profile the expression of glycan epitopes, including glycoproteins or glycolipids. Among these glycans, the expression of GD2 was found to be elevated on stem-like cell population. Further study would illustrate the relationship between GD2 and GBM stem cells.

Keywords: glioblastoma multiforme, SSEA-4, monoclonal antibody, glycolipid, cancer stem cell, ganglioside, targeted therapy, tumor-associated antigen, GD2

Table of Contents

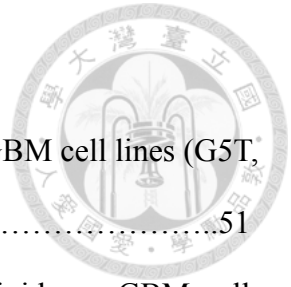

List of Figures

List of Supplementary Figures

List of Tables

Abbreviations

ADCC	antibody-dependent cellular cytotoxicity
APC	allophycocyanin
bFGF	basic fibroblast growth factor
CDC	complement-dependent cytotoxicity
CDC	cancer stem cell
Cer	ceramide
CNS	central nervous system
DHB	2,5-dihydroxybenzoic acid
D-PDMP	D-threo-1-phenyl-2-decanoylamino-3-morpholino-1-propanol
EGFR	epidermal growth factor receptor
FKBP4	FK-506 binding protein 4
FUT	fucosyltransferase
GAG	glycosaminoglycan
GalCer	galactosylceramide
GBM	glioblastoma multiforme
GlcCer	glucosylceramide
GPI	glycosylphosphatidylinositol
GSL	glycosphingolipid
hESC	human embryonic stem cell
Hex	hexose
HexNAc	*N-acetyl*hexosamine
HPTLC	high-performance thin-layer chromatography
HSPG	heparin-sulphate proteoglycan
IGF1R	insulin-like growth factor 1 receptor
IUPAC	International Union of Pure and Applied Chemistry
LacCer	lactosylceramide
LDH	lactate dehydrogenase
Lex	Lewis x
Ley	Lewis y
MAL II	*Maackia amurensis* lectin II
MALDI	matrix-assisted laser desorption/ionization
MS	mass spectrometry
NHS	N-Hydroxysuccinimide
NOD-SCID	non-obese diabetic/severe combined immunodeficient
Oct-4	octamer-binding transcription factor 4
PAGE	polyacrylamide gel electrophoresis

PBS	phosphate buffered saline
PCR	polymerase chain reaction
PDGFR	platelet-derived growth factor receptor
PI	propidium iodide
PTEN	phosphatase and tensin homolog
RBC	red blood cell
SDS	sodium dodecyl sulfate
sLex	sialyl Lewis x
SOX2	SRY (sex determining region Y)-box 2
SPG	sialyl paragloboside
SSEA-3	stage-specific embryonic antigen-3
SSEA-4	stage-specific embryonic antigen-4
sTn	sialyl Tn
TF	Thomsen-Friedenreich
VEGF	vascular endothelial growth factor
WHO	World Health Organization

CHAPTER1: INTRODUCTION

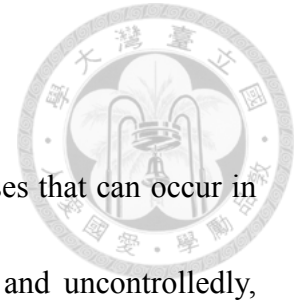

1.1 Perspective

Cancer, known as a malignant neoplasm, is a broad group of diseases that can occur in any part of human bodies. Cancer cells divide and grow rapidly and uncontrolledly, forming malignant tumors, invading nearby parts of the body and eventually metastasizing to other organs. Cancer is a leading cause of death worldwide, accounting for 7.9 million death (about 13% of all human deaths) in 2007 [1], and the rates are projected to continue rising as more people live to an old age and with modern lifestyles in the developing world. Besides conventional therapies for cancer, including surgery, chemotherapy and radiation therapy, the scientists are making great efforts in elucidating the basic tumor biology and developing novel therapies against cancers for decades. Among hundreds of different types of cancers, our study focuses on glioblastoma multiforme (GBM), one of most deadly human cancers, examining for novel biomarkers with therapeutic potentials in GBM and GBM tumor initiating cells.

1.2 Overview of glioblastoma multiforme

GBM is one of the most aggressive and malignant cancers of the central nervous system (CNS). In CNS, neuronal cells and glial cells work together to maintain a functional nervous system. GBM phenotypically resembles astrocytes, one kind of glial cells, and therefore is a type of astrocytoma, one kind of gliomas. According to World Health

Organization (WHO) grading system, based on histological characteristics, astrocytomas are classified into four prognostic grades: grade I (pilocytic astrocytoma), grade II (diffuse astrocytoma), grade III (anaplastic astrocytoma) and grade IV (GBM) [2]. Anaplastic astrocytomas are characterized by increased cellularity, nuclear atypia, and mitotic activity. As the name implies, glioblastoma is multiforme; all GBM tumors may not be generated equal, containing regions of microvascular proliferation, pseudopalisading necrosis, and pleomorphic nuclei and cells. Besides, GBM is genetically heterogeneous. GBM can be separated into two main subtypes based on the biologic and genetic differences. For decades, it has been known that some low grade or anaplastic astrocytomas can recur, progress and transform into GBM over a period of years. These have been traditionally termed secondary GBMs, whereas *de novo* GBM tumors are named as primary GBMs [3, 4]. Primary GBM is characterized by epidermal growth factor receptor (EGFR) amplification and mutations (40~60%; < 10% in secondary GBMs) [5], loss of heterozygosity of chromosome 10q [6], deletion of phosphatase and tensin homologue on chromosome 10 (PTEN) [7], and p16 deletion [8, 9]. Secondary GBM is characterized by mutations in the p53 tumor-suppressor gene [5], overexpression of the platelet-derived growth factor receptor (PDGFR) [10], promoter methylation of *RB1* and $p14^{ARF}$, loss of heterozygosity of chromosome 10q [11], and mutations in NADP+-dependent isocitrate dehydrogenase [12, 13]. The median age of

primary GBM patients is about 62, and the median age of secondary GBM is about 45 [7, 14]. GBM is more 40% more common in men than in women and twice as common in Caucasians as in AAs [15]. Primary GBM is rarely seen in younger patients. GBM is also the most common primary CNS malignant tumor in the USA and European countries, with about 3 in 100,000 people newly diagnosed with GBM each year, accounting for over 51% of all gliomas [15]. In Taiwan, there are about 200 people diagnosed with GBM each year. The etiology of GBM in unknown, and many factors that increase the risk of developing GBM have been suggested; however, the only established risk factor is exposure to ionizing radiation [16]. Cellular phones are known to emit small amount of non-ionizing electromagnetic radiation, and because the use of cellular phone has become prevalent worldwide, electromagnetic radiation exposure due to cellular phone use has become a concern but not yet been proven [16-18]. Other suspected risk factors include head trauma, pesticide exposure, polyvinyl chloride, and alcohol consumption. Symptoms of GBM are variable and depend on the size and the location of the tumor. The common symptoms and signs for patients with GBM are progressive headaches, seizures and focal neurologic deficits. GBM patients often display a multitude of varying symptoms; therefore, diagnosis is more commonly made following surgical resection. Standard treatment for GBM patients includes surgical resection, chemotherapy, and radiation therapy. Maximal surgical resection is the first

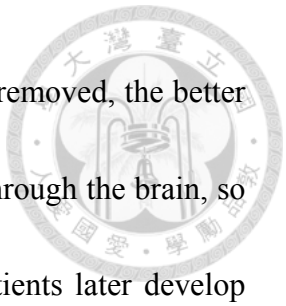

stage of treatment of GBM. The greater the extent the tumor can be removed, the better prognosis the patients have [19]. GBM cells are widely infiltrative through the brain, so a complete resection of GBM tumor is impossible. Most GBM patients later develop recurrent tumors either near the original site or at more distant "satellite lesions" within the brain. After the efficacy of radiation therapy was reported in the 1970s [20], radiation therapy becomes a standard treatment of GBM following surgery. Chemotherapy is administrated in conjugation with radiation therapy. While there are many different chemotherapeutic agents available for the treatment of GBM, the most commonly used agent is Temozolomide [21]. Temozolomide is an oral alkylating agent, and inhibits DNA repair mechanism in tumor cells [22]. Temozolomide is associated with the lowest incidence of recurrence and longer survival rates of gliomas. Although advances in medical management have improved the quality for life for GBM patients, the effect on GBM survival has been modest. The median survival time from the time of diagnosis without any treatment is 3 months, and for GBM patients with treatment is about 14-15 months [23]. Five-year survival rates are about 13% for patients aged 14-15 years, and only 1% for those aged ≥ 75 years [24]. Because of these challenges, new approaches are needed. Better understanding of the genetic and proteomic changes in GBM tumorigenesis can be translated into new therapeutic treatments, especially molecule-based targeted therapies.

1.3 Glycosylation

Glycans, assemblies of sugars, are one of the fundamental components of cells and may also be the most abundant and diverse biopolymers in nature. The mammalian glycome is estimated to be between hundreds and thousands of glycan structures. Glycosylation produce numerous types of glycans (or glycoconjugates) that are attached to proteins, lipids, or other organic molecules. Protein glycosylation includes N-linked glycosylation, O-linked glycosylation, and proteoglycans. The oligosaccharide chain (N-glycan) is linked to asparagine residues of proteins, especially in the tripeptide sequence Asn-X-Ser/Thr where X could be any amino acid except Pro or Asp. This sequence is known as a glycosylation sequon. O-linked glycosylation is the attachment of O-glycans to oxygen atom of serine and threonine residues of proteins [25, 26]. Proteoglycans are highly glycosylated proteins, consisting of a “core protein” with one or more covalently attached glycosaminoglycans (GAGs), long unbranched polysaccharides with a repeating disaccharide unit [27]. Although GAGs are also attached to serine residues of core proteins, they are biosynthesized by different pathways. Lipid glycosylation adds glycans to lipids and produces glycolipids, glyceroglycolipids, and glycosphingolipids (GSLs) [28]. Glypiation, glycosylphosphatidylinositol (GPI) covalently linked to the C-terminus of a protein, is widely detected on various surface proteins [29]. There are other less common types of

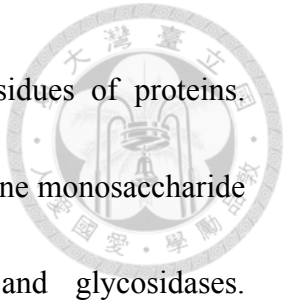

glycosylation, for example, on lysine, tryptophan, or tyrosine residues of proteins. Glycans are synthesized in an ordered and sequential manner from nine monosaccharide building blocks by the cooperation of glycosyltransferases and glycosidases. Glycosyltransferases transfer a glycosyl donor to another molecule covalently, and glycosidases hydrolyze specific glycan linkage. Gene transcription of glycosyltransferases and glycosidases has a great impact on the formation of glycans. Cell-type-specific expression of glycosylation genes reflects on the distinct pattern of glycans displayed. Analysis of transcriptional levels of enzymes relevant to glycan structures is helpful in predicting glycan expression patterns [30]. Glycosylation, like other post-translational modification, affects the functions of proteins in many different ways. Glycans can promote or inhibit intra- and intermolecular binding, regulating the interactions of proteins with other molecules. By this regulation and binding to lectins (glycan binding proteins), glycans involve in multiple cellular mechanisms, such as protein folding [31], signal transduction, receptor activation [32, 33], molecular trafficking and clearance [34], cell adhesion [35], and endocytosis [36]. Because of the diversity of glycan structures, the information and functions of glycans are numerous and have been a major focus for the past decades.

1.4 Glycosphingolipids

Glycosphingolipids (GSLs) are a subtype of glycolipids containing a long-chain amino alcohol, sphingosine. Sphingosine is linked to a fatty acid via an amide bond to form a ceramide, the lipid moiety of GSLs. The fatty acids of ceramides varied widely, with acyl chain lengths ranging from 14 to 26 carbon atoms (or greater). Most of the fatty acids are saturated or mono-unsaturated, and the most common fatty acid are palmitic (C16:0) and stearic (C18:0) non-hydroxy fatty acid [37]. The diversity of ceramides affects the presentation of the attached glycan on the cell membranes. Addition of one or more sugars on a ceramide produces GSLs, and the first sugars linked to ceramide are generally β-linked galactose (GalCer) or glucose (GlcCer). GalCer and its analog sulfatide are major glycans in the brain, enriched in myelin-forming cells and oligodendrocytes [38], while GlcCer is abundant in certain tissues, like skin [39]. Typically, a galactose is transferred to GlcCer on glucose moiety with β1-4 linkage by the lactosylceramide synthase, forming lactosylceramide (LacCer) [40, 41], which play an important role as a precursor for the synthesis of complex GSLs [42]. Further elongations of the glycan on LacCer by different glycosyltransferases generate a series of neutral "core" structures that constitute the basis of the nomenclature of GSLs (Fig. S1). Therefore, ganglio-series GSLs are based on the neutral core structure Galβ1-3GalNAcβ1-4Galβ1-4GlcβCer, whereas neolacto-series GSLs are based on the core structure Galβ1-4GlcNAcβ1-3Galβ1-4GlcβCer, lacto-series on

Galβ1-3GlcNAcβ1-3Galβ1-4GlcβCer, globo-series on Galα1-4Galβ1-4GlcβCer, and isoglobo-series on Galα1-3Galβ1-4GlcβCer. Abbreviations for the subfamily have been recommended by International Union of Pure and Applied Chemistry (IUPAC) to make the nomenclature simple; Gg stands for ganglio-, Lc for lacto-, nLc for neolacto-, Gb for globo-, and iGb for isoglobo-. The designation of the structure family is followed by the number of monosaccharide units of the GSL, and the suffix "ceramide" (Cer) [43]; for example, Galβ1-3GlcNAcβ1-3Galβ1-4GlcβCer is commonly called Lc4Cer. Base on certain modification of GSLs, GSLs could be further classified as neutral (with no charged sugars or ionic groups), sialylated (with one or more sialic acid residues), or sulfated. Generally, all sialylated GSLs are considered as gangliosides whether they belong to ganglio-series GSLs or not. The expression pattern of these GSL subtypes is tissue-specific. For example, ganglio-series GSLs are predominantly expressed in the brain [44], and neolacto-series GSLs are distributed on certain hematopoietic cells [45], and lacto-series GSLs are mainly in secretory organs, and globo-series GSLs are mostly expressed in erythrocytes [46]. The specific distribution of GSLs indicates that different functions of GSLs in these tissues.

1.5 Globo-series GSLs

The GSLs of globo-series feature a Galα1-4Gal linkage to lactosylceramides, and this

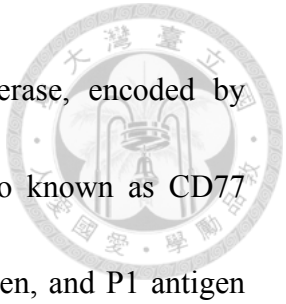

linkage is catalyzed by lactosylceramide 4-alpha-galactosyltransferase, encoded by *A4GALT* gene (Fig. S2) [47]. Globotriosylceramide (Gb3Cer), also known as CD77 antigen and Pk antigen, globoside (Gb4Cer), also known as P antigen, and P1 antigen (Galα1-4nLc4Cer) constitute the basis of P-blood group system [48]. The P1 red blood cell (RBC) phenotype is defined as P1 and P antigens on RBC and is the most common phenotype with a prevalence of approximately 75%. The P2 RBC phenotype indicates the absence of P1, with a prevalence of about 25%. The rare Pk (absence P and P1) and p (absence of Pk, P and P1) phenotypes are resulted from the inactivating mutations in the *B3GALNT1* and *A4GALT* genes, respectively [49, 50]. Gb3/CD77 is also a differentiation antigen of B cell lineage [51], and a receptor for Shiga Toxin and Verotoxin 1 (VT1) [52]. Galactosyl globoside (Gb5Cer) and sialyl galactosyl globoside (sialyly Gb5Cer, SGG, MSGG), also known as stage-specific embryonic antigen-3 (SSEA-3) and SSEA-4, respectively, are widely used as cell-surface markers to define human embryonic stem cells (hESCs) [53, 54]. SSEA-3 and -4 are expressed on hESCs and human embryonal carcinoma cells and downregulated as these cells differentiate [53, 55]. In addition to P-blood group, partial of the ABH blood group activity is contributed from globo-series GSLs, Globo H and Globo A [56].

1.6 Glycans in cancers

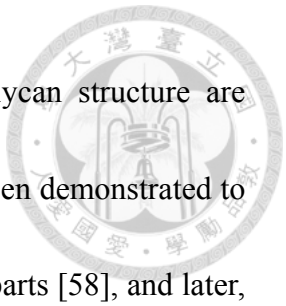

Altered glycosylation is a feature of cancer cells, and several glycan structure are well-known tumor markers [57]. In 1969, healthy fibroblasts have been demonstrated to have smaller membrane glycoprotein than their transformed counterparts [58], and later, histological studies showed that healthy and malignant tissue displayed different patterns of lectins binding [59]. Recently, more and more cancer-associated cell surface glycans have been described with monoclonal antibodies and mass spectrometry [60]. These findings illustrate the molecular changes during malignant transformation and provide novel ideas for developing therapies against cancers. The alterations of glycosylation include over- and down-expression of specific natural glycans, as well as neo-expression of glycans normally expressed on the embryonic tissues, so called oncofetal antigens. Most of these glycan changes are resulted from the altered expression of glycosyltransferases in the Golgi of cancer cells. The most common change is the overall increase in the size and branching of N-linked glycans [61]. This increase is usually caused by the increased activity of N-acetylglucosaminyltransferase V (GlcNAc-TV, also known as MGAT5) [62]. The increased branching, followed by terminal sialylation through upregulation of sialyltransferases, leads to a global increase of sialic acid content on cancer cells [63]. In addition to change in the core structures of glycans, several terminal glycan epitopes are overexpressed on tumor cells, such as sialyl Lewis x (sLex), sialyl Tn (sTn), Lewis y (Ley), Globo H, and polysialic acid

[64-66]. Many tumors also exhibit increased expression of certain glycoproteins and glycolipids, especially the gangliosides. Mucin, a highly O-glycosylated glycoproteins, is overexpressed in many epithelial tumor [67]. Gangliosides, normally observed in neural system, and are found to be elevated in many tumors, such as GD2, GD3 and fucosyl GM1 [65, 68]. Tumor progression contains a variety of alterations in intercellular and intracellular signaling. Some of these glycans have been characterized as key mediators in pathophysiological events during tumor progress. Activation of insulin-like growth factor 1 receptor (IGF1R) through its own N-glycosylation, and ERBB2 (a member of epidermal growth factor receptor family) through O-glycans on mucins are involved in the growth and proliferation of cancer cells [69]. The enhanced expression of sialic acids on tumor cells might help cell detachment from neighboring cells through charge repulsion and polysialylation is usually correlated with increased invasiveness and poor prognosis [70, 71]. Specific heparin-sulphate proteoglycans (HSPGs), which bind to lot of growth factor and pro-angiogenic factor, are overproduced and may play crucial roles in tumor growth and angiogenesis [72, 73]. Furthermore, certain gangliosides overexpressed by tumors are often shed into bloodstream and can lead to immune silencing, probably through the inhibition of co-stimulatory molecule synthesis and suppression of dendritic-cell maturation [74-76]. Therefore, investigation of the change and the role of glycans during tumor progression

would provide not only knowledge on glycobiology and cancer biology but also new targets for anti-cancer therapy.

1.7 Glioma-associated GSLs

Tumor-associated GSLs, especially gangliosides, have attracted lots of interest in tumor research. Several tumor-associated gangliosides have been discovered and studied on gliomas. Elevation of monosialylated gangliosides GM3 and GM2 and their disialylated derivatives GD3 and GD2 were observed in glioma biopsies [77-79]. GM3 is also found in medulloblastomas and meningiomas [80], and normally expressed in a variety of cells and tissues, including normal brain [81] and RBC [82]. The increase of GD3 was most significant, and besides gliomas, GD3 is reported as a tumor-associated ganglioside in melanoma [83], leukemia [84], lung cancer [85] , and breast cancer [86]. However, the correlation between GD3 and malignancy remains obscure [79, 87-89]. Ganglioside GD2 is well known tumor-associated ganglioside in neuroblastoma [90], melanoma [91], and small cell lung cancer [92], but only expressed with a modest level in normal tissues. A novel lacto-series gangliosides, 3'-isoLM1 (sialyl Lc4, NeuAcα2-3Galβ1-3GlcNAcβ1-3Galβ1-4GlcβCer), was fist isolated from the human glioma cell line D-54 MG xenografts in nude mice [93]. Later, the existence of 3'-isoLM1 was verified in human glioma biopsies [94], and with monoclonal antibody

against 3'-isoLM1, SL-50, 3'-isoLM1 was detected in an invading subset of glioma cells [87]. Analyses of D-54 MG xenografts also revealed the existence of 3'6'-isoLD1 (disialyl Lc4, NeuAcα2-3Galβ1-3(NeuAcα2-6)GlcNAcβ1-3Galβ1-4GlcβCer), the disialylated form of 3'-isoLM1 [93]. The expression of 3'6'-isoLD1 was validated in frozen sections of glial tumors with monoclonal antibodies [95]. 3'-isoLM1, unlikely its neolacto-series isomer, sialyl paragloboside (SPG), is not found in normal brain or in RBC. Moreover, 3'-isoLM1 and 3'6'-isoLD1 are detected only in fetal human brain during the first trimester [96]. Since some of these glioma-associated gangliosides are rarely expressed or even absent in normal tissues, they are suitable for targeted therapy [97]. Hence, these glioma-associated GSLs would provide new targets for development of new therapies against gliomas.

1.8 Target therapy of GBM

Traditionally, chemotherapy and radiation therapy for treatment of cancer are designed to aim at proliferating cancer cells with minimal effect on non-cancerous cells. However, this strategy only has modest effect on GBM patients, and more effective therapeutic options are needed. Targeted therapy is such a choice, which GBMs are highly suitable for. GBM tumors have a set of genetic alterations and signaling pathway disruption, providing potential targets. As mentioned above, both EGFR and PDGFR are

overexpressed in GBM and the enhanced signaling pathways are involved in the proliferation and survival of GBM cells. A number of synthetic kinase inhibitors have been developed and are in clinical trial, such as erlotinib and gefitinib for EGFR [98-100], and imatinib for PDGFR [101]. Deletion of PTEN make the PTEN/Akt pathway and downstream, mTOR, appealing targets for therapy [102]. Moreover, the inhibitor of vascular endothelial growth factor (VEGF)/VEGFR pathway, bevacizumab (monoclonal antibody against VEGF), suppress the proliferation of GBM cells as well as angiogenesis which is crucial for GBM tumors [103-105]. In addition to interfering the function of target proteins, monoclonal antibodies against specific molecules on cell surface also stimulate the patient's immune system to attack those cells [106], since these naked (unarmed) monoclonal antibodies can potentially trigger antibody-dependent cellular cytotoxicity (ADCC) and complement dependent cytotoxicity (CDC). Furthermore, these antibodies can combined with conventional cytotoxic therapies to generate armed antibodies or radionuclides [107], and even deliver liposomes to tumor cells [108].

1.9 GBM stem cells

Many studies have reported that brain tumors recur after standard treatment are more resist to further therapy. This phenomena is not only found on GBM but also on several

other cancers [109, 110]. Besides, GBM tumors, as well as most of other tumors, exhibit functional heterogeneity between subtypes of tumor cells [111]. The tumor heterogeneity and the concept of resistant cells within tumor mass prompted the hypothesis of so called cancer stem cell (CSC), or cancer stem-like cells, or TICs [112]. The first solid evidence of CSCs have been revealed in 1997, a subpopulation of leukaemic cells (CD34+/CD38-) is capable of initiating tumors in immunodeficient mice [113]. Since then, cells with characteristics of CSC and their specific surface makers have been reported in various hematopoietic and solid tumors, including colon, breast and lung cancer, melanoma and brain tumor [114-122]. Cancer stem-like cells in GBM were first reported in 2002, successfully isolating stem-like cells from clinical tumor specimens using an in vitro culture system [123]. The first surface marker for isolation of GBM stem-like cells is CD133, a cholesterol-binding membrane protein of unknown biological function [122]. CD133, also a marker for normal neural stem cells,-positive GBM cells exhibit stem cell properties in vitro, and as few as 100 CD133+ cells are capable of initiating a tumor that was a phenocopy of the original tumors. A number of surface molecules have been demonstrated as useful markers for isolation of GBM stem-like cells, such as integrin α6, SSEA-1 (Lewis X), and A2B5 [124-126]. It remain to be determined to what extent the isolated cells fulfill the properties of CSC, and more precise definition of marker sets and understanding the

cellular and genetic mechanisms within CSC would improve the development of therapeutic strategy.

1.10 Significance and rationale

We examined the expression of surface glycans on GBM and GBM-stem like cells by a panel of anti-glycan antibodies. Then, the specificity of the antibody was assayed with glycan array, and the expression and the identity of the glycan antigen were analyzed by immunoblotting and mass spectrometry. We further examined the expression of SSEA-4, which was found highly expressed in the GBM cell lines, in the clinical specimens of gliomas with immunohistochemistry. Since SSEA-4 generally is not expressed in normal tissues, we tested whether SSEA-4 has the potential as a therapeutic target by the use of monoclonal antibody in the in vitro cytotoxicity assay and the in vivo tumor growth experiment. We also profiled the expression levels of SSEA-4 in other 13 cancer cell lines, to verify whether SSEA-4 might be expressed in various tumors in addition to GBM. On the other hand, we utilized the in intro culture system to enrich cells with the CSC properties, tested the stemness and the tumorigenicity of this subpopulation, and examined the differences of surface glycans between GBM and GBM stem-like cells. The reliability of these GBM stem-like cell-specific markers will be examined in the following experiments.

CHAPTER 2: MATERAILS AND METHODS

2.1 Reagents

Anti-Le^x, anti-sLe^x, and anti-GD2 antibodies were purchased from BD Biosciences (Franklin Lakes, NJ). Anti-GD1a, anti-GT1b and Alexa Fluor® 488 anti-A2B5 antibodies were purchased from Millipore (Billerica, MA). Anti-GM1 and anti-GM2 antibodies were purchased from Calbiochem (Merck, Darmstadt, Germany). Anti-Le^y and anti-sTn antibodies were purchased from Abcam (Cambridge, UK). Anti-TF antibody was purchased from Thermo Scientific (Waltham, MA). Anti-Tn antibody was purchased from DakoCytomation (Glostrup, Denmark). Fluorescence-labelled or purified MC813-70 and MC631 were purchased from Biolegend (San Diego, CA). MC813-70 ascites were purchased from Developmental Studies Hybridoma Bank at the University of Iowa. The usages of these antibodies in individual experiments were descried in the following paragraphs.

2.2 Flow Cytometry

Cells (1×10^5) were stained with 0.5μg Alexa Flour 488-conjugated anti-SSEA-3 mAb (MC-631), anti-SSEA-4 mAb (MC813-70) or allophycocyanin (APC)-conjugated anti-Globo H mAb (VK9, a gift from Philip O. Livingston, Memorial Sloan-Kettering Cancer Center, New York, NY) in 50 μL FACS buffer (PBS solution with 1% FBS) on ice for 30 min. For lectin staining, cells were incubated in lectin binding buffer [1%

BSA, 0.5 × Carbo-Free Blocking buffer (Vector Laboratories, Burlingame, CA), 2 mM $MgCl_2$, 2 mM $CaCl_2$] containing biotinylated lectin for 30 min on ice. After being washed twice with lectin binding buffer, cells were incubated with streptavidin-APC (1:500 diluted in FACS buffer; Biolegend) on ice for 30 min. After washing twice with 200 μL FACS buffer, cells were resuspended in 200 μL FACS buffer containing 1 μg/ml propidium iodide (PI) and subjected to analysis. Data acquisition was performed on a FACSCanto (BD Biosciences) with FACSDiva software (BD Biosciences), and data analyses were performed using FlowJo software (TreeStar, Ashland, OR). Live cells (PI-negative) were gated for analysis. For methanol washing, cells were washed and fixed with 4% paraformaldehyde in PBS for 15 min at room temperature, followed by incubation in methanol for 10 min before staining with specific antibodies.

2.3 Cell Culture

U-251, U-138, LN-18, T98, LN-229, U87, U-373, Hs683, D54MG, GBM 8401, GBM 8901, G5T, G9T, SNB75, A172 and SF126 cells were routinely maintained in high glucose DMEM (Life Technologies, Carlsbad, CA) supplemented with 10% FBS (Biological Industries, Israel). DBTRG cells were maintained in RPMI 1640 (Life Technologies) with 10% FBS.

2.4 Immunofluorescent Staining

Cells were plated on tissue culture plastic chamber slides (Nunc, Roskilde, Denmark) overnight to allow sufficient attachment, fixed with 4% paraformaldehyde for 15 min at room temperature, washed three times with PBS, and then blocked with 3% BSA in PBS. Cells were then incubated overnight with 10 μg/mL of mAb MC813-70 (Biolegend), washed three times with PBS and incubated for 2 h at room temperature with 5 μg/ml FITC-conjugated anti-mouse IgG (eBioscience, San Diego, CA). Nuclei were counterstained with Hoechst 33342 (2 μg/mL, Life Technologies). All images were acquired by an Olympus IX71 microscope.

2.5 Immunohistochemistry

For MC813-70 staining on normal brain and GBM specimens, three different tissue microarray slides (Biomax, Rockville, MD), comprising a total of 19 normal brain sections and 55 GBM sections were tested. The slides were dried at 56°C for 1 h, deparaffinized in xylene and rehydrated in graded alcohols, followed by treating with blocking buffer [2% Blocking Reagent (Roche, Basel, Switzerland) in PBS with 0.1% Triton X-100] for 30 min at room temperature. The slides were then incubated at 4°C for overnight with mAb MC813-70 (10 μg/mL in blocking buffer). After gently washing with PBST, the immunoreactivity on specimens was detected with

SuperSensitive™ Polymer-HRP IHC Detection System (BioGenex, Fremont, CA), and the slides were counterstained with hematoxylin and prepped for mounting.

2.6 Glycan Array Fabrication

Microarrays were printed (BioDot; Cartesian Technologies, Irvine, CA) by robotic pin (SMP3; TeleChem International Inc., Sunnyvale, CA) with the deposition of ~0.6 nL per spot. Amine-containing glycans in printing buffer (300 mM sodium phosphate, pH 8.5, 0.01% Triton X-100) were spotted onto *N*-Hydroxysuccinimide (NHS)-activated glass slides. Each glycan was printed at 100 μM in a replicate of four or 50 μM in a replicate of six for Kd determination. Printed slides were allowed to incubate in 80% humidity for 30 min, followed by desiccation for overnight. Remaining NHS groups were blocked by immersing the slides for 1 h in SuperBlock (PBS) Blocking Buffer (Pierce, Appleton, WI).

2.7 Antibody Binding Assay

MAb MC813-70 Alexa Fluor 647 (Biolegend) was prepared in 100 μL of PBS-B-T (pH 7.4, with 3% BSA and 0.05% Tween-20) and applied to cover the grid. After incubation in a moist chamber for 30 minutes, the slides were rinsed with PBST and deionized

water and blow-dried. The slides were scanned at 635 nm in genepix 4300A (Molecular device, Sunnyvale, CA). Data were analyzed by GenePix Pro-6.0 (Molecular Devices).

2.8 Sialidase Treatment

Cells were washed and resuspended in PBS buffer at 1×10^7 cells/mL. Cells were incubated with or without 500 mU α2,3 sialidase (NEB, Ipswich, MA)/10^6 cells/100 μL for 1 h at 37°C, and washed twice with FACS buffer followed by surface staining and flow cytometry. The efficiency of sialidase treatment was measured by biotinylated *Maackia amurensis* lectin II (MAL II; Vector Laboratories), which recognizes α2,3-linked sialic acids.

2.9 Extraction of Glycosphingolipids

Cells (4×10^7) were harvested, washed with PBS and homogenized in water. Per 3 vol. homogenate was added with 8 vol. methanol and 4 vol. chloroform and the sample was incubated in a bath sonicator for 30 min. After centrifugation at 3000 × *g* for 15 min, the pellet was repeatedly extracted with 4:8:3 chloroform/methanol/water, and the combined supernatant was dried under a stream of nitrogen. The total lipid extract was then dissolved in chloroform/methanol/water (30/60/8, v/v/v), and gangliosides were purified by DEAE-Sephadex A-25 (GE Healthcare, Buckinghamshire, UK) based

anion-exchange chromatography. Unbound flow-through containing neutral glycolipids was collected and dried. After washing with chloroform/methanol/water (30/60/8, v/v/v), gangliosides were eluted with chloroform/methanol/aqueous NaCl (0.02, 0.2 and 0.8 M stepwisely) (30/60/8, v/v/v), followed by desalting with Sep-Pak C18 Cartridges (Waters, Milford, MA). The extracts were dried under nitrogen and the ganglioside residues as well as neutral glycolipid residues were redissolved in 100 μL chloroform/methanol (2/1, v/v).

2.10 High-Performance Thin-Layer Chromatography

GSLs were separated on glass-packed silica gel 60 precoated high-performance thin-layer chromatography (HPTLC) plates (Merck). Gangliosides were chromatographed in chloroform/methanol/water (120/85/20, v/v/v) and neutral GSLs in chloroform/methanol/water (120/70/17, v/v/v), respectively, each supplemented with 2 mM $CaCl_2$. For analytic purposes, GSLs were stained with 0.3% orcinol in 3 M H_2SO_4 and then transferred to a preheated heating plate (110 °C) until bluepurple spots appeared. For preparative purposes, gangliosides were stained with 0.02% primulin (Sigma, St. Louis, MO) in acetone/water (4/1, v/v). Spots of gangliosides were marked with a pencil under UV light and scraped from the plate with an adsorbent scraper (Sigma) and the gangliosides were extracted with chloroform/methanol/water (30/60/8,

v/v/v) under sonication for 10 min. The silica was removed by centrifugation, re-extracted again, and the combined supernatant were dried and redissolved in methanol.

2.11 TLC Immunostaining

GSLs were separated on HPTLC plates as described above. After chromatography, the TLC plate was air-dried, immersed in 2.1% poly(isobutyl-methacrylate) (Sigma) in hexane/chloroform (42:8, v/v) three times and soaked in PBS at 37°C for overnight. The plate was dried, blocked with in PBS for 30 min at room temperature and reacted with MC813-70 or MC-631 (5 μg/mL) for 2 h at room temperature. Gently washed with PBST (0.05% Tween-20) for three times, the plate was incubated with biotinylated secondary antibody (1 μg/mL) for 1 h, followed by incubation with streptavidin-alkaline phosphatase (1:1000; Millipore). After washing with PBST, the TLC plate was developed with NBT/BCIP (Thermo Scientific)

2.12 MALDI-MS Profiling and MS/MS Analysis

MALDI-MS analysis of permethylated glycans were conducted in an ABI 4700 Proteomics Analyzer (Applied Biosystems, Foster City, CA) using 2,5-dihydroxybenzoic acid (DHB) as the matrix (10 mg/mL). MALDI-MS/MS

sequencing with low- and high-energy collision-induced dissociation was operated in a Q/TOF Ultima MALDI (Waters Micromass) and a 4700 Proteomics Analyzer using the DHB matrix as described above.

2.13 Complement-Dependent Cytotoxicity Assay

The CDC activity of anti-SSEA4 (MC813-70) mAb was measured by lactate dehydrogenase (LDH)-release assay using the CytoTox 96® Non-Radioactive Cytotoxicity Assay kit (Promega, Fitchburg, WI). Cells (1×10^4) were plated in each well of 96-well plates and washed with PBS twice after growth for overnight. The cells were then incubated with 1 μg of MC813-70 or mouse IgG3 isotype control in 50 μL phenol red-free DMEM or RPMI with rabbit complement (dilution of 1:5; Life Technologies). After incubation in a 5% CO2 incubator at 37ºC for 1 h, the degree of cell lysis was determined by measuring the amount of LDH released into the culture supernatant. Maximum LDH release was determined by lysing the cells with Lysis Solution provided by the kit. Percentage of specific lysis was calculated according to the equation: % lysis = [experimental release – spontaneous release] / [maximum release – spontaneous release] × 100.

2.14 In vivo Tumor Growth

BALB/cAnN.Cg-Foxn1nu/CrlNarl mice were purchased from National Laboratory Animal Center (Taiwan) and maintained under specific pathogen-free conditions. The health status of animal was monitored daily. Procedures involving animals and their care were conducted according to Academia Sinica Institutional Animal Care and Utilization Committee in compliance with national and international laws and policies. DBTRG cells (1×10^7/250 μL PBS) were subcutaneously injected to the flank regions of mice (8- to 10-weeks old) to generate the xenograft model. On day 11, 15 and 19, each mouse was peritoneally injected with 200 μg of MC813-70 (purified from the ascites) or mouse IgG3 isotype control Ab. The tumor size was determined by vernier caliper by measuring the length (L) and width (W), and the tumor volume was calculated (in mm^3) as $1/2 \times LW^2$.

2.15 Neurosphere culture

For neurosphere formation, GBM cell lines were maintained in the ultra-low attachment dish (Corning, Corning, NY) with neurobasal media (Invitrogen), containing 1.0X N2, 1.0X B27 supplement (Invitrogen), and human recombinant basic fibroblast growth factor (bFGF) and EGF (20 ng/ml each; PeproTech, Rocky Hill, NJ). The media were refreshed every 3 days and all cells were cultured in 5% CO2 and humidified atmosphere at 37oC. For detection of self-renewal ability, after neurosphere formation

was generated, neurosphere cells were dissociated and plated in 96-well plates in 0.2 ml volume media. Media were added every 3 days for 3 weeks. The number of neurospheres whose diameter is over 100 um were calculated.

2.16 Quantitative real- time polymerase chain reaction

Total RNA were extracted using RNeasy kit (QIAGEN, Venlo, Netherlands) according to the manufacturer's instructions. 2 μg of total RNA was used for cDNA synthesis using RevertAid First Strand cDNA Synthesis Kit (Thermo Scientific) The Maxima SYBR Green/ ROX qPCR Master Mix (Thermo Scientific) reaction system was used, and reactions were run on an ABI Prism 7900HT sequence detection system (Advanced Biosystems, Foster City, CA). Sequences of the primers used were listed in Table 1. Quantitative PCR results were first normalized to the GAPDH transcript level to yield Δthreshold cycle values. The results are expressed as $2^{-\Delta Ct}$, according to the method described by Livak and Schmittgen [127].

2.17 SDS-PAGE and western blot

Cells were harvested and washed with PBS and lysed in lysis buffer, containing 150 mM NaCl, 100 mM phosphate buffer pH 7.2, 1% NP-40, 10% glycerol, 1x protease inhibitor and 1x phosphatase inhibitor. Supernatant was collected by centrifugation at

14,000 x g for 10 min at 4°C. Protein concentration was determined according to the BCA method (Pierce). The protein sample were mixed with 4x sample buffer (Invitrogen) and boiled for 5 min at 95°C, separated on 10% SDS-polyacrylamide gels (PAGE), and then transferred to PVDF membrane (Millipore). The membrane blots were blocked in PBS containing 5% non-fat milk for 1 hr at room temperature, and incubated with primary antibody overnight at 4°C. After washing with PBST with 0.1% Tween-20, the blots were incubated with secondary antibody conjugated with horseradish peroxidase (Millipore). Then the blots were washed with TBST, and immunoreacted bands were detected with ECL reagents (Millipore) and exposed on ImageQuant LAS 4000 (GE Healthcare).

CHAPTER 3: RESULTS

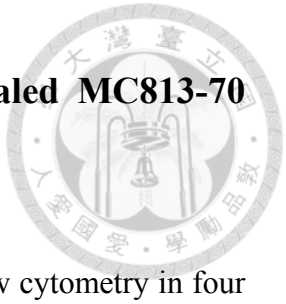

3.1 Flow cytometric analysis of glycan epitopes revealed MC813-70 binds to GBM cell lines

We analyzed the expression levels of various glycan epitopes by flow cytometry in four human GBM cell lines: G5T, LN-18, U-138 and U-251. The glycan epitopes examined include O-linked glycans (Tn, sTn, TF), Lewis antigens (Le^x, Le^y and sLe^x), complex gangliosides [GM2, GM1, GD1a, GD2, GT1b and A2B5 (c-series gangliosides)], and globo-series GSLs (SSEA-3, SSEA-4 and Globo H). The results showed that most of these four GBM cell lines expressed high levels of Tn, TF, Le^x, and Le^y, a low level of sLe^x, and no sTn (Table 2, Fig. 1). In addition, these four GBM cell lines were positive for all the gangliosides we examined although the expression levels varied (Fig. 1).

Regarding the expression levels of globo-series GSLs, U-251 showed a weak MC813-70 (anti-SSEA-4) staining, and G5T, U-138 and LN-18 displayed a high MC813-70 staining intensity (Table 2, Fig. 2B). Positive MC631 (anti-SSEA-3A) staining was only observed on G5T among these four cell lines, and none was positive for VK9 (anti-Globo H) staining (Table 2, Fig. 2C). After these findings, we further looked into the expression patterns of globo-series GSLs in more GBM cell lines, and we found that of the 17 GBM cell lines, nine showed strong MC813-70 staining signal (SSEA-4^{hi}); three were weakly stained (SSEA-4^{lo}), and five were not stained by MC813-70 (Fig. 2B). Nine out of 17 cell lines were positive for MC631 staining and six

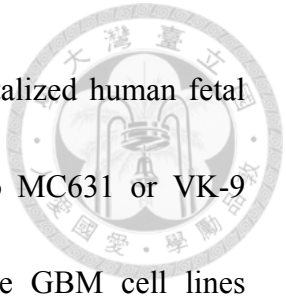

were positive for VK9 staining (Fig. 2A, C). SVG p12, an immortalized human fetal glia cell, showed a very weak MC813-70 staining signal, but no MC631 or VK-9 staining signal. These results indicated that most (70.6%) of the GBM cell lines examined were positively stained by MC813-70.

3.2 Examination of MC813-70 specificity by glycan microarray

Previous studies indicate that mAb MC813-70 recognizes the NeuAcα2-3Galβ1-3GalNAc epitope in SSEA-4 glycolipid (sialyl Gb_5Cer) and the glycoproteins with an extended core 1 O-glycan structure [54, 128]. In addition, MC813-70 shows cross-reactivity toward GM1b and GD1a when these two gangliosides are immobilized at a very high concentration/density. We used a glycan microarray, a platform for studying the interactions between glycans and glycan-binding proteins [129], to investigate the binding specificity of MC813-70. As shown in Fig. 2, we found that among the 152 chemically synthesized glycans on the glycan microarray, (Fig. 3), MC813-70 only recognizes the SSEA-4 hexasaccharide with Neu5Ac or Neu5Gc at the terminal position (No. 12, 49; Fig. 4A). Compared with previous ELISA results [54], MC813-70 did not show any binding to GM1b (No. 104) or GD1a (No. 106), both of which contain the terminal trisaccharide epitope of SSEA-4 (NeuAcα2-3Galβ1-3GalNAc) with a different linkage (β1-4) to lactose at the reducing

end. In addition, MC813-70 did not bind to sialyl Lc4 (No. 111), a glioma-associated GSL, with similar terminal glycan structure of SSEA-4 (NeuAcα2-3Galβ1-3GlcNAcβ1-3). We also used the glycan array to determine the dissociation constants of MC813-70 with SSEA-4 hexasaccharide on surface, and the Kd value for the interaction was 4.21 ± 0.26 nM (Fig. 4B). These results showed that MC813-70 is highly specific for SSEA-4.

3.3 Verification of MC813-70 staining on GBM cell lines by HPTLC immunostaining

To exclude the possibility that MC813-70 may bind to the extended core 1 O-glycan on glycoproteins in GBM cells, we treated DBTRG cells with methanol to remove lipids before staining with MC813-70. Upon methanol treatment, the immunoreactivity of MC813-70 disappeared, as analyzed by immunofluorescence microscopy (Fig. 5A) and flow cytometry (Fig. 5B), suggesting that the immunoreactivity of MC813-70 was toward glycolipids, not glycoproteins. To further verify the expression of SSEA-4, we next purified the gangliosides using anion-exchange chromatography, developed the purified gangliosides on HPTLC plates, and visualized by orcinol-H_2SO_4 stain or immunoblotting. As shown in Fig. 6, the purified gangliosides from three different GBM cell lines exhibited similar patterns (Fig. 6, left panel, lane 1-3), with abundant

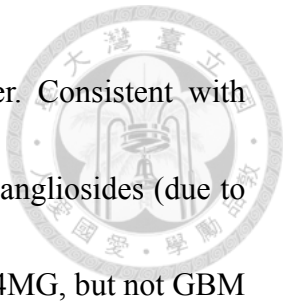

GM3, GM2, Neu5Ac-(n)Lc4/Gg4Cer and Neu5Ac2-(n)Lc4/Gg4Cer. Consistent with the results of flow cytometric analysis, MC813-70 recognized two gangliosides (due to a different chain length of fatty acids) on TLC from DBTRG and D54MG, but not GBM 8901 cells (Fig. 6). The positions of the immuno-reactive double bands in GBM gangliosides were the same as in the gangliosides purified from 2102Ep cells (Fig. 6, lane 4), embryonal carcinoma cells known to express a high level of SSEA-4 glycolipid [54]. A double-band developed at a shorter distance than MC813-70 positive glycolipid was detected by MC813-70 in YAC-1 cells (Fig. 6, lane 5), in which GM1b is a major ganglioside [130], supporting that MC813-70 harbors a weak cross-reactivity toward GM1b. Immunoblotting with MC631 revealed that it could also recognize MC813-70 positive glycolipid with a lower affinity than MC813-70 did (Fig. 6, right panel). To examine the number of sialic acids on MC813-70 positive glycolipids, we eluted gangliosides in gradient salt conditions and performed immunoblotting with MC813-70. The result supported that MC813-70 reactive gangliosides were monosialylated as the two bands appeared at the fraction eluted in low salt condition (Fig. 7). These result indicated a monosialyl ganglioside with the same TLC mobility of SSEA-4 is expressed in GBM cell lines.

3.4 Sialidase treatment confirms the structure of MC813-70 antigen as

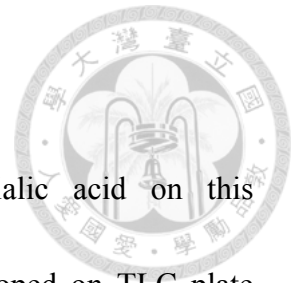

an α2,3-sialyl globo-series GSL

We next used sialidases to elucidate the linkage of the sialic acid on this MC813-70-reactive monosialoganglioside. The gangliosides developed on TLC plate were treated with α2,3-sialidase or the sialidase that cleaves all linkages of sialic acids, and blotted with MC813-70 and MC631. The results in Fig. 8 showed that the immunoreactivity of MC813-70 disappeared after sialidase treatment (Fig. 8, middle panel), while MC631 could detect strong signals (Fig. 8, right panel) at the positions resembled MC813-70 reactive doublets, indicating the presence of an α2,3-linked sialic acid and the remnant glycolipid belonging to globo-series.. Next, we performed the MC631 staining on α2,3-sialidase-treated DBTRG cells (Fig. 9), and the result showed that when treating with α2,3-sialidase, the cells became MC813-70 negative and MC631 positive, supporting that the GBM cells did express SSEA-4. The activity of α2,3-sialidase was validated by the decreased intensity of MAL II staining.

3.5 Analysis of DBTRG gangliosides by mass spectrometry indicates the presence of SSEA-4 glycolipid

We analyzed the gangliosides from DBTRG cells by MALDI-MS profiling (Fig. 10). The spectra were dominated by several major peaks that occurred in signal clusters due to the expected heterogeneity of the ceramide portions. Based on the *m/z* values of

major molecular ions, as fitted to permethylation of hexose (Hex), *N-acetyl*hexosamine (HexNAc), or NeuAc residues, in combination with sphingosine and fatty acyl chains, the respective gangliosides profiles were assigned. Consistent with the HPTLC results, the MS profiling revealed that the major species of gangliosides in DBTRG cells were GM3, GM2, Neu5Ac-(n)Lc4/Gg4Cer, and Neu5Ac2-(n)Lc4/Gg4Cer. The signal with Neu5Ac-Hex4-HexNAc-Cer (*m/z* = 2025.2) that represented SSEA-4, although with low intensity, was also detected, reflecting the existence of SSEA-4 in DBTRG cells. These data support that the MC813-70 reactive ganglioside was SSEA-4, and despite of being a minor constituent of total gangliosides, SSEA-4 was expressed in GBM cells.

3.6 Expression of SSEA-4 in GBM tissues

SSEA-4 is a widely used marker for stem cells, but the information about the expression of SSEA-4 in GBM tissues as well as normal brain tissues was limited. To understand if SSEA-4 is overexpressed in clinical GBM specimens, in addition to GBM cell lines, we analyzed the expression of SSEA-4 among astrocytomas from grade I to IV and normal brain tissues by immunohistochemistry on human tissue microarrays (Fig. 11). The staining intensity was graded as 0 (negative), 1+ (weak), 2+ (moderate), 3+ (strong), as shown in Fig. 11D. We found that 38 out of 55 GBM tissue specimens (69%) were positive for MC813-70 staining, and around half of GBM specimens were intensely

stained (≥2+). As shown in the positive specimens, SSEA-4 was situated on the plasma membrane of GBM cells (Fig. 11B, inset), where most of GSLs locate. Furthermore, 55-60% of grade I, II and III astrocytoma specimens were stained by MC813-70 despite of weaker intensity, and the scores of SSEA-4 intensity was positively correlated with the grades of astrocytomas (Fig. 11C). On the contrary, most normal brain tissues were SSEA-4 negative (Fig. 11A). These results indicated SSEA-4 was highly expressed in GBM tumors.

3.7 MC813-70 Mediates CDC against GBM Cell Lines

To test if targeting SSEA-4 would trigger complement-dependent cytotoxicity (CDC) in GBM cells, GBM cell lines were treated with MC813-70 and rabbit complement, and the degree of CDC was evaluated by detecting the level of released lactate dehydrogenase caused by cell death. Fig. 12 showed that in the presence of complement, mAb MC813-70 remarkably reduced the number of viable GBM cells. We observed a significant CDC in SSEA-4^{hi} GBM cell lines: 71.7% cytotoxicity of DBTRG, 46.6% of LN-229, 67% of G5T, and 65.4% of LN-18 cells. MC813-70-mediated CDC did not kill two GBM cell lines, Hs683 and U87, which expressed low or no SSEA-4. Therefore, the level of MC813-70 mediated CDC positively correlated with the expression level of SSEA-4 in each GBM cell line, and it is possible that only the cells with enough

amounts of SSEA-4 would be bound by enough amounts of MC813-70 and therefore are susceptible to CDC.

3.8 MC813-70 Suppresses Brain Tumor Growth *in Vivo*

To check if MC813-70 was able to suppress GBM tumor growth *in vivo*, MC813-70 was administered to the nude mice injected with DBTRG cells subcutaneously, when the tumors grew to palpable bumps (15-30 mm^3at day 11 post-injection). MC813-70 (200 μg) was given intraperitoneally to each mouse every four days for a total of three times, with an irrelevant mouse IgG3 (isotype control) injected in parallel for comparison. The experiment revealed that the administration of MC813-70 could inhibit DBTRG tumor growth (Fig. 13). The growth of DBTRG tumors were completely suppressed in two of three mice treated with MC813-70, and the third mice developed tumor after the cease of antibody treatment. Comparing to the mice receiving MC813-70 treatment, DBTRG tumor grew aggressively (with the tumor volume of 184 mm^3 in average at day 31) in the control group injected with mouse IgG3. These data demonstrated that MC813-70 was able to inhibit the growth of SSEA-4-expressing GBM tumors, possibly through CDC and ADCC *in vivo*.

3.9 Expression of SSEA-4 in Various Cancer Cell Lines

SSEA-4 has been reported to be expressed on renal carcinoma [131], basaloid lung cancer [132], epithelial ovarian carcinoma [133], breast cancer [134], and oral cancer [135]. Here, we analyzed the expression levels of SSEA-3, Globo H and SSEA-4 on various cancer cell lines by flow cytometry. As shown in Table 3, we have examined a total of 134 cancer cell lines (17 brain cancer cell lines, 20 lung cancer cell lines, 23 breast cancer cell lines, 13 oral cancer cell lines, 2 esophageal cancer cell lines, 6 gastric cancer cell lines, 10 liver cancer cell lines, 5 bile duct cancer cell lines, 8 pancreatic cancer cell lines, 7 colon cancer cell lines, 6 renal cancer cell lines, 4 cervical cancer cell lines, 9 ovarian cancer cell lines and 4 prostate cancer cell lines), and the names and the expressed GSLs of these cell lines are listed in Table 4. We found that SSEA-4 was expressed in every type of cancer cell line (96 of 134). Globo H was also expressed in many of cancer cell lines (88 of 134), preferentially in lung, breast, pancreas, colon, stomach, mouth, liver, kidney cancer cell lines. We also observed that many of cancer cell lines (70 of 134) expressed SSEA-4 and Globo H simultaneously. On the other hand, the expression of SSEA-3 always followed a high expression of SSEA-4, indicating that SSEA-4 and Globo H were the major globo-series GSLs on the cancer cells. To validate the identity of SSEA-4, we purified the gangliosides from nine MC813-70-positive cell lines as well as TF1a, a MC813-70-negative leukemia cell line, and performed immunostaining on HPTLC plates. As expected, SSEA-4 was detected in these nine

cancer cell lines but not TF1a (Fig. 14), and the intensity was well correlated with the geometric mean fluorescence intensity as examined by flow cytometry. The slight differences of mobility of SSEA-4 in various cell lines could be resulted from the chain-length variations in the sphingoid base or fatty acid. These results revealed that SSEA-4 could be expressed in a variety of cancer cell lines in addition to GBM.

3.10 Cells maintained in in vitro neurosphere culture expressed higher levels of stemness genes

In order to enrich cells with properties of CSCs, we employed the neurosphere culture system and cultured cells in the ultra-low attachment dish to prevent differentiation [136, 137]. After 10 day, most of GBM cell lines show the formation of neurospheres (Fig. 15), while the other cells within culture died. We analyzed the stemness of neurosphere cells from six of GBM cell lines by evaluating the expression of stemness genes. SOX2, OCT4 and NANOG are transcription factors expressed in specific stage of embryonic stem cells and maintained the pluripotent ability. Nestin, a type VI intermediate filament protein, expressed in the early stage of development in the nervous system and in myogenic and other tissues [138]. CD133 (prominin 1) has been found in hematopoietic stem cells, endothelial progenitor cells and neuronal stem cell. In the real-time RT-PCR and western blotting, we observed that the gene and protein

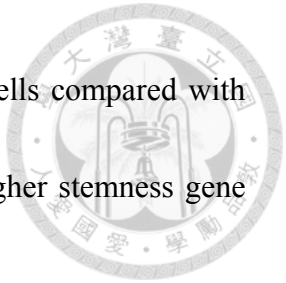

expressions of stemness genes were increased in the neurosphere cells compared with parental cell (Fig. 16, 17). Hence, the neurosphere cells showed higher stemness gene expression in our in vitro enrichment system.

3.11 Neurosphere cells show higher potential of self-renewal and tumorogenicity

We performed sphere formation assay to test self-renewal capacities of parental and neurosphere cells. Even within neurospheres, only a small percentage of cells, that possess self-renewal capacity, reform into a secondary neurosphere [122]. In the self-renewal assay, cells derived from neurospheres generated more and bigger secondary spheres (Fig. 18A), indicating that neurosphere population have higher percentage of total cells with self-renewal capacity. To examine the tumor-initiating ability, non-obese diabetic/severe combined immunodeficient (NOD-SCID) mice were subcutaneously injected with neurosphere and parental cells. Results showed that when injecting with the 10^4 cells, the cells from neurospheres grew faster than parental cells, suggesting that neurosphere cells possessed greater tumorigenicity than parental cells in vivo.

3.12 Expression of GD2 is increased in neurosphere cells

We stained parental cells and neurosphere cells with antibodies against different types

of glycans, including the ganglio- and globo-GSLs, Lewis antigens, mucin-type O-glycans and several glycoproteins that have been used as markers to identify stem cells. The expression profile of various surface glycans were summarized in Table 5. Among these surface glycans, the change of GD2 expression was most significant and consistently observed in all neurosphere cells derived from different GBM cell lines (Fig. 19). However, Lewis X, a well-known marker for pluripotent stem cells, did not show any significant difference in these neurosphere and parental cells. All GBM cells and GBM neurosphere cells are CD44+, CD90+ and CD45-. Interestingly, we also observed the loss of CD24 expression in neurosphere cells; therefore, most neurospheres are CD44+/CD24-, a marker set of breast cancer stem cell.

CHAPTER 4: DISCUSSION

In the present study, we evaluated the expression of globo-series GSLs on human GBM cell lines, and found that SSEA-4 was highly expressed in most GBM cell lines, while SSEA-3 and Globo H were also expressed at lower levels. The data from sialidase-treatment and MS confirmed the identity of SSEA-4 (α2-3 sialyl galactosylgloboside) in GBM cell lines. In addition, immunohistochemical studies demonstrated that SSEA-4 was expressed in nearly 70% of GBM tumor specimens, but barely expressed in normal brain tissues. These findings, for the first time, indicate that SSEA-4 is overexpressed in GBM tissues.

SSEA-4, first identified in 1983 [54], is expressed in a variety of human cell lines including embryonic carcinoma (EC), embryonic stem (ES), and induced pluripotent stem (iPS) cells. SSEA-4 is down-regulated upon differentiation, making it a widely used marker to characterize human ES cells and monitor their differentiation. Nonetheless, the information about the distribution of SSEA-4 in normal tissues is limited. SSEA-4 was reported to be expressed as a minor GLS in erythrocytes [54] and on the epithelial cells of several glandular tissues, such as breast, colon, gastrointestinal tract, kidney, lung, ovary, pancreas, rectum, stomach, testes, thymus and uterine cervix [139]. With regard to the expression pattern of SSEA-4 in solid tumors, it was found on renal cell carcinomas in 1997 by Saito *et al.*[131] using immunohistochemistry with

RM1, another SSEA-4 mAb. In the last few years, SSEA-4 has been reported to be expressed on breast cancer cells and breast cancer stem cells [134], basaloid lung cancer [132], epithelial ovarian carcinoma [133], and oral cancer [135]. The relationship between the expression level of SSEA-4 and the tumor malignancy differs in various types of cancers; while the expression of SSEA-4 in basaloid lung cancer associates with poor prognosis [132], the reduction of SSEA-4 is correlated with more advanced tumor stage and tumor cell differentiation in ovarian cancer [133]. Here, we examined the expression of SSEA-4. Not only in GBM/grade IV astrocytoma, SSEA-4 was also detected in lower grades of astrocytoma (grade I, ~55%; II, ~55%; III, ~60%). Nevertheless, there appears to be a trend that higher expression of SSEA-4 is associated with higher grade of astrocytomas. We propose that SSEA-4 may play an active role during tumor progression of astrocytomas, and may serve as a potential therapeutic target in patients with GBM as well as low grade astrocytomas. Furthermore, we provided evidence that SSEA-4 was expressed in multiple cancer cell lines, including lung, breast, ovarian, prostate, colon, and pancreatic cancers. Further clinical specimens from other cancers should be detected for their expression of SSEA-4 to confirm if SSEA-4 can serve as a marker for cancers.

Although SSEA-4 has been discovered for over 20 years, the molecular function of

SSEA-4 has not been tested experimentally. Brimble *et al.* depleted SSEA-3 and -4 in hESCs with D-threo-1-phenyl-2-decanoylamino-3-morpholino-1-propanol (D-PDMP), an inhibitor for glucosylceramide synthase, and found that D-PDMP treatment did not alter the gene expression profile of hESCs or alter their capacity to differentiate *in vitro*, suggesting that SSEA-4 is not essential for hESCs pluripotency [140]. On the other hand, Van Slambrouck *et al.* demonstrated that clustering of monosialyl-Gb5 induces the invasion of MCF-7 breast cancer cells through activation of FAK/c-Src signaling pathway [141]. Recently, SSEA-4 was reported to bind to FK-506 binding protein 4 (FKBP4), and may thus affect the transportation of SSEA-4 to the cell surface and the downstream signaling pathway [142].

In addition to SSEA-4, we have examined the expression of two more globo-series GSLs, SSEA-3 and Globo H. Unlike SSEA-4, SSEA-3 was mainly expressed in those cell lines with high expression of SSEA-4. Together with the results that the expression of Globo H was only observed in six of the GBM cell lines we tested, the data indicated that SSEA-4 was the major globo-series GSL in GBM, and once SSEA-3 was synthesized, it would be efficiently converted to SSEA-4 [139]. It has been suggested that an α2,3-sialyltransferase, encoded by *ST3GAL2* gene, is the major SSEA-4 synthase, which is closely related to renal carcinogenesis [143], and the mRNA level of *ST3GAL2*

is increased in renal and colorectal carcinomas [144]. We also observed that the mRNA level of *ST3GAL2*, but not *fucosyltransferase (FUT) 1* and *2*, was abundant in GBM cell lines (Fig. 25). This may explain why SSEA-4 is the predominant globo-series GSL in GBM cells. It is also interesting to correlate the mRNA levels of *A4GALT*, *ST3GAL2*, *FUT1* and *FUT2* with the expression of globo-series GSLs in GBM, to aid the detection of globo-series GSLs with small amounts of tumor specimens.

As shown in Fig. 8, besides SSEA-4, there is one more GSL that would be recognized by MC631 after the removal of sialic acids on it. The upper doublet on the HTPLC plate was SSEA-4, sialyl Gb_5Cer, and the structure of lower doublet was proposed to be a sialylated SSEA-4, disialyl Gb_5Cer, which could not be recognized by either MC813-70 or MC631. According to the position of the sialic acids, there are three reported isomers of disialyl Gb_5Cer: V3NeuAcαIV6NeuAcα-Gb_5Cer, V3(NeuAcα)2-Gb_5Cer, and V6NeuAcαV3NeuAcα-Gb_5Cer. The expression of these three GSLs in normal human tissues are not well studied and seem to be rare [145], however, overexpression of V3NeuAcαIV6NeuAcα-Gb_5Cer is found on renal carcinomas [131]. The structure of the disialyl Gb_5Cer on GBM cells should be delineated and this disialyl Gb_5Cer could also be another GBM-associated GSL.

Cancer stem cells are a subpopulation of cancer cells, which are tumorigenic and possess self-renewal and the potential to differentiate to a heterogeneous population. The CSC concept has important therapeutic implications, but its investigation has been hampered both by a lack of consistency in the terms used for these cells and by how they are defined. A number of cell surface marker have proven useful for isolation of CSCs, such as CD133, CD44, CD24, THY-1 and ATP-binding cassette B5 ABCB5 [146]. Although SSEA-4 is a widely used stem cell marker for non-tumor cells, SSEA-4 (+) tumor cells showing characteristics of CSCs was reported on human HSC-4 oral cancer cells until recently [135]. Whether SSEA-4 (+) GBM cells possess the properties of CSC has not been studied yet. We expect even if SSEA-4 was essential for identifying GBM stem cells, other surface markers, such as CD44/SSEA-4 in oral cancer, should be included for more precise identification of CSCs since SSEA-4 is expressed in most of GBM cells and GBM tissue.

GD2, a b-series disialoganglioside, prominently expresses on the surface of neurosphere cultured from different GBM cell lines. Several reports indicated that GD2 is expressed on the surface mouse and human neural stem cells [147, 148], as well as breast cancer stem cell [149]. Notably, GD2 distribution is restricted in neurons, skin melanocytes, and sensory nerve fibers [150]. Therefore, the restricted expression of GD2 in normal

tissues makes it appropriate to be the therapeutic targets.

The current standard of care for GBM patients is maximum surgical resection combined with radiation and concomitant and adjuvant temozolomide therapy. Unfortunately, most cases of GBM recur, prompting the need to develop new treatment strategies. Targeted therapy, which blocks tumor growths by interfering specific molecules with small molecules or mAbs, is a growing part of many cancer treatment regimens [151], e.g., a series of anti-EGFRvIII mAbs have been generated for GBM therapy [106, 152]. Moreover, anti-glycolipid targeted therapy is showing great promise in the treatment of several cancers [153], such as anti-GD2 in neuroblastoma [90]. In addition, a recent report indicates that a Globo H-DT vaccine can elicit specific IgG against not only Globo H, but also SSEA-3 and SSEA-4 [134]. The expression profile of these three unique glycolipids on different types of cancer cell lines as shown in Table 3 provides a new direction in cancer vaccine therapy. In addition, our finding of high-level SSEA-4 expression on GBM provides a potential new target for GBM diagnosis and therapy.

CHAPTER 5: FIGURES

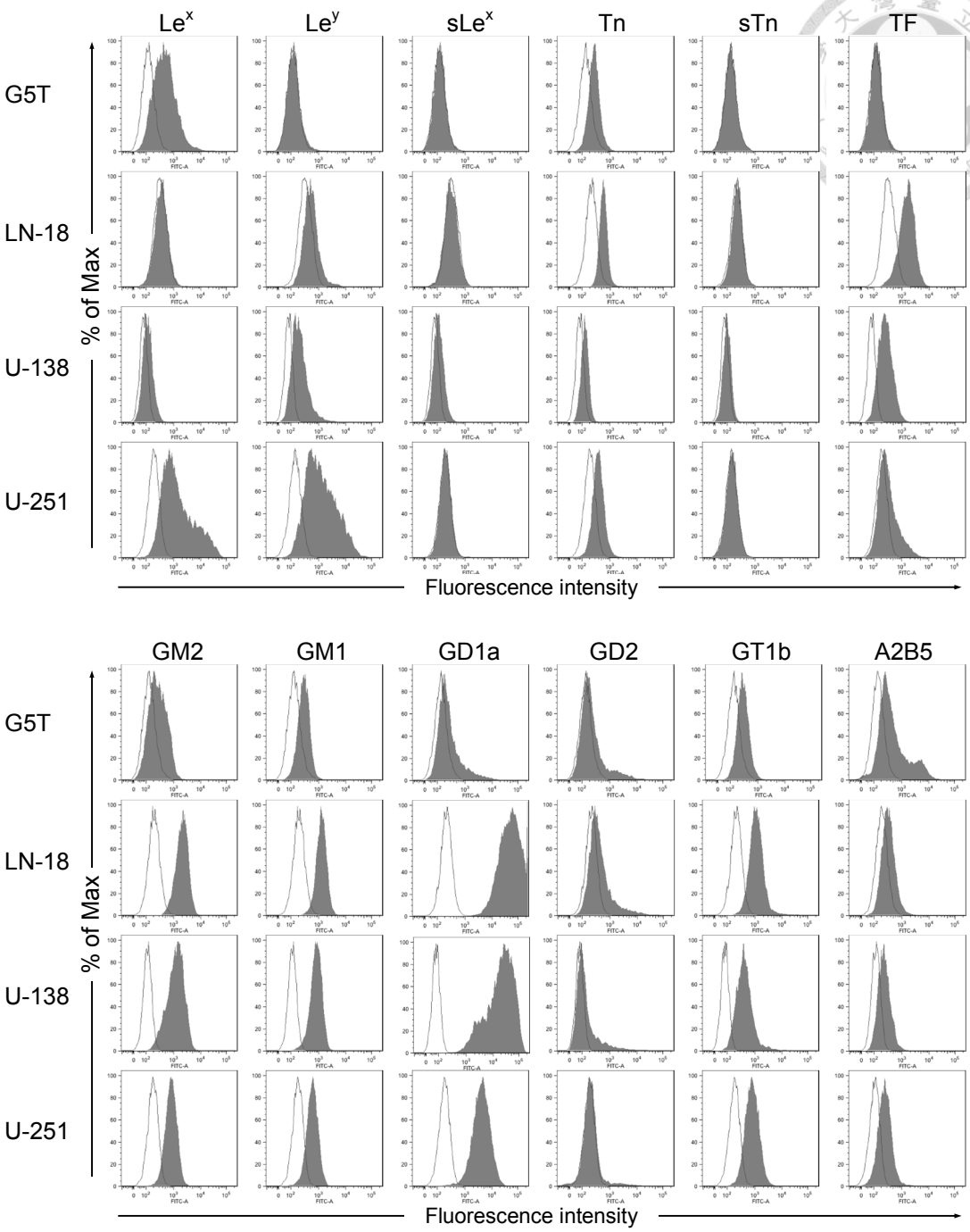

Figure 1. Flow cytometric analyses of glycan-related molecules on GBM cell lines (G5T, LN-18, U-138, and U-251). Expression of Lewis antigens (Le^x, Le^y and sLe^x), O-linked glycans (Tn, sTn, and TF), complex gangliosides [GM2, GM1, GD1a, GD3, GD2, GT1b and A2B5 (c-series gangliosides)] were analyzed. Cells (1×10^5) were incubated with optimal concentrations of the primary antibodies and fluorescent-labeled secondary antibodies, and analyzed by FACSCanto flow cytometer. The histograms of the cells stained with MC813-70 and isotype control are shown in gray and white, respectively.

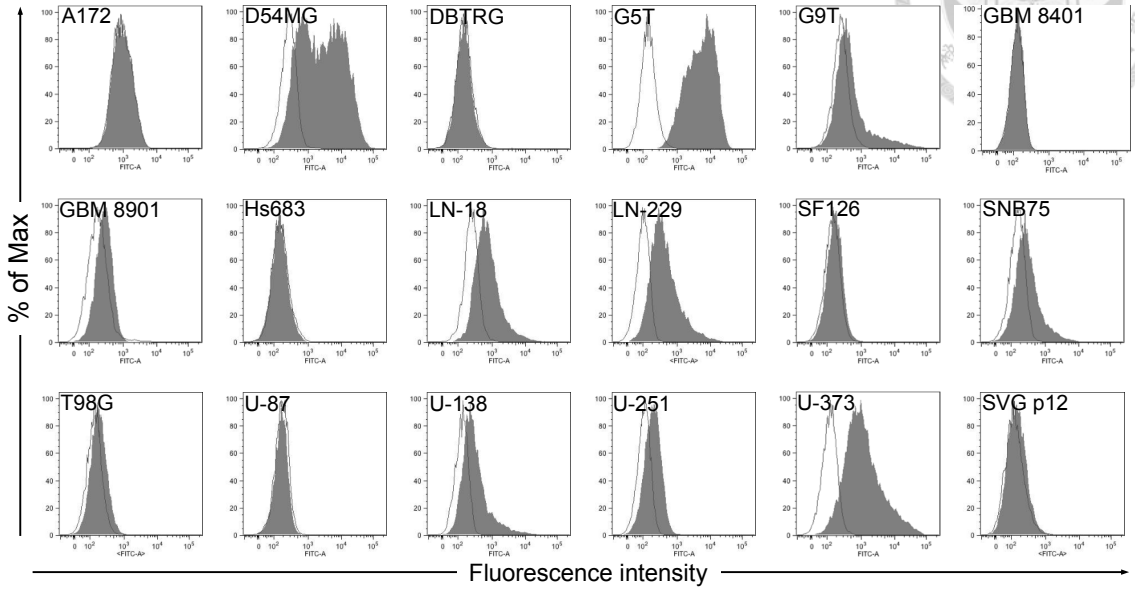
A
MC631 (anti-SSEA-3)
A172
D54MG
DBTRG
G5T
G9T
GBM 8401
GBM 8901
Hs683
LN-18
LN-229
SF126
SNB75
T98G
U-87
U-138
U-251
U-373
SVG p12
% of Max
Fluorescence intensity

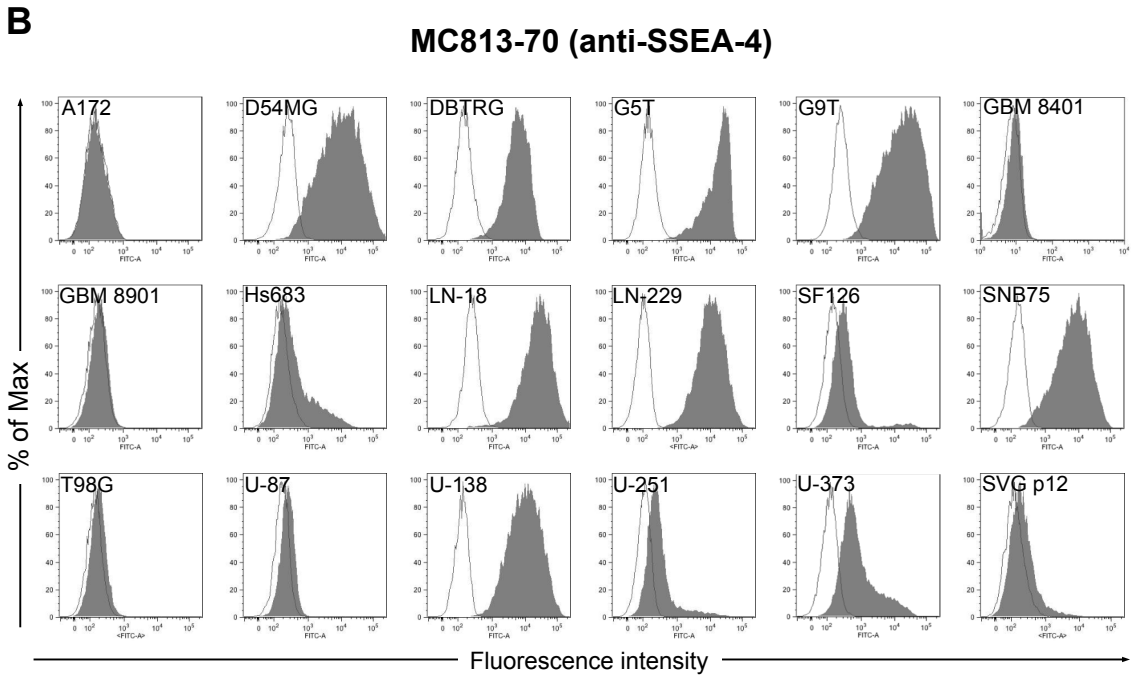
B
MC813-70 (anti-SSEA-4)
A172
D54MG
DBTRG
G5T
G9T
GBM 8401
GBM 8901
Hs683
LN-18
LN-229
SF126
SNB75
T98G
U-87
U-138
U-251
U-373
SVG p12
% of Max
Fluorescence intensity

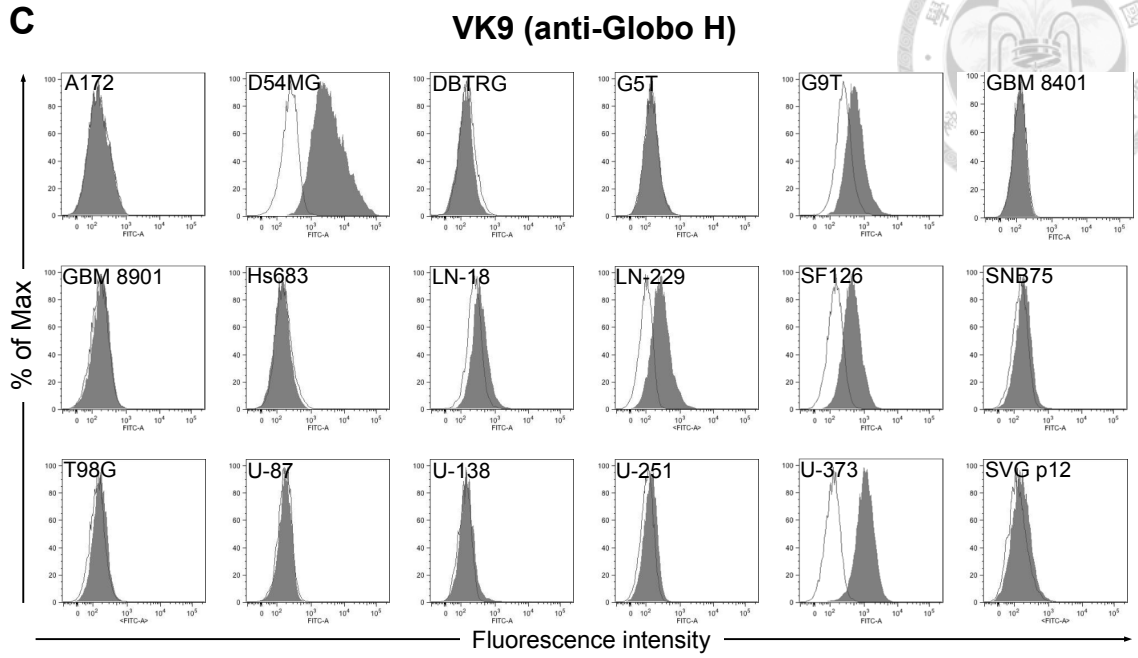

Figure 2. Flow cytometric analyses of globo-series glycosphingolipids on GBM cell lines. Expression of SSEA-3 (A), SSEA-4 (B), and Globo H (C) were analyzed. Cells (1×10^5) were incubated with Alexa Fluor 488-conjuagated MC631, Alexa Fluor 488-conjuagated MC813-70 or APC-conjuagated VK9, and analyzed by FACSCanto flow cytometer. All the cells examined were GBM cell lines except SVG p12, which is a normal human fetal glial cell line transformed with SV40 large T antigen. The histograms of the cells stained with the monoclonal antibody and isotype control are shown in gray and white, respectively.

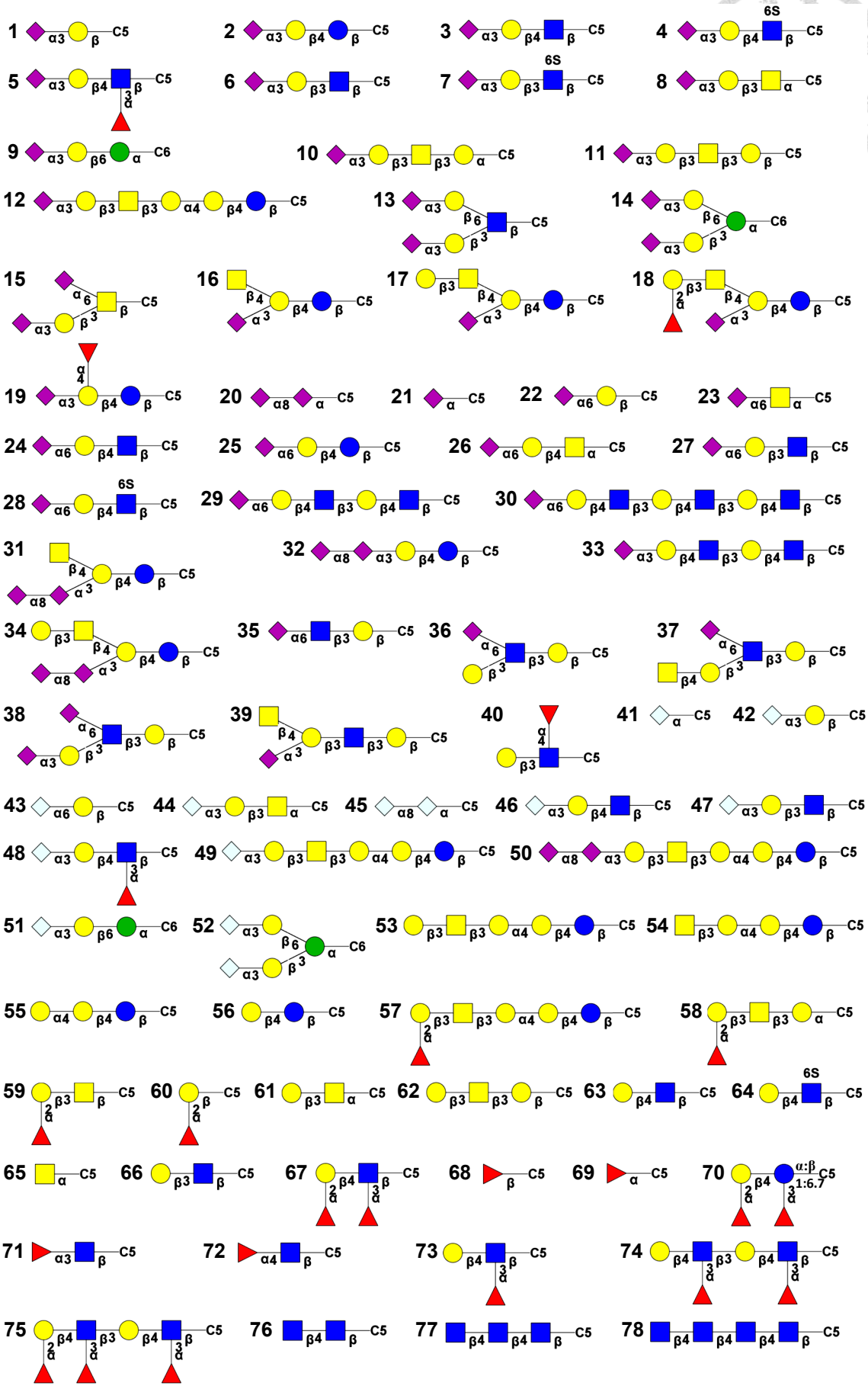
1 α3 β C5
2 α3 β4 β C5
3 α3 β4 β C5
4 6S α3 β4 β C5
5 α3 β4 β C5 3 α
6 α3 β3 β C5
7 6S α3 β3 β C5
8 α3 β3 α C5
9 α3 β6 α C6
10 α3 β3 β3 α C5
11 α3 β3 β3 β C5
12 α3 β3 β3 α4 β4 β C5
13 α3 β6 β C5 α3 β3
14 α3 β6 α C6 α3 β3
15 α6 β C5 α3 β3 α4
16 β4 β C5 α3 β4
17 β3 β4 β C5 α3 β4
18 2 α β3 β4 β C5 α3 β4
19 α4 α3 β4 β C5
20 α8 α C5
21 α C5
22 α6 β C5
23 α6 α C5
24 α6 β4 β C5
25 α6 β4 β C5
26 α6 β4 α C5
27 α6 β3 β C5
28 6S α6 β4 β C5
29 α6 β4 β3 β4 β C5
30 α6 β4 β3 β4 β3 β4 β C5
31 β4 α8 α3 β4 β C5
32 α8 α3 β4 β C5
33 α3 β4 β3 β4 β C5
34 β3 β4 α8 α3 β4 β C5
35 α6 β3 β C5
36 α6 β3 β3 β C5
37 α6 β4 β3 β C5
38 α6 α3 β3 β C5
39 β4 α3 β3 β3 β C5
40 α4 β3 C5
41 α C5
42 α3 β C5
43 α6 β C5
44 α3 β3 α C5
45 α8 α C5
46 α3 β4 β C5
47 α3 β3 β C5
48 α3 β4 β C5 3 α
49 α3 β3 β3 α4 β4 β C5
50 α8 α3 β3 β3 α4 β4 β C5
51 α3 β6 α C6
52 α3 β6 α C6 α3 β3
53 β3 β3 α4 β4 β C5
54 β3 α4 β4 β C5
55 α4 β4 β C5
56 β4 β C5
57 2 α β3 β3 α4 β4 β C5
58 2 α β3 β3 α C5
59 2 α β3 β C5
60 2 α β C5
61 β3 α C5
62 β3 β3 β C5
63 β4 β C5
64 6S β4 β C5
65 α C5
66 β3 β C5
67 2 α β4 β C5 3 α
68 β C5
69 α C5
70 2 α β4 α:β 1:6.7 C5 3 α
71 α3 β C5
72 α4 β C5
73 β4 β C5 3 α
74 β4 β3 β4 β C5 3 α 3 α
75 2 α β4 β3 β4 β C5 3 α 3 α
76 β4 β C5
77 β4 β4 β C5
78 β4 β4 β4 β C5

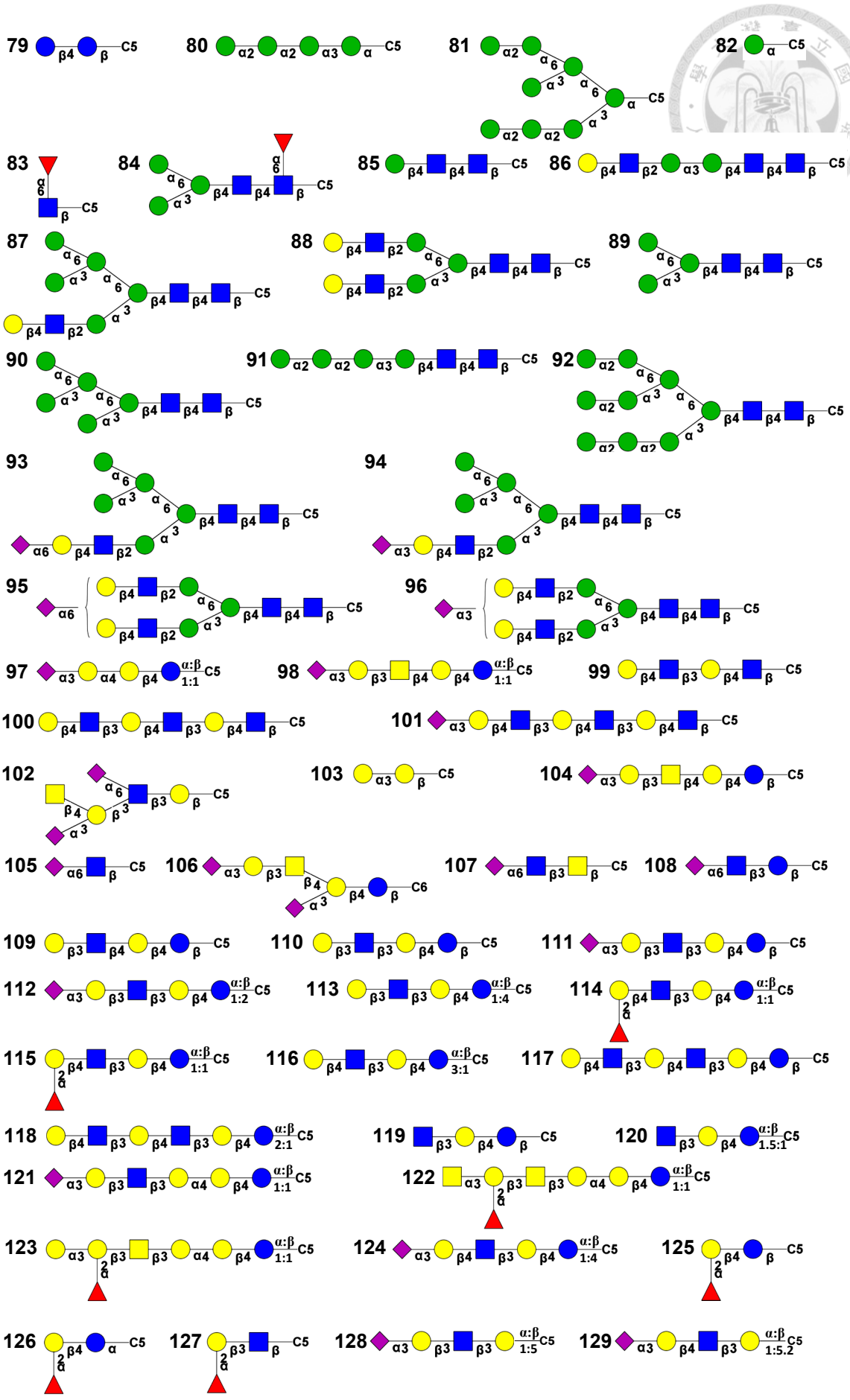
79
80
81
82
83
84
85
86
87
88
89
90
91
92
93
94
95
96
97
98
99
100
101
102
103
104
105
106
107
108
109
110
111
112
113
114
115
116
117
118
119
120
121
122
123
124
125
126
127
128
129

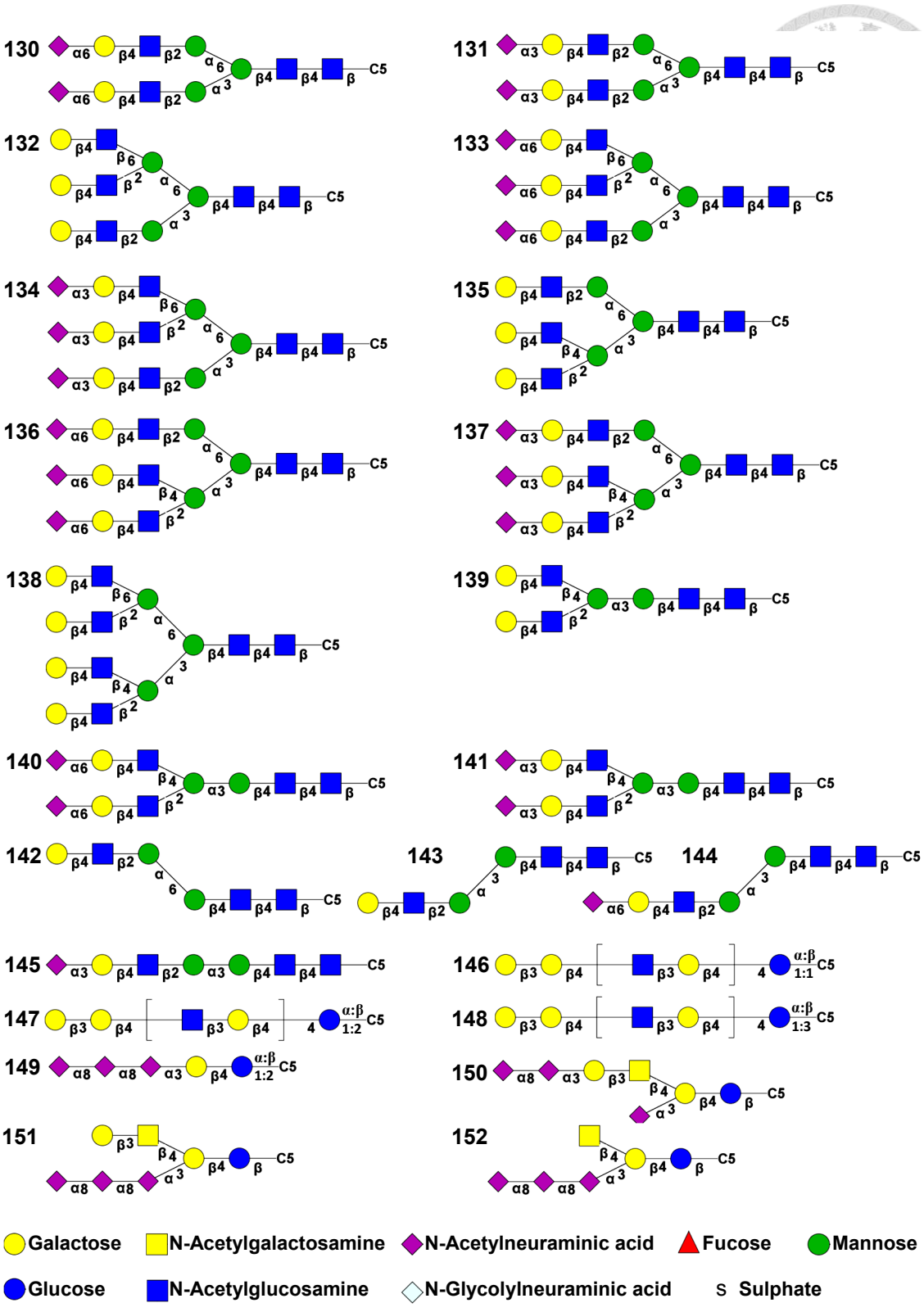

Figure 3. Chemical structures of 152 oligosaccharides on glycan microarray glass slide. The graphical notation of glycan structures in this figure is based on the symbols proposed by the Consortium for Functional Glycomics (CFG). Enantiomertic ratios are indicated for the glycans containing enantiomers. C5, C5H10NH2; C6, C6H12NH2.

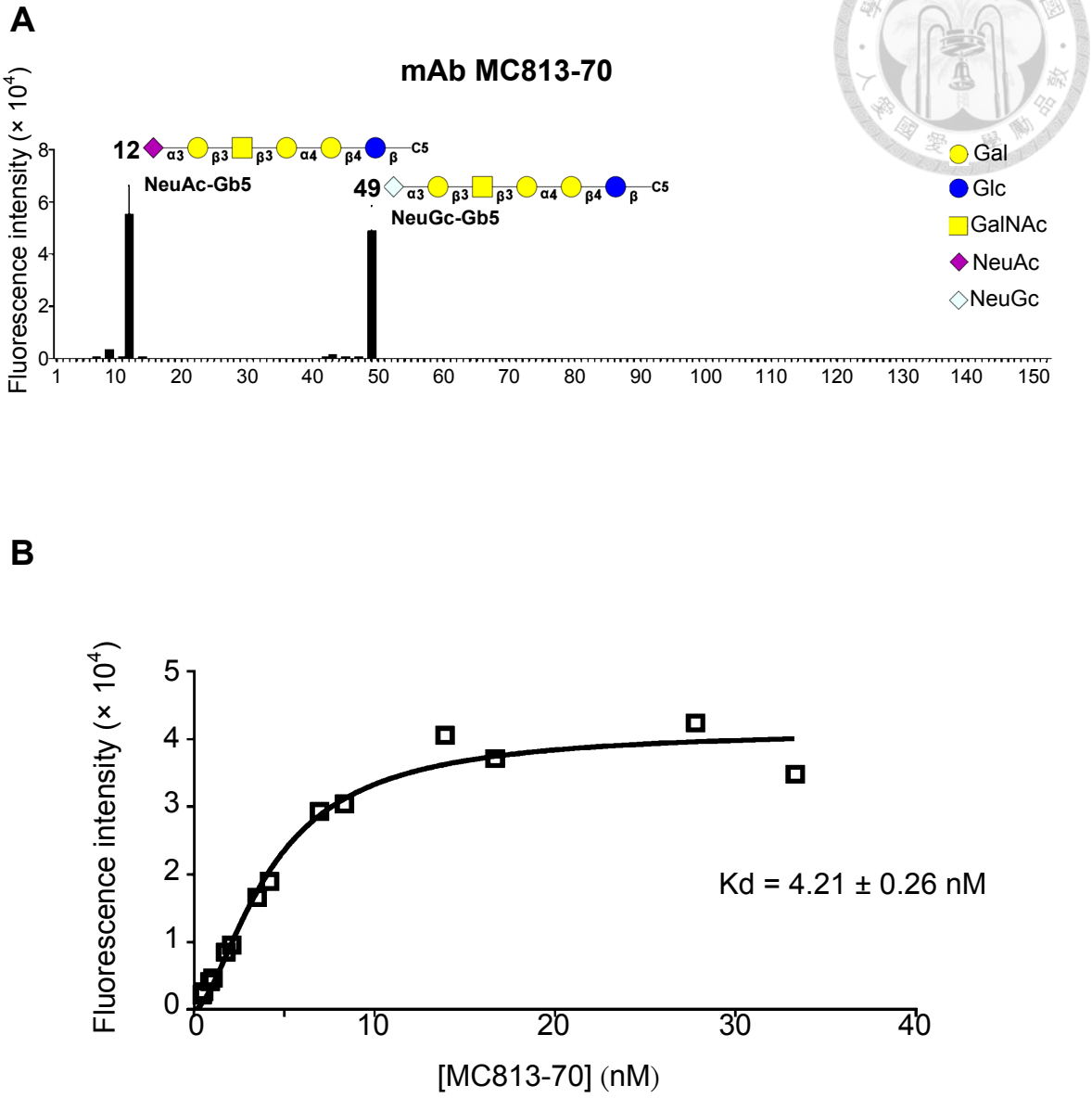

Figure 4. The glycan binding profile of mAb MC813-70. (A) The glycan microarrays on glass slides were interacted with Alexa Flour 647-conjugated MC813-70 (10 μg/mL) and read in an array scanner at 635 nm. Data are presented as mean ± SD. C5, C5H10NH2. (B) The binding curve of MC813-70 to SSEA-4 glycan was obtained by using different concentrations of Alexa Flour 647-conjugated MC813-70. The dissociation constant (Kd) of mAb MC813-70 toward SSEA-4 glycan was calculated and shown.

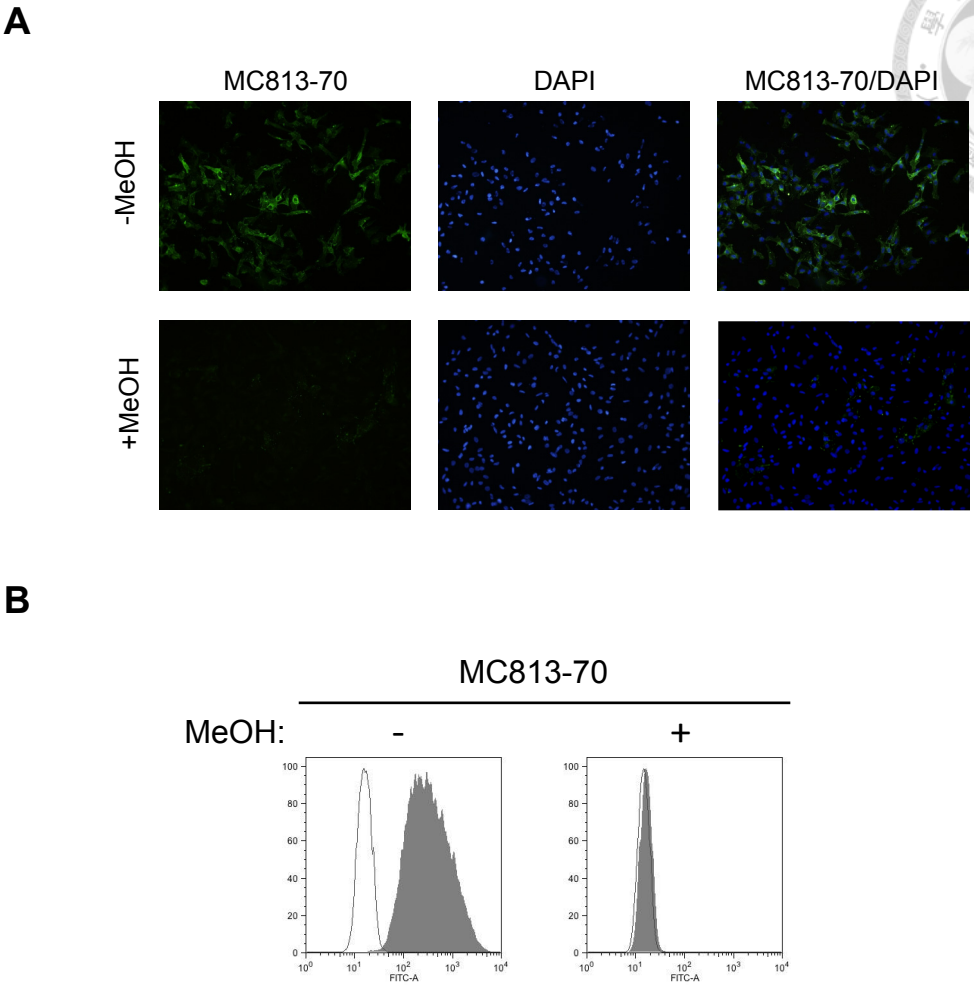

Figure 5. Effect of methanol on MC813-70 immunoreactivity toward GBM cells. DBTRG cells with or without methanol (MeOH) treatment were stained with MC813-70 and subjected to immunofluorescent microscopy (A) and flow cytometry (B). DBTRG cells showed positive immunofluorescent staining [Panel A, green color; Panel B, gray histogram], which disappeared after treatment with MeOH. For immunofluorescent microscopy, nuclei were stained with DAPI (blue), and for flow cytometry, staining with isotype control is shown as white histogram.

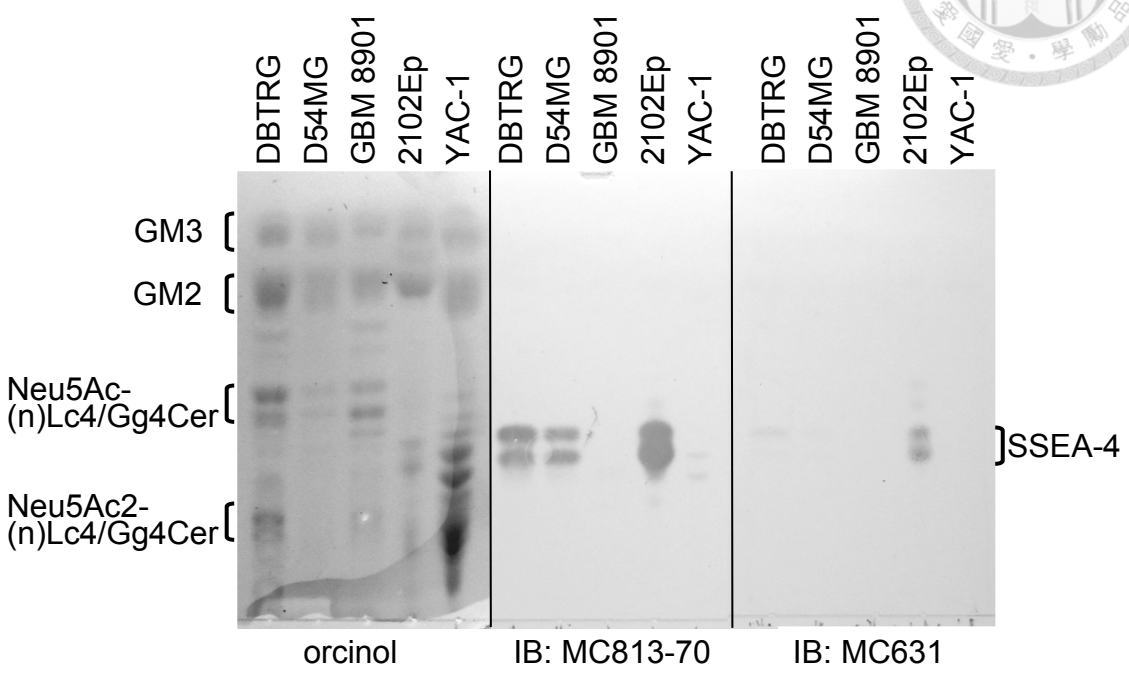

Figure 6. HPTLC profiles and immunostaining of gangliosides from GBM cell lines . Gangliosides extracted from GBM cell lines (DBTRG and D54MG, SSEA-4^+; GBM 8901, SSEA-4^-) were separated on an HPTLC plate and detected with orcinol (left panel), MC813-70 mAb (middle panel) or MC631 mAb (right panel). Gangliosides from 2012Ep (human embryonal carcinoma cell line) and YAC-1 (mouse lymphoma cell line) were applied to serve as the positive controls for SSEA-4 and GM1b, respectively.

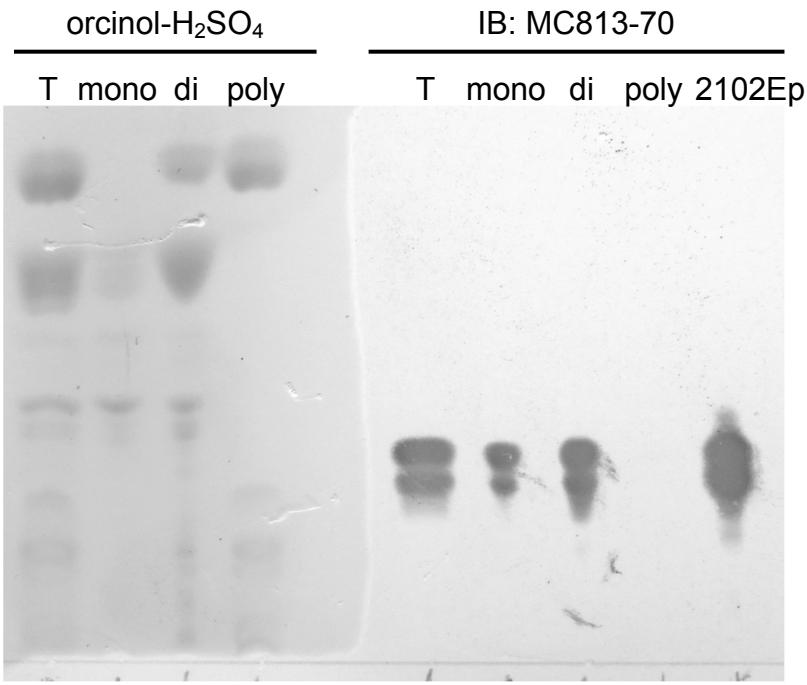

Figure 7. HPTLC profiles and MC813-70 immunostaining of gangliosides extracted from DBTRG cells. Gangliosides from DBTRG cells were bound to DEAE and eluted by 0.8 M NaCl at once (indicated as T) or fractionated into mono-, di-, and poly -sialylated gangliosides by stepwise elution with 0.02 M, 0.2 M, and 0.8 M NaCl (indicated as mono, di and poly). Gangliosides were separated on a HPTLC plate and detected by orcinol staining (left) or MC813-70 immunostaining (right). MC813-70-positive signals were detected in monosialylated gangliosides fraction. The gangliosides extracted from 2012Ep cells, which is known to express SSEA-4, was used as a positive control.

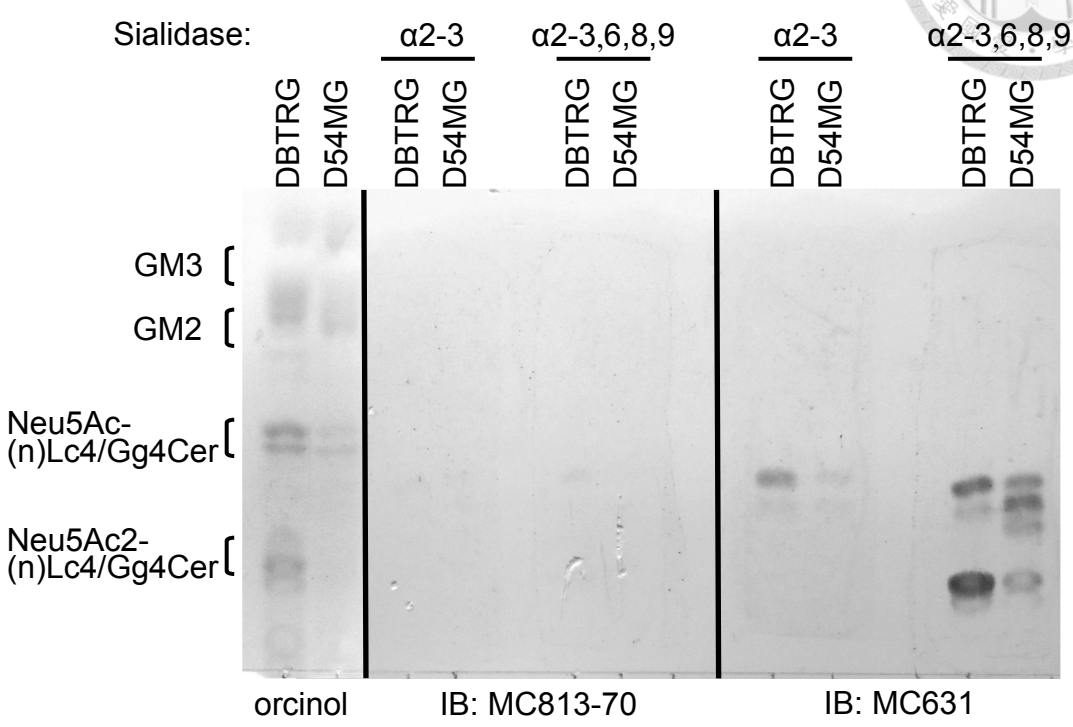

Figure 8. Desialylation of gangliosides from GBM cells affected MC813-70 and MC631 staining. Detection of on-HPTLC-desialylated gangliosides with MC813-70 mAb (middle panel) or MC631 mAb (right panel). The GBM-associated ganglioside originally recognized by MC813-70 showed MC813-70 (-) and MC631 (+) after sialidase treatment, as marked in the dashed rectangle.

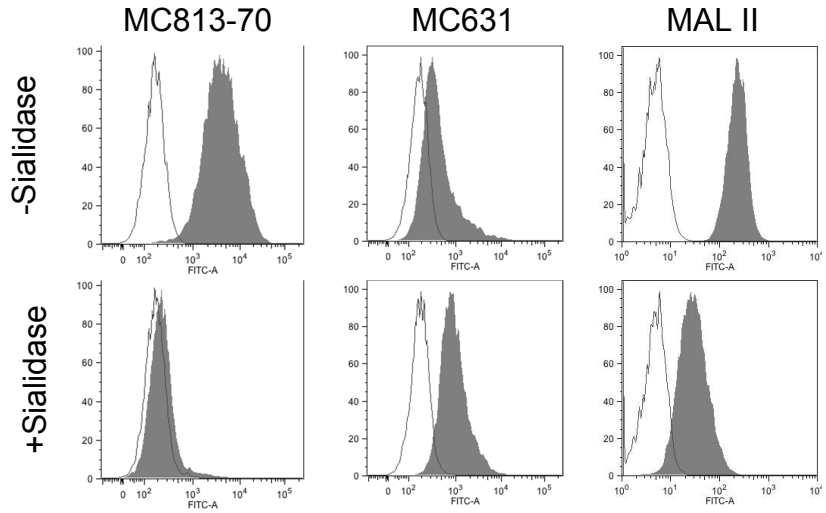

Figure 9. Desialylation of GBM cells affected MC813-70 and MC631 staining. DBTRG cells were treated with α2,3-sialidase prior to staining with MC813-70, MC631 and MAL II. Flow cytometric analysis showed that the intensity of MC631 staining increased and MC813-70 staining disappeared after sialidase treatment. The efficiency of sialidase treatment was monitored by staining with MAL II, which recognizes α2,3-linked sialic acids. The histograms of the cells stained with mAb and MAL II are shown in gray, and the histograms representing isotype control staining are shown in white.

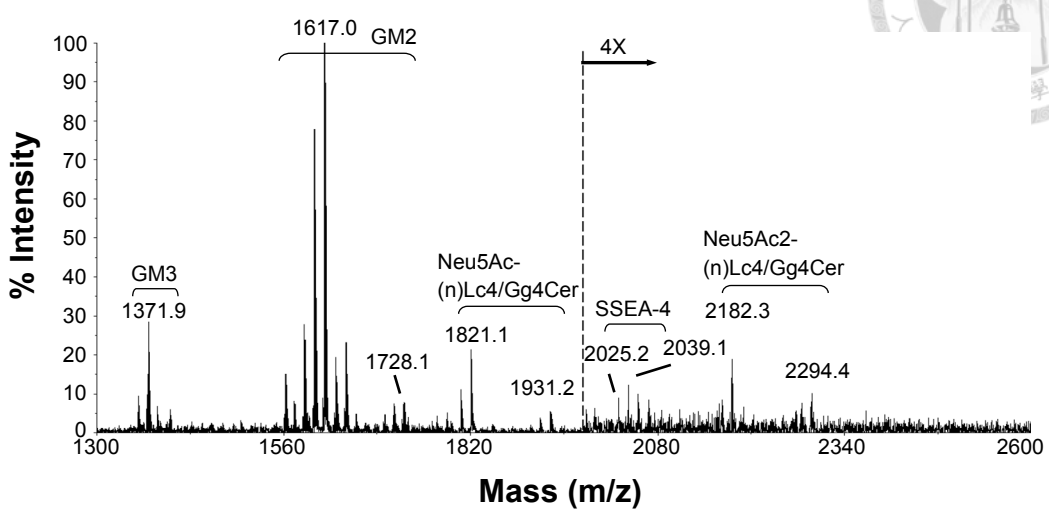

Figure 10. MALDI-MS profiles of gangliosides from GBM cell lines. The extracted gangliosides from DBTRG GBM cells were permethylated and analyzed by MALDI-MS. The major gangliosides in DBTRG cells were GM3 (*m/z* = 1371.9), GM2 (*m/z* = 1617.0), Neu5Ac-(n)Lc4/Gg4Cer (*m/z* = 1821.1), and Neu5Ac2-(n)Lc4/Gg4Cer (*m/z* = 2182.3). Although in a relatively weak signal, SSEA-4 (Neu5Ac-Hex4-HexNAc-Cer, *m/z* = 2025.2) was also observed. Gangliosides with the same glycan moiety but with different fatty acyl contents are bracketed.

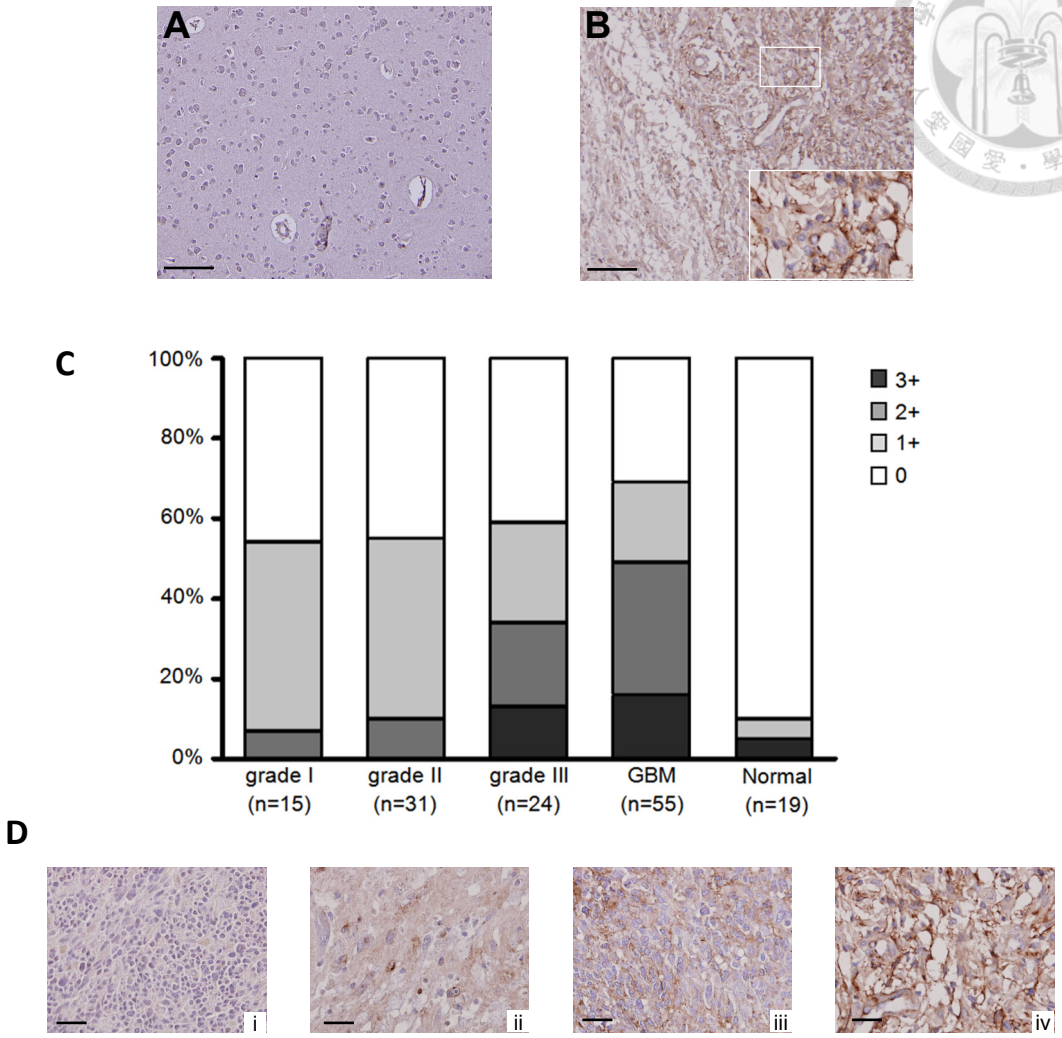

Figure 11. Expression of SSEA-4 in grade I-IV astrocytoma. (A & B) Representative images of normal brain tissues (A) and GBM (B) after immunohistochemical staining with MC-813-70. The inset in panel B shows a magnified picture of the small rectangular area. Scale bar, 100 μm. (C) Statistical results of SSEA-4 IHC. Grade I (n=15), grade II (n=31), grade III (n=24), grade IV (GBM, n=55) and normal brain tissues (n=19) were counterstained with hematoxylin after IHC. (D) The staining intensity of the tissues was graded as 0 (negative), 1+ (weak), 2+ (moderate), and 3+ (strong).

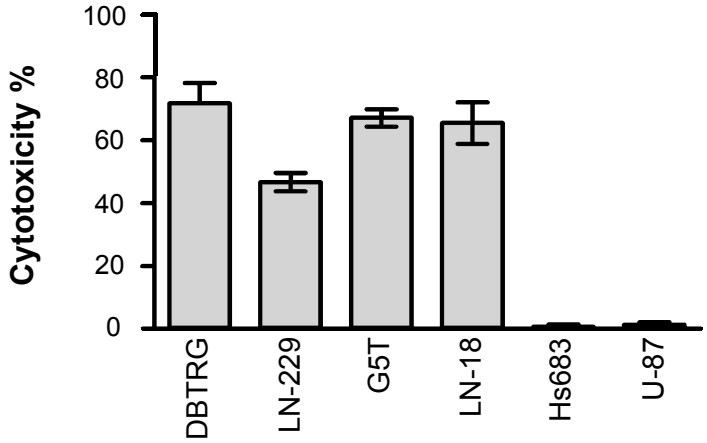

Figure 12. MC813-70 triggered CDC in GBM cells. GBM cell lines were treated with 20 μg/mL MC813-70 and rabbit complement to observe MC813-70-induced cell lysis. The CDC activity of MC813-70 was measured by lactate dehydrogenase (LDH) release assay as described in "Materials and Methods." The data are shown as mean ± SD.

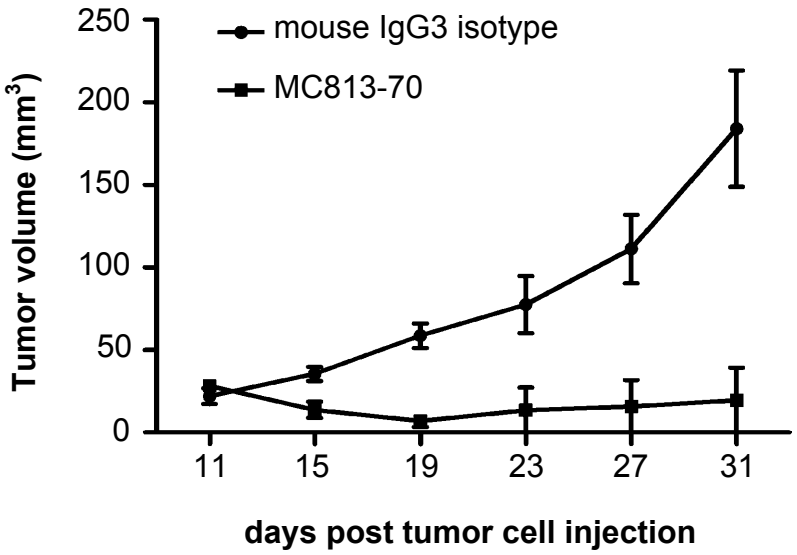

Figure 13. Inhibition of DBTRG tumor growth by MC813-70. Male nude mice were inoculated with DBTRG cells on the right flank at day 0, intraperitoneally administered with MC813-70 or mouse IgG3 isotype control (200 μg per dose) at day 11, 15, and 19, and sacrificed at day 31. The tumor volume in each group (n=3) was measured at different time points and shown as mean ± SD. *P*=0.001 was obtained by two-way ANOVA.

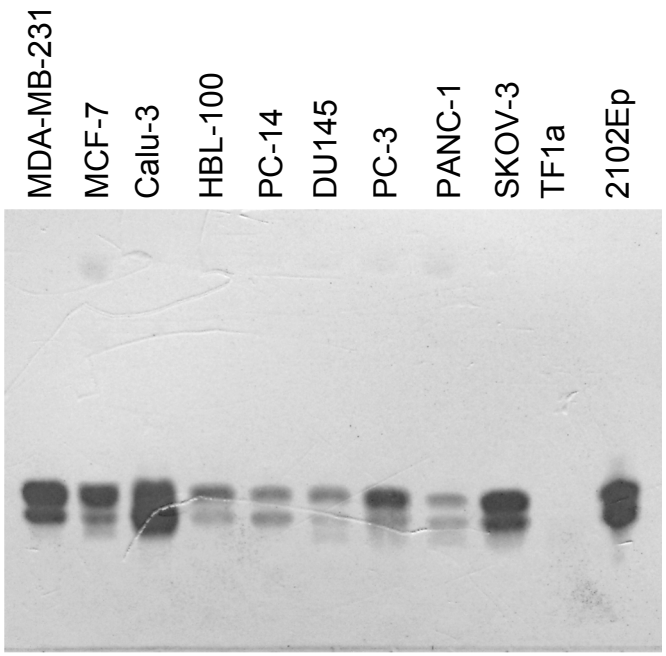

Figure 14. Immunostaining of SSEA-4 on HPTLC-separated gangliosides from cancer cells. Representative breast (MDA-MB-231, MCF-7 and HBL-100), lung (Calu-3 and PC-14), prostate (DU145 and PC-3), pancreatic (PANC-1), ovarian (SKOV-3), erythroleukemia (TF1a), and embryonal carcinoma (2012Ep) cell lines are shown.

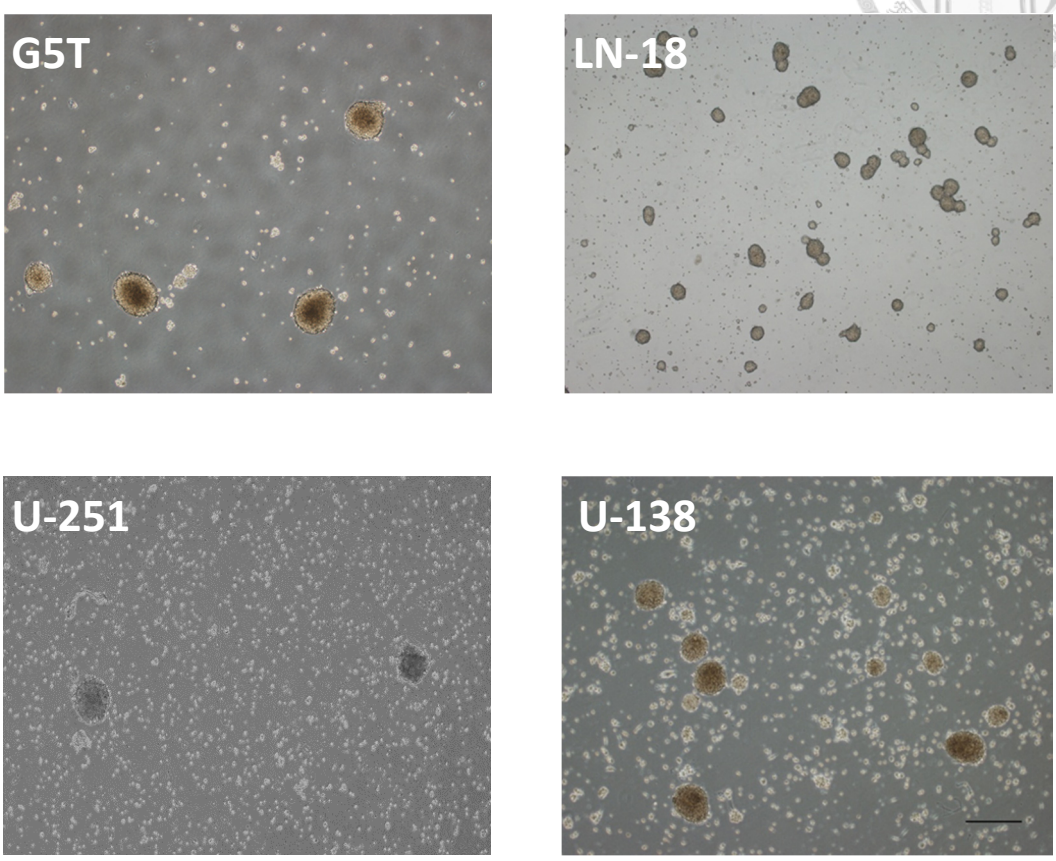

Figure 15. The morphology of neurospheres derived from GBM cancer cell lines. Representative images of GBM cells that were maintained in the neurosphere culture media after 10 days. Scale bar, 100 μm.

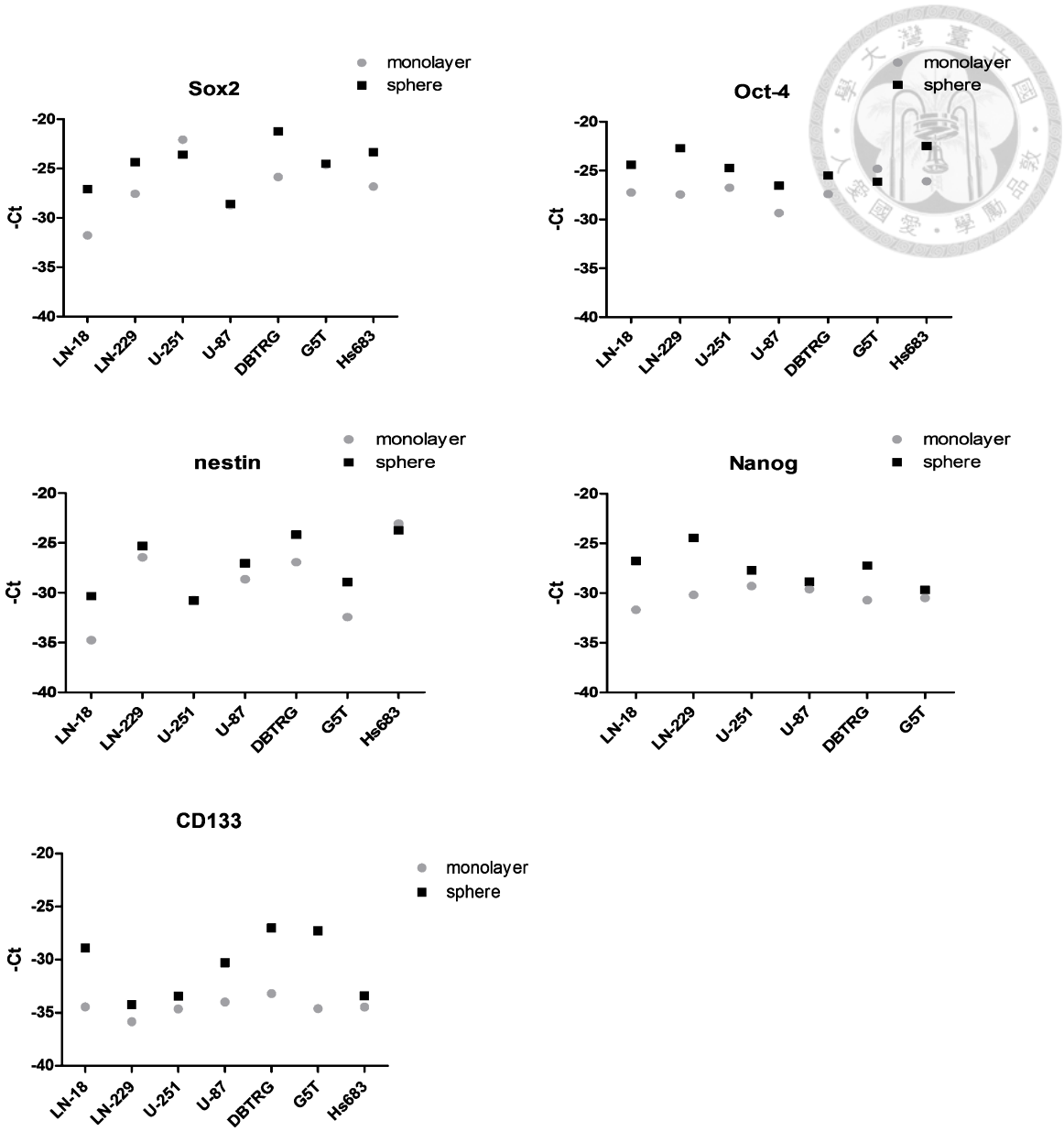

Figure 16. GBM neurosphere cells expressed higher levels of mRNA related to stemness genes . Total RNA was extracted from GBM cells as well as GBM neurosphere cells and reverse-transcribed to cDNA. The expression levels of *Sox2, Oct-4, nestin, Nanog, and CD133* were determined by real-time PCR and normalized against the expression level of *GAPDH*. The Ct value of *GAPDH* of each sample was adjusted to 15, and the normalized expression level of genes was shown as -(Ct).

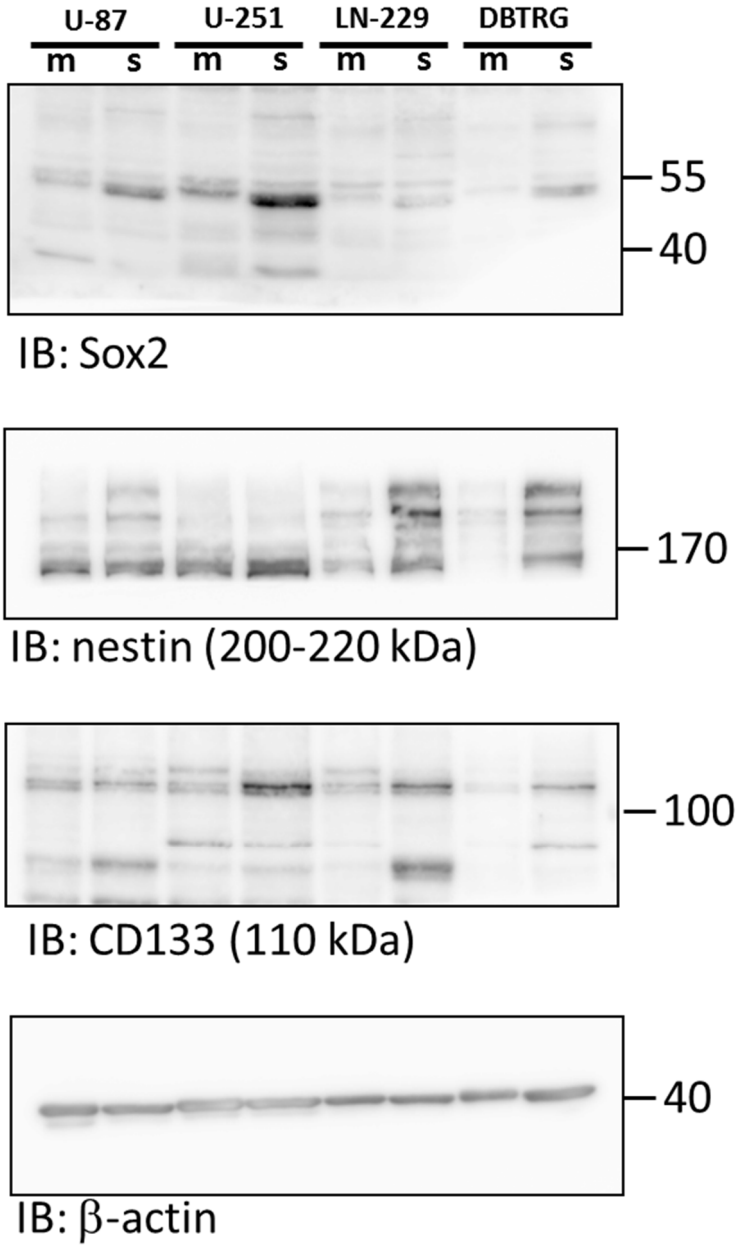

Figure 17. GBM neurosphere cells expressed higher levels of Sox2, nesitn, and CD133. Aliquots of total lysates (25 μg) were subjected to the SDS-PAGE and then immunoblotted with antibodies against Sox2, nestin, CD133, or β-actin.

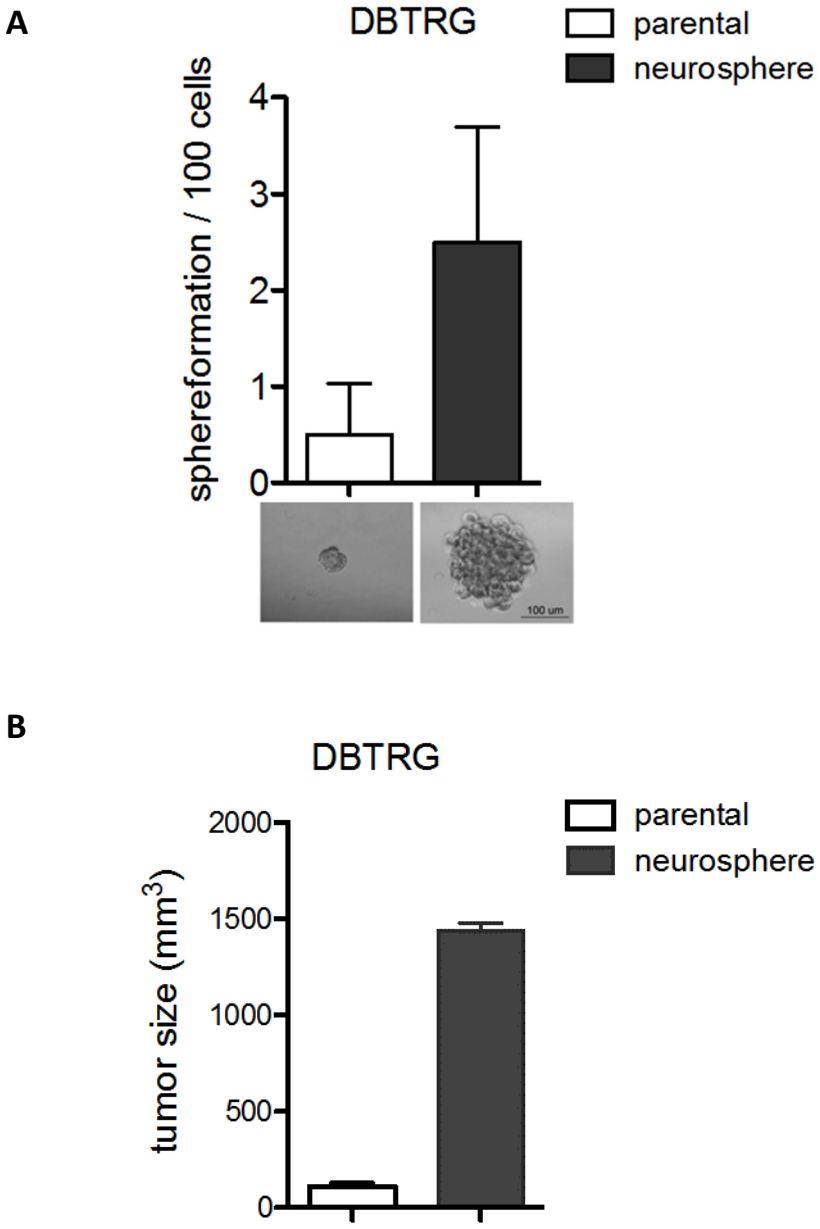

Figure 18. The cells derived from GBM neurospheres exhibited higher self-renewal potential and tumorogenicity. (A) 100 cells of DBTRG cells (parental) and DBTRG neurosphere cells were plated in 96-well plates with neurosphere culture media. After 3weeks, the number of neurospheres whose diameter is over 100 um were calculated. Representative images of neurospheres from two populations were shown. Scale bar, 100 μm. (B) 10^4 cells were injected into NOD-SCID mice subcutaneously, and the tumor volume was measured after 70 days. The data are shown as mean ± SD.

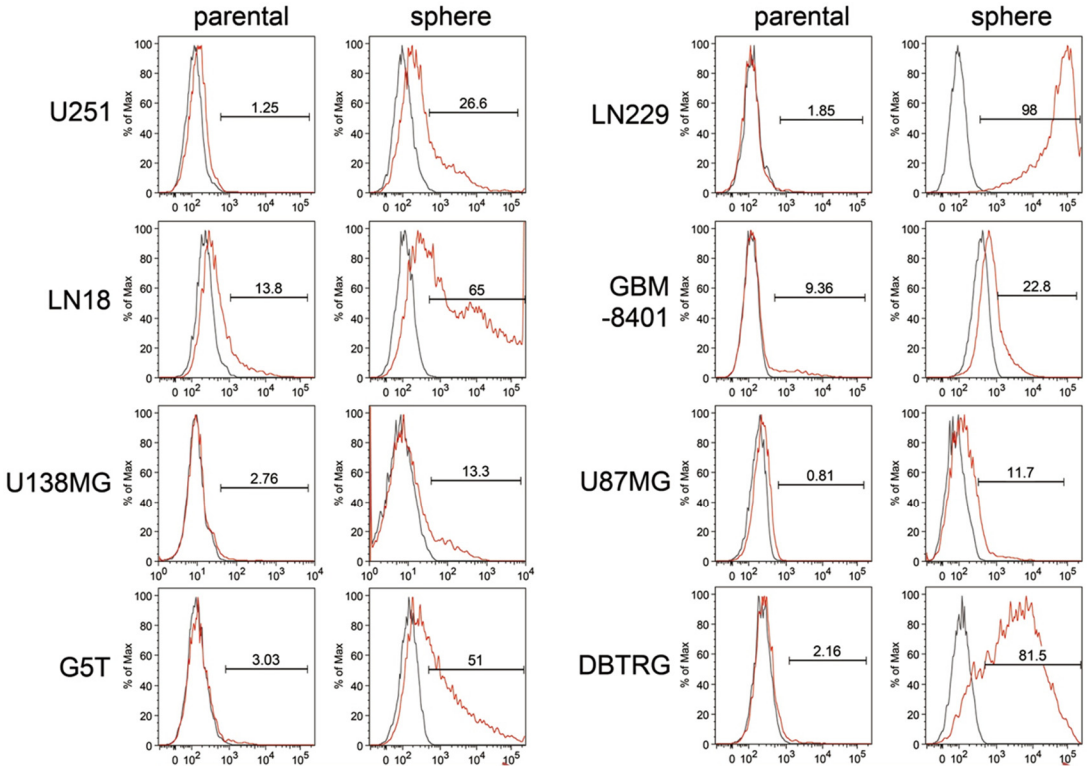

Figure 19. A higher amount of GD2 is expressed in GBM neurospheres. Cells (1×10^5) were incubated with optimal concentrations of the GD2 antibody and fluorescent-labeled secondary antibodies, and analyzed by FACSCanto flow cytometer. The histograms of the cells stained with MC813-70 and isotype control are shown in red line and grey line, respectively.

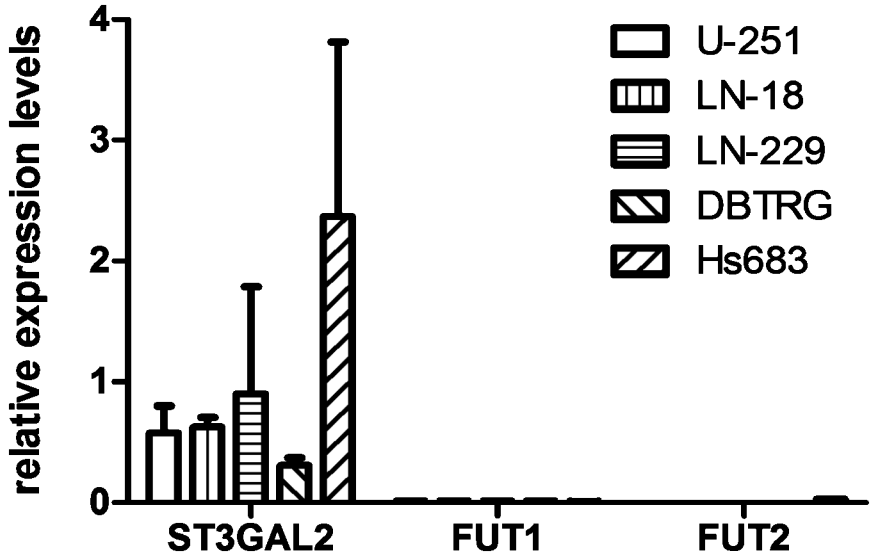

Figure 20. **Human GBM cell lines express a higher level of *ST3GAL2* than *FUT1* and *FUT2*.** Total RNA was extracted from GBM cell lines and reverse-transcribed to cDNA. The expression levels of *ST3GAL2*, *FUT1* and *FUT2* were determined by real-time PCR and normalized against the expression level of *GAPDH*.

CHAPTER 6: SUPPLEMENTARY FIGURES

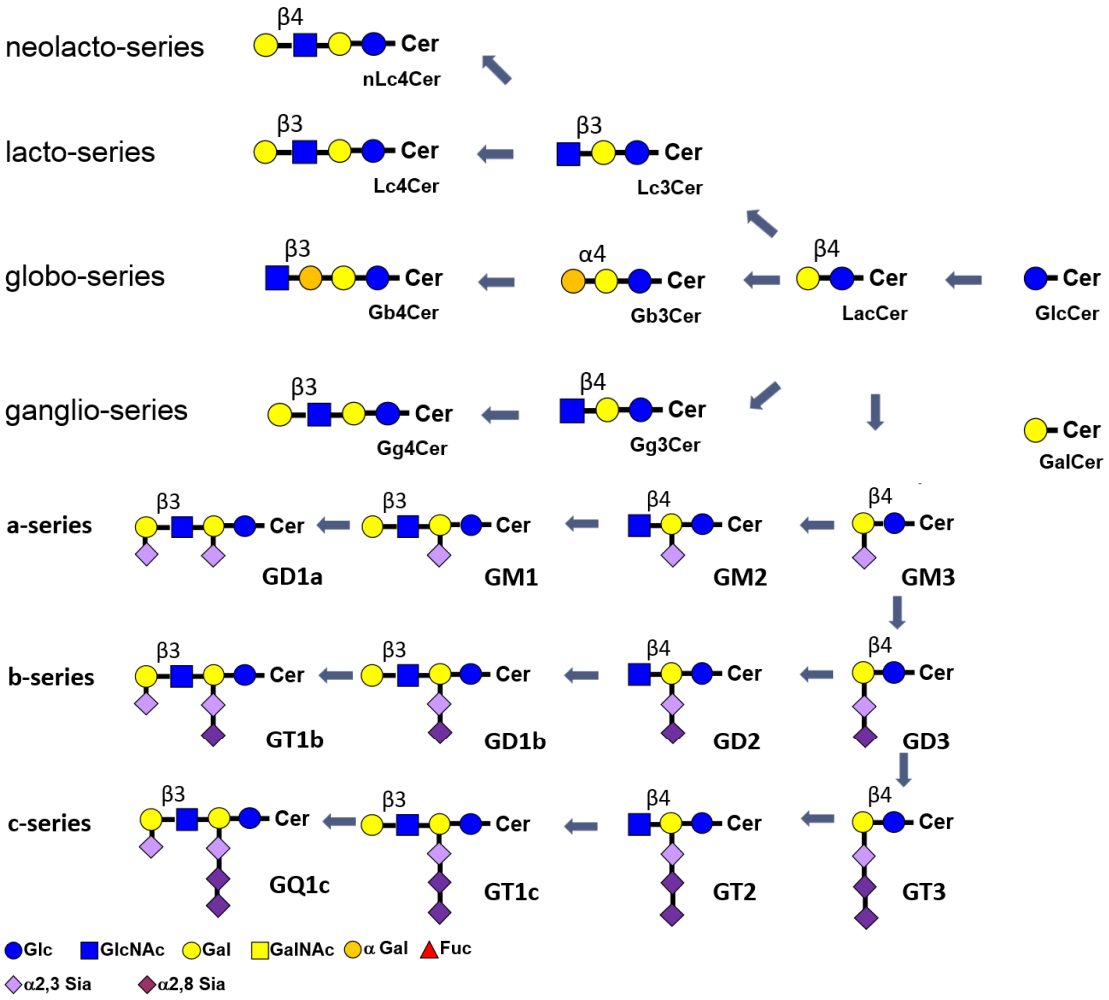

Supplementary Figure 1. Biosynthetic pathway of glycosphingolipids and gangliosides.

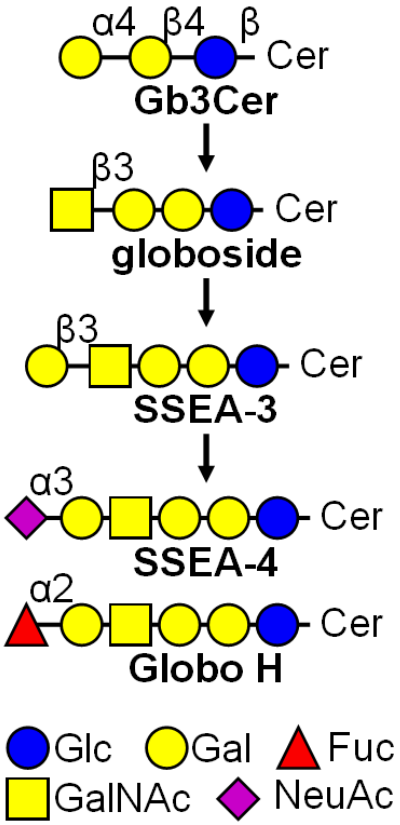

Supplementary Figure 2. Biosynthetic pathway of globo-series glycosphingolipids

CHAPTER 7: TABLES

Table 1. Forward and reverse primers of genes.

Gene name	Forward and reverse primers
SOX2	F 5’-CACATGAACGGCTGGAGCAA-3’ (20mer)
	R 5’-GGAGTGGGAGGAAGAGGTAAC-3’ (21mer)
OCT4	F 5’-GGTATTCAGCCAAACGACCATC-3’ (22mer)
	R 5’-TTCTCCAGGTTGCCTCTCACTC-3’ (22mer)
NANOG	F 5’-CGAAGAATAGCAATGGTGTGAC-3’ (22mer)
	R 5’-GGTCTGAGTGTTCCAGGAGTG-3’ (21mer)
NESTIN	F 5’-CTCCAAGACTTCCCTCAGCTTTC-3’ (23mer)
	R 5’-GGGCTCTGATCTCTGCATCTACA-3’ (23mer)
CD133	F 5’-CCTCATGGTTGGAGTTGGATT-3’ (21mer)
	R 5’-GAGTGCCGTAAGTGCCTCTA-3’ (20mer)
GAPDH	F 5’-GCTGTTGTCATACTTCTCATG-3’ (21mer)
	R 5’-TCTTCCAGGAGCGAGATCCC-3’ (20mer)

Table 2. Expression profiles of glycan-related epitopes in GBM cell lines (LN-18, U-138, U-251 and G5T).

Antigens	LN-18	U-138	U-251	G5T
TF	83.3 ± 3.4	76.1 ± 17.7	12.8 ± 11.7	5.8 ± 0.2
Tn	77.7 ± 4.3	49.9 ± 28.5	54.2 ± 18.2	20.7 ± 12.5
sTn	5.1 ± 0.3	10.9 ± 5.9	5.3 ± 0.5	4.9 ± 0.8
Le^x	6.2 ± 0.7	22.2 ± 17.7	74.2 ± 14.6	76.5 ± 10.6
Le^y	29.3 ± 9.9	46.0 ± 31.3	61.9 ± 21.8	8.8 ± 1.2
sLe^x	4.8 ± 0.5	32.8 ± 1.7	8.2 ± 5.2	5.4 ± 0.3
GM2	82.8 ± 23.9	97.2 ± 2.7	89.8 ± 14.1	38.4
GM1	98.5 ± 0.1	97.9 ± 1.6	74.6 ± 30.2	39.4
GD1a	96.9 ± 4.4	99.3 ± 1.0	88.0 ± 9.9	27.6
GD2	43.4 ± 11.6	23.4 ± 9.7	10.3 ± 4.2	15.4 ± 8.9
GT1b	97.6 ± 3.3	96.1 ± 0.9	88.8 ± 1.5	30.1 ± 7.1
A2B5	58.2 ± 41.1	59.2 ± 12.0	36.6 ± 18.0	21.1 ± 11.4
SSEA-3	75.9 ± 16.2	38.9 ± 26.0	27.1 ± 24.8	97.7 ± 3.0
SSEA-4	99.6 ± 0.2	90.5 ± 16.4	43.1 ± 10.8	99.9 ± 0.1
Globo H	22.5	11.8	9.3 ± 4.0	5.5 ± 0.1

Expression of glycan-related epitopes was determined by flow cytometry as described in Materials and Methods. Values are mean ± SD % of positive cells in total cells.

Table 3. Expression of globo-series GSLs on cancer cell lines.

Tumor origin	SSEA-4+	SSEA-3+	Globo H+	SSEA4+ or SSEA3+ or Globo H+	SSEA-4+ SSEA-3+	SSEA-4+ Globo H+	SSEA-4+ SSEA-3+ Globo H+
Brain	12/17	9/17	6/17	12/17	9/17	6/17	5/17
Lung	13/20	5/20	13/20	16/20	5/20	10/20	5/20
Breast	17/23	6/23	14/23	18/23	6/23	13/23	6/23
Mouth	8/13	2/13	11/13	12/13	2/13	7/13	2/13
Esophagus	1/2	0/2	2/2	2/2	0/2	1/2	0/2
Stomach	4/6	3/6	6/6	6/6	3/6	4/6	3/6
Liver	6/10	4/10	9/10	9/10	4/10	6/10	4/10
Bile duct	2/5	1/5	3/5	3/5	1/5	2/5	1/5
Pancreas	8/8	3/8	6/8	8/8	3/8	6/8	3/8
Colon	5/7	0/7	6/7	7/7	0/7	4/7	0/7
Kidney	5/6	0/6	5/6	6/6	0/6	4/6	0/6
Cervix	3/4	2/4	1/4	3/4	2/4	1/4	0/4
Ovary	8/9	2/9	5/9	8/9	2/9	5/9	2/9
Prostate	4/4	1/4	1/4	4/4	1/4	1/4	0/4

Expression of globo-series GSLs was determined by flow cytometry. Those cell lines in which over 15% of total cells are positive in flow cytometry are labelled positive.

Table 4. Flow cytometry analysis of expression of globo-series GSLs on various cancer cell lines

Brain cancer

Cell line	Antigen	Cell line	Antigen	Cell line	Antigen
A172		D54MG	3,4,H	DBTRG	4
G5T	3,4	G9T	3,4,H	GBM 8401	
GBM 8901		Hs683	4	LN-18	3,4,H
LN-229	3,4,H	SF126	4,H	SNB75	3,4
T95G		U-138 MG	3,4	U-251 MG	3,4
U-373 MG	3,4,H	U-87 MG			

Lung cancer

Cell line	Antigen	Cell line	Antigen	Cell line	Antigen
A549	4,H	Calu-3	4	CL1	4
CL1-0	4,H	CL1-5	4,H	CL2	H
CL3		H1299		H1355	4,H
H157	3,4,H	H441	4,H	H460	
H480	3,4,H	H520	H	H661	3,4,H
H928	3,4,H	NuLi-1	3,4,H	PC-13	H
PC-14		PC-9	4		

Breast cancer

Cell line	Antigen	Cell line	Antigen	Cell line	Antigen
Au565		BT-20		BT-474	
BT-483		BT-549	4	DU4475	4,H
HBL-100	4,H	HBL-435		HCC1395	3,4,H
HCC1599	4,H	HCC1806	3,4,H	HCC1937	4
HCC38	4,H	Hs578T	3,4,H	MCF-7	3,4,H
MDA-MB-157	3,4,H	MDA-MB-231	3,4,H	MDA-MB-361	4,H
MDA-MB-453	4,H	MDA-MB-468	4	SK-BR-3	H
T47D	3,4,H	ZR75	4,H		

Oral cancer

Cell line	Antigen	Cell line	Antigen	Cell line	Antigen
Ca922	4,H	Cal27	4,H	HSC3	4,H
OC3	H	OECM1	H	SAS	H
SCC25	4	SCC4	3,4,H	Tu-183	H
Tw1.5	4,H	Tw2.6	4,H	UMSCC-1	3,4,H
YD-15	3,4,H				

Esophageal cancer

Cell line	Antigen	Cell line	Antigen
CE81T	H	KYSE70	4,H

Gastric cancer

Cell line	Antigen	Cell line	Antigen	Cell line	Antigen
AGS	H	AZ521	3,4,H	KATO III	3,4,H
NCI-N87	H	SCM-1	3,4,H	SNU-1	4,H

Liver cancer

Cell line	Antigen	Cell line	Antigen	Cell line	Antigen
59T	3,4,H	Changliver	H	HA22T	H
Hep3b	3,4,H	HepG2	4,H	Huh-7	4,H
J5	H	Mahlavu		NTU-BL	3,4,H
SK-HEP-1	3,4,H				

Bile duct cancer

Cell line	Antigen	Cell line	Antigen	Cell line	Antigen
HuccT1	3,4,H	SNU-1079		SNU-1196	H
SNU-245	4,H	SNU-308			

Pancreatic cancer

Cell line	Antigen	Cell line	Antigen	Cell line	Antigen
AsPC1	4	BxPC3	4,H	HPAC	4,H
KP-4	3,4,H	MIA PaCa-2	3,4,H	Panc0203	4,H
PANC1	4	PL45	3,4,H		

Colon cancer

Cell line	Antigen	Cell line	Antigen	Cell line	Antigen
CX-1	4,H	DLD-1	H	H3347	4,H
HCT1116	4	HT-29	H	SW480	4,H
SW620	4,H				

Renal cancer

Cell line	Antigen	Cell line	Antigen	Cell line	Antigen
769-P	3,4,H	A498	4	A704	H
ACHN	3,4,H	Caki-1	3,4,H	Caki-2	3,4,H

Cervical cancer

Cell line	Antigen	Cell line	Antigen	Cell line	Antigen
Hela	3,4	Hela 229	3,4	Hela S3	
ME-180	4,H				

Ovarian cancer

Cell line	Antigen	Cell line	Antigen	Cell line	Antigen
C33A	4	CAOV3	4	ES-2	4,H
NUGCC	3,4,H	OVCAR-3	4,H	SiHa	
SKOV3	4	TOV-112D	4,H	TOV-21G	3,4,H

Prostate cancer

Cell line	Antigen	Cell line	Antigen	Cell line	Antigen
22Rr1	4,H	Du145	4	hTERT-HPNE	3,4
PC-3	4				

Antigen: 3 = SSEA-3; 4 = SSEA-4; H = Globo H.

Table 5. Expression patterns of surface glycans on GBM and GBM neurosphere cells.

		LN-18		U-138		U-251		G5T	
	antibody	parental	sphere	parental	sphere	parental	sphere	parental	sphere
Ganglio-series	GM3	38.4 ± 1.2	11.8 ± 2.3	38.2 ± 17.8	5.3 ± 5.0	1.3 ± 6.8	5.6 ± 6.8	0.8 ± 0.1	1.2 ± 0.4
	GM2	68.2 ± 33.7	72.7 ± 23.6	76.3 ± 1.5	72.9 ± 22.1	84.2 ± 9.8	81.7 ± 9.8	7.5 ± 10.1	19.2 ± 26.6
	GM1	70.8 ± 8.7	61.5 ± 5.4	72.9 ± 15.1	71.7 ± 30.5	69.9 ± 23.8	58.4 ± 23.8	2.9 ± 3.5	14.5 ± 20.1
	GD1a	76.4 ± 24.8	94.8 ± 7.1	49.5 ± 69.0	50.2 ± 69.3	88.4 ± 3.3	90.8 ± 3.3	14.2	57.2
	GD2	18.7 ± 12.4	59.3 ± 3.3	7.5 ± 2.5	8.9 ± 2.6	5.4 ± 18.7	66.5 ± 18.7	7.6 ± 6.4	51.9 ± 1.6
	GT1b	77.0 ± 29.2	89.6 ± 1.4	48.4 ± 23.5	30.2 ± 8.3	59.6 ± 25.6	72.8 ± 25.6	4.0 ± 3.0	9.0 ± 3.8
	A2B5	19.9 ± 19.9	46.9 ± 14.8	8.3 ± 2.9	32.0 ± 18.9	23.3 ± 18.0	13.4 ± 18.0	5.5 ± 4.1	6.8 ± 1.7
Lewis antigen	LeX	6.3 ± 5.2	0.7 ± 0.0	3.1 ± 1.9	2.5 ± 1.1	71.0 ± 18.7	69.2 ± 18.7	44.4 ± 14.3	53.7 ± 4.9
	sLeX	5.6 ± 4.0	0.8 ± 0.2	4.3 ± 2.1	1.4 ± 0.2	19.4 ± 1.2	0.1 ± 1.2	0.8 ± 0.2	1.3 ± 0.6
	LeY	18.0 ± 2.3	7.9 ± 1.5	12.8 ± 8.0	45.6 ± 22.9	64.7 ± 2.9	91.0 ± 2.9	2.0 ± 0.5	22.6 ± 4.0
Globo-series	SSEA3	40.0 ± 14.2	6.5 ± 3.0	12.4 ± 8.7	0.9 ± 0.2	12.7 ± 8.4	5.9 ± 8.4	91.7 ± 9.0	56.5 ± 2.4
	SSEA4	98.2 ± 1.8	15.9 ± 4.8	82.8 ± 28.0	4.2 ± 1.8	43.1 ± 10.8	10.6 ± 10.8	99.8 ± 0.1	99.2 ± 0.1
	Globo H	5.29	0.45	1.2	0.3	4.5 ± 1.7	1.4 ± 1.7	0.8 ± 0.2	1.5 ± 0.7
O-glycan	TF	66.3 ± 7.8	10.5 ± 7.9	30.5 ± 20.1	18.4 ± 12.5	12.8 ± 28.4	46.3 ± 28.4	0.7 ± 0.2	12.0 ± 4.4
	Tn	6.7 ± 1.6	12.6 ± 1.3	2.3 ± 2.2	12.6 ± 10.3	42.1 ± 8.8	15.4 ± 8.8	2.1 ± 1.9	5.5 ± 1.6
	sTn	0.5 ± 0.4	0.6 ± 02	0.6 ± 0.3	0.6 ± 0.1	0.9 ± 0.9	0.1 ± 0.9	0.4 ± 0.2	0.3 ± 0.4
Glycoprotein	CD44	100 ± 0.0	99.1 ± 0.6	99.1 ± 0.6	99.8 ± 0.3	94.8 ± 0.2	94.9 ± 0.2	100.0 ± 0.1	99.8 ± 0.3
	CD24	21.0 ± 0.7	4.5 ± 2.0	3.0 ± 0.3	2.5 ± 0.6	3.8 ± 1.2	0.9 ± 1.2	99.9 ± 0.1	3.2 ± 2.3
	CD45	0.2 ± 0.0	0.4 ± 0.0	0.4 ± 0.2	0.4 ± 0.2	0.3 ± 0.8	0.1 ± 0.8	0.4 ± 0.1	0.3 ± 0.1
	CD90	94.3 ± 5.3	84.3 ± 0.6	90.0 ± 13.4	36.4 ± 8.8	94.8 ± 0.4	94.9 ± 0.4	98.1 ± 0.8	44.2 ± 18.7
	CD133/1	5.43	1.35	2.6 ± 1.1	1.4 ± 0.2	0.1 ± 0.4	0.8 ± 0.4	1.7 ± 1.3	1.9 ± 0.5
	CD133/2	3.3	1.47	2.9 ± 1.0	3.1 ± 1.3	N.D.	N.D.	1.8 ± 0.9	2.1 ± 1.4

Expression of glycan-related epitopes was determined by flow cytometry as described in Materials and Methods. Values are mean ± SD % of positive cells in total cells. N.D. stands for Not Detected.

CHAPTER 8: REFERENCES

1. Jemal, A., F. Bray, M.M. Center, J. Ferlay, E. Ward, and D. Forman, *Global cancer statistics.* CA Cancer J Clin, 2011. **61**(2): p. 69-90.
2. Louis, D.N., H. Ohgaki, O.D. Wiestler, W.K. Cavenee, P.C. Burger, A. Jouvet, B.W. Scheithauer, and P. Kleihues, *The 2007 WHO classification of tumours of the central nervous system.* Acta Neuropathol, 2007. **114**(2): p. 97-109.
3. Ohgaki, H. and P. Kleihues, *Genetic pathways to primary and secondary glioblastoma.* Am J Pathol, 2007. **170**(5): p. 1445-53.
4. Furnari, F.B., T. Fenton, R.M. Bachoo, A. Mukasa, J.M. Stommel, A. Stegh, W.C. Hahn, K.L. Ligon, D.N. Louis, C. Brennan, L. Chin, R.A. DePinho, and W.K. Cavenee, *Malignant astrocytic glioma: genetics, biology, and paths to treatment.* Genes Dev, 2007. **21**(21): p. 2683-710.
5. Watanabe, K., O. Tachibana, K. Sata, Y. Yonekawa, P. Kleihues, and H. Ohgaki, *Overexpression of the EGF receptor and p53 mutations are mutually exclusive in the evolution of primary and secondary glioblastomas.* Brain Pathol, 1996. **6**(3): p. 217-23; discussion 23-4.
6. Rasheed, B.K., R.E. McLendon, H.S. Friedman, A.H. Friedman, H.E. Fuchs, D.D. Bigner, and S.H. Bigner, *Chromosome 10 deletion mapping in human gliomas: a common deletion region in 10q25.* Oncogene, 1995. **10**(11): p. 2243-6.
7. Ohgaki, H., P. Dessen, B. Jourde, S. Horstmann, T. Nishikawa, P.L. Di Patre, C. Burkhard, D. Schuler, N.M. Probst-Hensch, P.C. Maiorka, N. Baeza, P. Pisani, Y. Yonekawa, M.G. Yasargil, U.M. Lutolf, and P. Kleihues, *Genetic pathways to glioblastoma: a population-based study.* Cancer Res, 2004. **64**(19): p. 6892-9.
8. Biernat, W., Y. Tohma, Y. Yonekawa, P. Kleihues, and H. Ohgaki, *Alterations of cell cycle regulatory genes in primary (de novo) and secondary glioblastomas.* Acta Neuropathol, 1997. **94**(4): p. 303-9.
9. Nakamura, M., T. Watanabe, U. Klangby, C. Asker, K. Wiman, Y. Yonekawa, P.

Kleihues, and H. Ohgaki, *p14ARF deletion and methylation in genetic pathways to glioblastomas.* Brain Pathol, 2001. **11**(2): p. 159-68.

10. Hermanson, M., K. Funa, M. Hartman, L. Claesson-Welsh, C.H. Heldin, B. Westermark, and M. Nister, *Platelet-derived growth factor and its receptors in human glioma tissue: expression of messenger RNA and protein suggests the presence of autocrine and paracrine loops.* Cancer Res, 1992. **52**(11): p. 3213-9.
11. Fujisawa, H., R.M. Reis, M. Nakamura, S. Colella, Y. Yonekawa, P. Kleihues, and H. Ohgaki, *Loss of heterozygosity on chromosome 10 is more extensive in primary (de novo) than in secondary glioblastomas.* Lab Invest, 2000. **80**(1): p. 65-72.
12. Yan, H., D.W. Parsons, G. Jin, R. McLendon, B.A. Rasheed, W. Yuan, I. Kos, I. Batinic-Haberle, S. Jones, G.J. Riggins, H. Friedman, A. Friedman, D. Reardon, J. Herndon, K.W. Kinzler, V.E. Velculescu, B. Vogelstein, and D.D. Bigner, *IDH1 and IDH2 mutations in gliomas.* N Engl J Med, 2009. **360**(8): p. 765-73.
13. Parsons, D.W., S. Jones, X. Zhang, J.C. Lin, R.J. Leary, P. Angenendt, P. Mankoo, H. Carter, I.M. Siu, G.L. Gallia, A. Olivi, R. McLendon, B.A. Rasheed, S. Keir, T. Nikolskaya, Y. Nikolsky, D.A. Busam, H. Tekleab, L.A. Diaz, Jr., J. Hartigan, D.R. Smith, R.L. Strausberg, S.K. Marie, S.M. Shinjo, H. Yan, G.J. Riggins, D.D. Bigner, R. Karchin, N. Papadopoulos, G. Parmigiani, B. Vogelstein, V.E. Velculescu, and K.W. Kinzler, *An integrated genomic analysis of human glioblastoma multiforme.* Science, 2008. **321**(5897): p. 1807-12.
14. Ohgaki, H., *Genetic pathways to glioblastomas.* Neuropathology, 2005. **25**(1): p. 1-7.
15. Ostrom, Q.T., H. Gittleman, P. Farah, A. Ondracek, Y. Chen, Y. Wolinsky, N.E. Stroup, C. Kruchko, and J.S. Barnholtz-Sloan, *CBTRUS Statistical Report: Primary Brain and Central Nervous System Tumors Diagnosed in the United States in 2006-2010.* Neuro Oncol, 2013. **15**(suppl 2): p. ii1-ii56.

16. Fisher, J.L., J.A. Schwartzbaum, M. Wrensch, and J.L. Wiemels, *Epidemiology of brain tumors.* Neurol Clin, 2007. **25**(4): p. 867-90, vii.

17. Inskip, P.D., R.E. Tarone, E.E. Hatch, T.C. Wilcosky, W.R. Shapiro, R.G. Selker, H.A. Fine, P.M. Black, J.S. Loeffler, and M.S. Linet, *Cellular-telephone use and brain tumors.* N Engl J Med, 2001. **344**(2): p. 79-86.

18. Lahkola, A., A. Auvinen, J. Raitanen, M.J. Schoemaker, H.C. Christensen, M. Feychting, C. Johansen, L. Klaeboe, S. Lonn, A.J. Swerdlow, T. Tynes, and T. Salminen, *Mobile phone use and risk of glioma in 5 North European countries.* Int J Cancer, 2007. **120**(8): p. 1769-75.

19. Lacroix, M., D. Abi-Said, D.R. Fourney, Z.L. Gokaslan, W. Shi, F. DeMonte, F.F. Lang, I.E. McCutcheon, S.J. Hassenbusch, E. Holland, K. Hess, C. Michael, D. Miller, and R. Sawaya, *A multivariate analysis of 416 patients with glioblastoma multiforme: prognosis, extent of resection, and survival.* J Neurosurg, 2001. **95**(2): p. 190-8.

20. Walker, M.D., E. Alexander, Jr., W.E. Hunt, C.S. MacCarty, M.S. Mahaley, Jr., J. Mealey, Jr., H.A. Norrell, G. Owens, J. Ransohoff, C.B. Wilson, E.A. Gehan, and T.A. Strike, *Evaluation of BCNU and/or radiotherapy in the treatment of anaplastic gliomas. A cooperative clinical trial.* J Neurosurg, 1978. **49**(3): p. 333-43.

21. Stupp, R., W.P. Mason, M.J. van den Bent, M. Weller, B. Fisher, M.J. Taphoorn, K. Belanger, A.A. Brandes, C. Marosi, U. Bogdahn, J. Curschmann, R.C. Janzer, S.K. Ludwin, T. Gorlia, A. Allgeier, D. Lacombe, J.G. Cairncross, E. Eisenhauer, and R.O. Mirimanoff, *Radiotherapy plus concomitant and adjuvant temozolomide for glioblastoma.* N Engl J Med, 2005. **352**(10): p. 987-96.

22. Hegi, M.E., A.C. Diserens, T. Gorlia, M.F. Hamou, N. de Tribolet, M. Weller, J.M. Kros, J.A. Hainfellner, W. Mason, L. Mariani, J.E. Bromberg, P. Hau, R.O.

Mirimanoff, J.G. Cairncross, R.C. Janzer, and R. Stupp, *MGMT gene silencing and benefit from temozolomide in glioblastoma.* N Engl J Med, 2005. **352**(10): p. 997-1003.

23. Van Meir, E.G., C.G. Hadjipanayis, A.D. Norden, H.K. Shu, P.Y. Wen, and J.J. Olson, *Exciting new advances in neuro-oncology: the avenue to a cure for malignant glioma.* CA Cancer J Clin, 2010. **60**(3): p. 166-93.
24. Krex, D., B. Klink, C. Hartmann, A. von Deimling, T. Pietsch, M. Simon, M. Sabel, J.P. Steinbach, O. Heese, G. Reifenberger, M. Weller, and G. Schackert, *Long-term survival with glioblastoma multiforme.* Brain, 2007. **130**(Pt 10): p. 2596-606.
25. Schachter, H., *The joys of HexNAc. The synthesis and function of N- and O-glycan branches.* Glycoconj J, 2000. **17**(7-9): p. 465-83.
26. Yan, A. and W.J. Lennarz, *Unraveling the mechanism of protein N-glycosylation.* J Biol Chem, 2005. **280**(5): p. 3121-4.
27. Esko, J.D. and S.B. Selleck, *Order out of chaos: assembly of ligand binding sites in heparan sulfate.* Annu Rev Biochem, 2002. **71**: p. 435-71.
28. Maccioni, H.J., C.G. Giraudo, and J.L. Daniotti, *Understanding the stepwise synthesis of glycolipids.* Neurochem Res, 2002. **27**(7-8): p. 629-36.
29. Kinoshita, T., K. Ohishi, and J. Takeda, *GPI-anchor synthesis in mammalian cells: genes, their products, and a deficiency.* J Biochem, 1997. **122**(2): p. 251-7.
30. Comelli, E.M., S.R. Head, T. Gilmartin, T. Whisenant, S.M. Haslam, S.J. North, N.K. Wong, T. Kudo, H. Narimatsu, J.D. Esko, K. Drickamer, A. Dell, and J.C. Paulson, *A focused microarray approach to functional glycomics: transcriptional regulation of the glycome.* Glycobiology, 2006. **16**(2): p. 117-31.
31. Parodi, A.J., *Role of N-oligosaccharide endoplasmic reticulum processing reactions in glycoprotein folding and degradation.* Biochem J, 2000. **348 Pt 1**: p.

1-13.

32. Ornitz, D.M. and P. Leder, *Ligand specificity and heparin dependence of fibroblast growth factor receptors 1 and 3.* J Biol Chem, 1992. **267**(23): p. 16305-11.

33. Miljan, E.A. and E.G. Bremer, *Regulation of growth factor receptors by gangliosides.* Sci STKE, 2002. **2002**(160): p. re15.

34. Park, E.I., Y. Mi, C. Unverzagt, H.J. Gabius, and J.U. Baenziger, *The asialoglycoprotein receptor clears glycoconjugates terminating with sialic acid alpha 2,6GalNAc.* Proc Natl Acad Sci U S A, 2005. **102**(47): p. 17125-9.

35. Lowe, J.B., *Glycan-dependent leukocyte adhesion and recruitment in inflammation.* Curr Opin Cell Biol, 2003. **15**(5): p. 531-8.

36. Partridge, E.A., C. Le Roy, G.M. Di Guglielmo, J. Pawling, P. Cheung, M. Granovsky, I.R. Nabi, J.L. Wrana, and J.W. Dennis, *Regulation of cytokine receptors by Golgi N-glycan processing and endocytosis.* Science, 2004. **306**(5693): p. 120-4.

37. Kolesnick, R., *The therapeutic potential of modulating the ceramide/sphingomyelin pathway.* J Clin Invest, 2002. **110**(1): p. 3-8.

38. Muse, E.D., H. Jurevics, A.D. Toews, G.K. Matsushima, and P. Morell, *Parameters related to lipid metabolism as markers of myelination in mouse brain.* J Neurochem, 2001. **76**(1): p. 77-86.

39. Holleran, W.M., Y. Takagi, G.K. Menon, G. Legler, K.R. Feingold, and P.M. Elias, *Processing of epidermal glucosylceramides is required for optimal mammalian cutaneous permeability barrier function.* J Clin Invest, 1993. **91**(4): p. 1656-64.

40. Togayachi, A., T. Akashima, R. Ookubo, T. Kudo, S. Nishihara, H. Iwasaki, A. Natsume, H. Mio, J. Inokuchi, T. Irimura, K. Sasaki, and H. Narimatsu, *Molecular cloning and characterization of UDP-GlcNAc:lactosylceramide beta*

1,3-N-acetylglucosaminyltransferase (beta 3Gn-T5), an essential enzyme for the expression of HNK-1 and Lewis X epitopes on glycolipids. J Biol Chem, 2001. **276**(25): p. 22032-40.

41. Henion, T.R., D. Zhou, D.P. Wolfer, F.B. Jungalwala, and T. Hennet, *Cloning of a mouse beta 1,3 N-acetylglucosaminyltransferase GlcNAc(beta 1,3)Gal(beta 1,4)Glc-ceramide synthase gene encoding the key regulator of lacto-series glycolipid biosynthesis.* J Biol Chem, 2001. **276**(32): p. 30261-9.
42. Hakomori, S. and Y. Igarashi, *Gangliosides and glycosphingolipids as modulators of cell growth, adhesion, and transmembrane signaling.* Adv Lipid Res, 1993. **25**: p. 147-62.
43. Chester, M.A., *IUPAC-IUB Joint Commission on Biochemical Nomenclature (JCBN). Nomenclature of glycolipids--recommendations 1997.* Eur J Biochem, 1998. **257**(2): p. 293-8.
44. Stryer, L., *Biochemistry*1975, San Francisco: W. H. Freeman. xii, 877 p.
45. Stults, C.L. and B.A. Macher, *Beta 1-3-N-acetylglucosaminyltransferase in human leukocytes: properties and role in regulating neolacto glycosphingolipid biosynthesis.* Arch Biochem Biophys, 1993. **303**(1): p. 125-33.
46. Kundu, S.K., A. Suzuki, B. Sabo, J. McCreary, E. Niver, R. Harman, and D.M. Marcus, *Erythrocyte glycosphingolipids of four siblings with the rare blood group p phenotype and their parents.* J Immunogenet, 1981. **8**(5): p. 357-65.
47. Keusch, J.J., S.M. Manzella, K.A. Nyame, R.D. Cummings, and J.U. Baenziger, *Cloning of Gb3 synthase, the key enzyme in globo-series glycosphingolipid synthesis, predicts a family of alpha 1, 4-glycosyltransferases conserved in plants, insects, and mammals.* J Biol Chem, 2000. **275**(33): p. 25315-21.
48. Marcus, D.M., M. Naiki, and S.K. Kundu, *Abnormalities in the glycosphingolipid content of human Pk and p erythrocytes.* Proc Natl Acad Sci U S A, 1976. **73**(9): p.

3263-7.

49. Suchanowska, A., R. Kaczmarek, M. Duk, J. Lukasiewicz, D. Smolarek, E. Majorczyk, E. Jaskiewicz, A. Laskowska, K. Wasniowska, M. Grodecka, E. Lisowska, and M. Czerwinski, *A single point mutation in the gene encoding Gb3/CD77 synthase causes a rare inherited polyagglutination syndrome.* J Biol Chem, 2012. **287**(45): p. 38220-30.

50. Okajima, T., Y. Nakamura, M. Uchikawa, D.B. Haslam, S.I. Numata, K. Furukawa, and T. Urano, *Expression cloning of human globoside synthase cDNAs. Identification of beta 3Gal-T3 as UDP-N-acetylgalactosamine:globotriaosylceramide beta 1,3-N-acetylgalactosaminyltransferase.* J Biol Chem, 2000. **275**(51): p. 40498-503.

51. Mangeney, M., Y. Richard, D. Coulaud, T. Tursz, and J. Wiels, *CD77: an antigen of germinal center B cells entering apoptosis.* Eur J Immunol, 1991. **21**(5): p. 1131-40.

52. Sandvig, K., *Shiga toxins.* Toxicon, 2001. **39**(11): p. 1629-35.

53. Thomson, J.A., J. Itskovitz-Eldor, S.S. Shapiro, M.A. Waknitz, J.J. Swiergiel, V.S. Marshall, and J.M. Jones, *Embryonic stem cell lines derived from human blastocysts.* Science, 1998. **282**(5391): p. 1145-7.

54. Kannagi, R., N.A. Cochran, F. Ishigami, S. Hakomori, P.W. Andrews, B.B. Knowles, and D. Solter, *Stage-specific embryonic antigens (SSEA-3 and -4) are epitopes of a unique globo-series ganglioside isolated from human teratocarcinoma cells.* EMBO J, 1983. **2**(12): p. 2355-61.

55. Reubinoff, B.E., M.F. Pera, C.Y. Fong, A. Trounson, and A. Bongso, *Embryonic stem cell lines from human blastocysts: somatic differentiation in vitro.* Nat Biotechnol, 2000. **18**(4): p. 399-404.

56. Clausen, H., K. Watanabe, R. Kannagi, S.B. Levery, E. Nudelman, Y. Arao-Tomono, and S. Hakomori, *Blood group A glycolipid (Ax) with globo-series structure which is specific for blood group A1 erythrocytes: one of the chemical bases for A1 and A2 distinction.* Biochem Biophys Res Commun, 1984. **124**(2): p. 523-9.

57. Hakomori, S., *Glycosylation defining cancer malignancy: new wine in an old bottle.* Proc Natl Acad Sci U S A, 2002. **99**(16): p. 10231-3.

58. Meezan, E., H.C. Wu, P.H. Black, and P.W. Robbins, *Comparative studies on the carbohydrate-containing membrane components of normal and virus-transformed mouse fibroblasts. II. Separation of glycoproteins and glycopeptides by sephadex chromatography.* Biochemistry, 1969. **8**(6): p. 2518-24.

59. Saussez, S., H. Marchant, N. Nagy, C. Decaestecker, S. Hassid, A. Jortay, M.P. Schuring, H.J. Gabius, A. Danguy, I. Salmon, and R. Kiss, *Quantitative glycohistochemistry defines new prognostic markers for cancers of the oral cavity.* Cancer, 1998. **82**(2): p. 252-60.

60. Adamczyk, B., T. Tharmalingam, and P.M. Rudd, *Glycans as cancer biomarkers.* Biochim Biophys Acta, 2012. **1820**(9): p. 1347-53.

61. Lau, K.S. and J.W. Dennis, *N-Glycans in cancer progression.* Glycobiology, 2008. **18**(10): p. 750-60.

62. Dennis, J.W., S. Laferte, C. Waghorne, M.L. Breitman, and R.S. Kerbel, *Beta 1-6 branching of Asn-linked oligosaccharides is directly associated with metastasis.* Science, 1987. **236**(4801): p. 582-5.

63. van Beek, W.P., L.A. Smets, and P. Emmelot, *Increased sialic acid density in surface glycoprotein of transformed and malignant cells--a general phenomenon?* Cancer Res, 1973. **33**(11): p. 2913-22.

64. Sell, S., *Cancer-associated carbohydrates identified by monoclonal antibodies.*

Hum Pathol, 1990. **21**(10): p. 1003-19.

65. Hakomori, S. and Y. Zhang, *Glycosphingolipid antigens and cancer therapy.* Chem Biol, 1997. **4**(2): p. 97-104.

66. Taylor-Papadimitriou, J. and A.A. Epenetos, *Exploiting altered glycosylation patterns in cancer: progress and challenges in diagnosis and therapy.* Trends Biotechnol, 1994. **12**(6): p. 227-33.

67. Hollingsworth, M.A. and B.J. Swanson, *Mucins in cancer: protection and control of the cell surface.* Nat Rev Cancer, 2004. **4**(1): p. 45-60.

68. Hakomori, S., *Traveling for the glycosphingolipid path.* Glycoconj J, 2000. **17**(7-9): p. 627-47.

69. Girnita, L., M. Wang, Y. Xie, G. Nilsson, A. Dricu, J. Wejde, and O. Larsson, *Inhibition of N-linked glycosylation down-regulates insulin-like growth factor-1 receptor at the cell surface and kills Ewing's sarcoma cells: therapeutic implications.* Anticancer Drug Des, 2000. **15**(1): p. 67-72.

70. Bogenrieder, T. and M. Herlyn, *Axis of evil: molecular mechanisms of cancer metastasis.* Oncogene, 2003. **22**(42): p. 6524-36.

71. Seidenfaden, R., A. Krauter, F. Schertzinger, R. Gerardy-Schahn, and H. Hildebrandt, *Polysialic acid directs tumor cell growth by controlling heterophilic neural cell adhesion molecule interactions.* Mol Cell Biol, 2003. **23**(16): p. 5908-18.

72. Iozzo, R.V. and J.D. San Antonio, *Heparan sulfate proteoglycans: heavy hitters in the angiogenesis arena.* J Clin Invest, 2001. **108**(3): p. 349-55.

73. Kleeff, J., T. Ishiwata, A. Kumbasar, H. Friess, M.W. Buchler, A.D. Lander, and M. Korc, *The cell-surface heparan sulfate proteoglycan glypican-1 regulates growth factor action in pancreatic carcinoma cells and is overexpressed in human pancreatic cancer.* J Clin Invest, 1998. **102**(9): p. 1662-73.

74. Wolfl, M., W.Y. Batten, C. Posovszky, H. Bernhard, and F. Berthold, *Gangliosides inhibit the development from monocytes to dendritic cells.* Clin Exp Immunol, 2002. **130**(3): p. 441-8.

75. Caldwell, S., A. Heitger, W. Shen, Y. Liu, B. Taylor, and S. Ladisch, *Mechanisms of ganglioside inhibition of APC function.* J Immunol, 2003. **171**(4): p. 1676-83.

76. Crespo, F.A., X. Sun, J.G. Cripps, and R. Fernandez-Botran, *The immunoregulatory effects of gangliosides involve immune deviation favoring type-2 T cell responses.* J Leukoc Biol, 2006. **79**(3): p. 586-95.

77. Fredman, P., H. von Holst, V.P. Collins, A. Ammar, B. Dellheden, B. Wahren, L. Granholm, and L. Svennerholm, *Potential ganglioside antigens associated with human gliomas.* Neurol Res, 1986. **8**(2): p. 123-6.

78. Jennemann, R., A. Rodden, B.L. Bauer, H.D. Mennel, and H. Wiegandt, *Glycosphingolipids of human gliomas.* Cancer Res, 1990. **50**(23): p. 7444-9.

79. Traylor, T.D. and E.L. Hogan, *Gangliosides of human cerebral astrocytomas.* J Neurochem, 1980. **34**(1): p. 126-31.

80. Ravindranath, M.H. and R.F. Irie, *Gangliosides as antigens of human melanoma.* Cancer Treat Res, 1988. **43**: p. 17-43.

81. Vanier, M.T., M. Holm, J.E. Mansson, and L. Svennerholm, *The distribution of lipids in the human nervous system--V. Gangliosides and allied neutral glycolipids of infant brain.* J Neurochem, 1973. **21**(6): p. 1375-84.

82. Ando, S. and T. Yamakawa, *Separation of polar glycolipids from human red blood cells with special reference to blood group-A activity.* J Biochem, 1973. **73**(2): p. 387-96.

83. Pukel, C.S., K.O. Lloyd, L.R. Travassos, W.G. Dippold, H.F. Oettgen, and L.J. Old, *GD3, a prominent ganglioside of human melanoma. Detection and characterisation by mouse monoclonal antibody.* J Exp Med, 1982. **155**(4): p.

1133-47.

84. Siddiqui, B., J. Buehler, M.W. DeGregorio, and B.A. Macher, *Differential expression of ganglioside GD3 by human leukocytes and leukemia cells.* Cancer Res, 1984. **44**(11): p. 5262-5.

85. Fuentes, R., R. Allman, and M.D. Mason, *Ganglioside expression in lung cancer cell lines.* Lung Cancer, 1997. **18**(1): p. 21-33.

86. Cazet, A., S. Groux-Degroote, B. Teylaert, K.M. Kwon, S. Lehoux, C. Slomianny, C.H. Kim, X. Le Bourhis, and P. Delannoy, *GD3 synthase overexpression enhances proliferation and migration of MDA-MB-231 breast cancer cells.* Biol Chem, 2009. **390**(7): p. 601-9.

87. Fredman, P., H. von Holst, V.P. Collins, B. Dellheden, and L. Svennerholm, *Expression of gangliosides GD3 and 3′-isoLM1 in autopsy brains from patients with malignant tumors.* J Neurochem, 1993. **60**(1): p. 99-105.

88. Berra, B., S.M. Gaini, and L. Riboni, *Correlation between ganglioside distribution and histological grading of human astrocytomas.* Int J Cancer, 1985. **36**(3): p. 363-6.

89. Nakamura, O., E. Ishihara, M. Iwamori, T. Nagai, M. Matsutani, K. Nomura, and K. Takakura, *[Lipid composition of human malignant brain tumors].* No To Shinkei, 1987. **39**(3): p. 221-6.

90. Yu, A.L., A.L. Gilman, M.F. Ozkaynak, W.B. London, S.G. Kreissman, H.X. Chen, M. Smith, B. Anderson, J.G. Villablanca, K.K. Matthay, H. Shimada, S.A. Grupp, R. Seeger, C.P. Reynolds, A. Buxton, R.A. Reisfeld, S.D. Gillies, S.L. Cohn, J.M. Maris, and P.M. Sondel, *Anti-GD2 antibody with GM-CSF, interleukin-2, and isotretinoin for neuroblastoma.* N Engl J Med, 2010. **363**(14): p. 1324-34.

91. Cahan, L.D., R.F. Irie, R. Singh, A. Cassidenti, and J.C. Paulson, *Identification of a human neuroectodermal tumor antigen (OFA-I-2) as ganglioside GD2.* Proc

Natl Acad Sci U S A, 1982. **79**(24): p. 7629-33.

92. Cheresh, D.A., J. Rosenberg, K. Mujoo, L. Hirschowitz, and R.A. Reisfeld, *Biosynthesis and expression of the disialoganglioside GD2, a relevant target antigen on small cell lung carcinoma for monoclonal antibody-mediated cytolysis.* Cancer Res, 1986. **46**(10): p. 5112-8.

93. Mansson, J.E., P. Fredman, D.D. Bigner, K. Molin, B. Rosengren, H.S. Friedman, and L. Svennerholm, *Characterization of new gangliosides of the lactotetraose series in murine xenografts of a human glioma cell line.* FEBS Lett, 1986. **201**(1): p. 109-13.

94. Fredman, P., H. von Holst, V.P. Collins, L. Granholm, and L. Svennerholm, *Sialyllactotetraosylceramide, a ganglioside marker for human malignant gliomas.* J Neurochem, 1988. **50**(3): p. 912-9.

95. Wikstrand, C.J., P. Fredman, L. Svennerholm, P.A. Humphrey, S.H. Bigner, and D.D. Bigner, *Monoclonal antibodies to malignant human gliomas.* Mol Chem Neuropathol, 1992. **17**(2): p. 137-46.

96. Svennerholm, L., K. Bostrom, P. Fredman, J.E. Mansson, B. Rosengren, and B.M. Rynmark, *Human brain gangliosides: developmental changes from early fetal stage to advanced age.* Biochim Biophys Acta, 1989. **1005**(2): p. 109-17.

97. Kato, Y., C.T. Kuan, J. Chang, M.K. Kaneko, J. Ayriss, H. Piao, V. Chandramohan, C. Pegram, R.E. McLendon, P. Fredman, J.E. Mansson, and D.D. Bigner, *GMab-1, a high-affinity anti-3'-isoLM1/3',6'-isoLD1 IgG monoclonal antibody, raised in lacto-series ganglioside-defective knockout mice.* Biochem Biophys Res Commun, 2010. **391**(1): p. 750-5.

98. Uhm, J.H., K.V. Ballman, W. Wu, C. Giannini, J.C. Krauss, J.C. Buckner, C.D. James, B.W. Scheithauer, R.J. Behrens, P.J. Flynn, P.L. Schaefer, S.R. Dakhill, and K.A. Jaeckle, *Phase II evaluation of gefitinib in patients with newly diagnosed*

Grade 4 astrocytoma: Mayo/North Central Cancer Treatment Group Study N0074. Int J Radiat Oncol Biol Phys, 2011. **80**(2): p. 347-53.

99. Peereboom, D.M., D.R. Shepard, M.S. Ahluwalia, C.J. Brewer, N. Agarwal, G.H. Stevens, J.H. Suh, S.A. Toms, M.A. Vogelbaum, R.J. Weil, P. Elson, and G.H. Barnett, *Phase II trial of erlotinib with temozolomide and radiation in patients with newly diagnosed glioblastoma multiforme.* J Neurooncol, 2010. **98**(1): p. 93-9.
100. Prados, M.D., S.M. Chang, N. Butowski, R. DeBoer, R. Parvataneni, H. Carliner, P. Kabuubi, J. Ayers-Ringler, J. Rabbitt, M. Page, A. Fedoroff, P.K. Sneed, M.S. Berger, M.W. McDermott, A.T. Parsa, S. Vandenberg, C.D. James, K.R. Lamborn, D. Stokoe, and D.A. Haas-Kogan, *Phase II study of erlotinib plus temozolomide during and after radiation therapy in patients with newly diagnosed glioblastoma multiforme or gliosarcoma.* J Clin Oncol, 2009. **27**(4): p. 579-84.
101. Ranza, E., G. Mazzini, A. Facoetti, and R. Nano, *In-vitro effects of the tyrosine kinase inhibitor imatinib on glioblastoma cell proliferation.* J Neurooncol, 2010. **96**(3): p. 349-57.
102. Kubota, N., S. Okada, T. Inada, K. Ohnishi, and T. Ohnishi, *Wortmannin sensitizes human glioblastoma cell lines carrying mutant and wild type TP53 gene to radiation.* Cancer Lett, 2000. **161**(2): p. 141-7.
103. Stefanik, D.F., W.K. Fellows, L.R. Rizkalla, W.M. Rizkalla, P.P. Stefanik, A.B. Deleo, and W.C. Welch, *Monoclonal antibodies to vascular endothelial growth factor (VEGF) and the VEGF receptor, FLT-1, inhibit the growth of C6 glioma in a mouse xenograft.* J Neurooncol, 2001. **55**(2): p. 91-100.
104. Bao, S., Q. Wu, S. Sathornsumetee, Y. Hao, Z. Li, A.B. Hjelmeland, Q. Shi, R.E. McLendon, D.D. Bigner, and J.N. Rich, *Stem cell-like glioma cells promote tumor angiogenesis through vascular endothelial growth factor.* Cancer Res, 2006.

66(16): p. 7843-8.

105. Vredenburgh, J.J., A. Desjardins, J.P. Kirkpatrick, D.A. Reardon, K.B. Peters, J.E. Herndon, 2nd, J. Marcello, L. Bailey, S. Threatt, J. Sampson, A. Friedman, and H.S. Friedman, *Addition of bevacizumab to standard radiation therapy and daily temozolomide is associated with minimal toxicity in newly diagnosed glioblastoma multiforme.* Int J Radiat Oncol Biol Phys, 2012. **82**(1): p. 58-66.
106. Mishima, K., T.G. Johns, R.B. Luwor, A.M. Scott, E. Stockert, A.A. Jungbluth, X.D. Ji, P. Suvarna, J.R. Voland, L.J. Old, H.J. Huang, and W.K. Cavenee, *Growth suppression of intracranial xenografted glioblastomas overexpressing mutant epidermal growth factor receptors by systemic administration of monoclonal antibody (mAb) 806, a novel monoclonal antibody directed to the receptor.* Cancer Res, 2001. **61**(14): p. 5349-54.
107. Carter, P., *Improving the efficacy of antibody-based cancer therapies.* Nat Rev Cancer, 2001. **1**(2): p. 118-29.
108. Siwak, D.R., A.M. Tari, and G. Lopez-Berestein, *The potential of drug-carrying immunoliposomes as anticancer agents. Commentary re: J. W. Park et al., Anti-HER2 immunoliposomes: enhanced efficacy due to targeted delivery. Clin. Cancer Res., 8: 1172-1181, 2002.* Clin Cancer Res, 2002. **8**(4): p. 955-6.
109. Alvero, A.B., R. Chen, H.H. Fu, M. Montagna, P.E. Schwartz, T. Rutherford, D.A. Silasi, K.D. Steffensen, M. Waldstrom, I. Visintin, and G. Mor, *Molecular phenotyping of human ovarian cancer stem cells unravels the mechanisms for repair and chemoresistance.* Cell Cycle, 2009. **8**(1): p. 158-66.
110. Matsui, W., Q. Wang, J.P. Barber, S. Brennan, B.D. Smith, I. Borrello, I. McNiece, L. Lin, R.F. Ambinder, C. Peacock, D.N. Watkins, C.A. Huff, and R.J. Jones, *Clonogenic multiple myeloma progenitors, stem cell properties, and drug resistance.* Cancer Res, 2008. **68**(1): p. 190-7.

111. Heppner, G.H. and B.E. Miller, *Tumor heterogeneity: biological implications and therapeutic consequences.* Cancer Metastasis Rev, 1983. **2**(1): p. 5-23.

112. Reya, T., S.J. Morrison, M.F. Clarke, and I.L. Weissman, *Stem cells, cancer, and cancer stem cells.* Nature, 2001. **414**(6859): p. 105-11.

113. Bonnet, D. and J.E. Dick, *Human acute myeloid leukemia is organized as a hierarchy that originates from a primitive hematopoietic cell.* Nat Med, 1997. **3**(7): p. 730-7.

114. Al-Hajj, M., M.S. Wicha, A. Benito-Hernandez, S.J. Morrison, and M.F. Clarke, *Prospective identification of tumorigenic breast cancer cells.* Proc Natl Acad Sci U S A, 2003. **100**(7): p. 3983-8.

115. Castor, A., L. Nilsson, I. Astrand-Grundstrom, M. Buitenhuis, C. Ramirez, K. Anderson, B. Strombeck, S. Garwicz, A.N. Bekassy, K. Schmiegelow, B. Lausen, P. Hokland, S. Lehmann, G. Juliusson, B. Johansson, and S.E. Jacobsen, *Distinct patterns of hematopoietic stem cell involvement in acute lymphoblastic leukemia.* Nat Med, 2005. **11**(6): p. 630-7.

116. Cox, C.V., R.S. Evely, A. Oakhill, D.H. Pamphilon, N.J. Goulden, and A. Blair, *Characterization of acute lymphoblastic leukemia progenitor cells.* Blood, 2004. **104**(9): p. 2919-25.

117. Eramo, A., F. Lotti, G. Sette, E. Pilozzi, M. Biffoni, A. Di Virgilio, C. Conticello, L. Ruco, C. Peschle, and R. De Maria, *Identification and expansion of the tumorigenic lung cancer stem cell population.* Cell Death Differ, 2008. **15**(3): p. 504-14.

118. Fang, D., T.K. Nguyen, K. Leishear, R. Finko, A.N. Kulp, S. Hotz, P.A. Van Belle, X. Xu, D.E. Elder, and M. Herlyn, *A tumorigenic subpopulation with stem cell properties in melanomas.* Cancer Res, 2005. **65**(20): p. 9328-37.

119. Galli, R., E. Binda, U. Orfanelli, B. Cipelletti, A. Gritti, S. De Vitis, R. Fiocco, C.

Foroni, F. Dimeco, and A. Vescovi, *Isolation and characterization of tumorigenic, stem-like neural precursors from human glioblastoma.* Cancer Res, 2004. **64**(19): p. 7011-21.

120. O'Brien, C.A., A. Pollett, S. Gallinger, and J.E. Dick, *A human colon cancer cell capable of initiating tumour growth in immunodeficient mice.* Nature, 2007. **445**(7123): p. 106-10.
121. Ricci-Vitiani, L., D.G. Lombardi, E. Pilozzi, M. Biffoni, M. Todaro, C. Peschle, and R. De Maria, *Identification and expansion of human colon-cancer-initiating cells.* Nature, 2007. **445**(7123): p. 111-5.
122. Singh, S.K., C. Hawkins, I.D. Clarke, J.A. Squire, J. Bayani, T. Hide, R.M. Henkelman, M.D. Cusimano, and P.B. Dirks, *Identification of human brain tumour initiating cells.* Nature, 2004. **432**(7015): p. 396-401.
123. Ignatova, T.N., V.G. Kukekov, E.D. Laywell, O.N. Suslov, F.D. Vrionis, and D.A. Steindler, *Human cortical glial tumors contain neural stem-like cells expressing astroglial and neuronal markers in vitro.* Glia, 2002. **39**(3): p. 193-206.
124. Lathia, J.D., J. Gallagher, J.M. Heddleston, J. Wang, C.E. Eyler, J. Macswords, Q. Wu, A. Vasanji, R.E. McLendon, A.B. Hjelmeland, and J.N. Rich, *Integrin alpha 6 regulates glioblastoma stem cells.* Cell Stem Cell, 2010. **6**(5): p. 421-32.
125. Ogden, A.T., A.E. Waziri, R.A. Lochhead, D. Fusco, K. Lopez, J.A. Ellis, J. Kang, M. Assanah, G.M. McKhann, M.B. Sisti, P.C. McCormick, P. Canoll, and J.N. Bruce, *Identification of A2B5+CD133- tumor-initiating cells in adult human gliomas.* Neurosurgery, 2008. **62**(2): p. 505-14; discussion 514-5.
126. Son, M.J., K. Woolard, D.H. Nam, J. Lee, and H.A. Fine, *SSEA-1 is an enrichment marker for tumor-initiating cells in human glioblastoma.* Cell Stem Cell, 2009. **4**(5): p. 440-52.
127. Livak, K.J. and T.D. Schmittgen, *Analysis of relative gene expression data using*

real-time quantitative PCR and the 2(-Delta Delta C(T)) Method. Methods, 2001. **25**(4): p. 402-8.

128. Kannagi, R., S.B. Levery, F. Ishigami, S. Hakomori, L.H. Shevinsky, B.B. Knowles, and D. Solter, *New globoseries glycosphingolipids in human teratocarcinoma reactive with the monoclonal antibody directed to a developmentally regulated antigen, stage-specific embryonic antigen 3.* J Biol Chem, 1983. **258**(14): p. 8934-42.
129. Wang, C.C., Y.L. Huang, C.T. Ren, C.W. Lin, J.T. Hung, J.C. Yu, A.L. Yu, C.Y. Wu, and C.H. Wong, *Glycan microarray of Globo H and related structures for quantitative analysis of breast cancer.* Proc Natl Acad Sci U S A, 2008. **105**(33): p. 11661-6.
130. Zarei, M., J. Muthing, J. Peter-Katalinic, and L. Bindila, *Separation and identification of GM1b pathway Neu5Ac- and Neu5Gc gangliosides by on-line nanoHPLC-QToF MS and tandem MS: toward glycolipidomics screening of animal cell lines.* Glycobiology, 2010. **20**(1): p. 118-26.
131. Saito, S., S. Orikasa, M. Satoh, C. Ohyama, A. Ito, and T. Takahashi, *Expression of globo-series gangliosides in human renal cell carcinoma.* Jpn J Cancer Res, 1997. **88**(7): p. 652-9.
132. Gottschling, S., K. Jensen, A. Warth, F.J. Herth, M. Thomas, P.A. Schnabel, and E. Herpel, *Stage-specific embryonic antigen-4 is expressed in basaloid lung cancer and associated with poor prognosis.* Eur Respir J, 2013. **41**(3): p. 656-63.
133. Ye, F., Y. Li, Y. Hu, C. Zhou, and H. Chen, *Stage-specific embryonic antigen 4 expression in epithelial ovarian carcinoma.* Int J Gynecol Cancer, 2010. **20**(6): p. 958-64.
134. Huang, Y.L., J.T. Hung, S.K. Cheung, H.Y. Lee, K.C. Chu, S.T. Li, Y.C. Lin, C.T. Ren, T.J. Cheng, T.L. Hsu, A.L. Yu, C.Y. Wu, and C.H. Wong,

Carbohydrate-based vaccines with a glycolipid adjuvant for breast cancer. Proc Natl Acad Sci U S A, 2013. **110**(7): p. 2517-22.

135. Noto, Z., T. Yoshida, M. Okabe, C. Koike, M. Fathy, H. Tsuno, K. Tomihara, N. Arai, M. Noguchi, and T. Nikaido, *CD44 and SSEA-4 positive cells in an oral cancer cell line HSC-4 possess cancer stem-like cell characteristics.* Oral Oncol, 2013.
136. Yuan, X., J. Curtin, Y. Xiong, G. Liu, S. Waschsmann-Hogiu, D.L. Farkas, K.L. Black, and J.S. Yu, *Isolation of cancer stem cells from adult glioblastoma multiforme.* Oncogene, 2004. **23**(58): p. 9392-400.
137. Kempermann, G., *Adult neurogenesis : stem cells and neuronal development in the adult brain*2006, New York: Oxford University Press. x, 426 p.
138. Michalczyk, K. and M. Ziman, *Nestin structure and predicted function in cellular cytoskeletal organisation.* Histol Histopathol, 2005. **20**(2): p. 665-71.
139. Chang, W.W., C.H. Lee, P. Lee, J. Lin, C.W. Hsu, J.T. Hung, J.J. Lin, J.C. Yu, L.E. Shao, J. Yu, C.H. Wong, and A.L. Yu, *Expression of Globo H and SSEA3 in breast cancer stem cells and the involvement of fucosyl transferases 1 and 2 in Globo H synthesis.* Proc Natl Acad Sci U S A, 2008. **105**(33): p. 11667-72.
140. Brimble, S.N., E.S. Sherrer, E.W. Uhl, E. Wang, S. Kelly, A.H. Merrill, Jr., A.J. Robins, and T.C. Schulz, *The cell surface glycosphingolipids SSEA-3 and SSEA-4 are not essential for human ESC pluripotency.* Stem Cells, 2007. **25**(1): p. 54-62.
141. Van Slambrouck, S. and W.F. Steelant, *Clustering of monosialyl-Gb5 initiates downstream signalling events leading to invasion of MCF-7 breast cancer cells.* Biochem J, 2007. **401**(3): p. 689-99.
142. Hung, T.C., C.W. Lin, T.L. Hsu, C.Y. Wu, and C.H. Wong, *Investigation of SSEA-4 binding protein in breast cancer cells.* J Am Chem Soc, 2013. **135**(16): p. 5934-7.

143. Saito, S., H. Aoki, A. Ito, S. Ueno, T. Wada, K. Mitsuzuka, M. Satoh, Y. Arai, and T. Miyagi, *Human alpha2,3-sialyltransferase (ST3Gal II) is a stage-specific embryonic antigen-4 synthase.* J Biol Chem, 2003. **278**(29): p. 26474-9.

144. Kudo, T., Y. Ikehara, A. Togayachi, K. Morozumi, M. Watanabe, M. Nakamura, S. Nishihara, and H. Narimatsu, *Up-regulation of a set of glycosyltransferase genes in human colorectal cancer.* Lab Invest, 1998. **78**(7): p. 797-811.

145. Kundu, S.K., B.E. Samuelsson, I. Pascher, and D.M. Marcus, *New gangliosides from human erythrocytes.* J Biol Chem, 1983. **258**(22): p. 13857-66.

146. Visvader, J.E. and G.J. Lindeman, *Cancer stem cells in solid tumours: accumulating evidence and unresolved questions.* Nat Rev Cancer, 2008. **8**(10): p. 755-68.

147. Haraguchi, M., S. Yamashiro, A. Yamamoto, K. Furukawa, K. Takamiya, K.O. Lloyd, and H. Shiku, *Isolation of GD3 synthase gene by expression cloning of GM3 alpha-2,8-sialyltransferase cDNA using anti-GD2 monoclonal antibody.* Proceedings of the National Academy of Sciences of the United States of America, 1994. **91**(22): p. 10455-9.

148. Yanagisawa, M., T. Taga, K. Nakamura, T. Ariga, and R.K. Yu, *Characterization of glycoconjugate antigens in mouse embryonic neural precursor cells.* Journal of neurochemistry, 2005. **95**(5): p. 1311-20.

149. Battula, V.L., Y. Shi, K.W. Evans, R.Y. Wang, E.L. Spaeth, R.O. Jacamo, R. Guerra, A.A. Sahin, F.C. Marini, G. Hortobagyi, S.A. Mani, and M. Andreeff, *Ganglioside GD2 identifies breast cancer stem cells and promotes tumorigenesis.* J Clin Invest, 2012. **122**(6): p. 2066-78.

150. Svennerholm, L., K. Bostrom, P. Fredman, B. Jungbjer, J.E. Mansson, and B.M. Rynmark, *Membrane lipids of human peripheral nerve and spinal cord.* Biochim Biophys Acta, 1992. **1128**(1): p. 1-7.

151. Green, M.R., *Targeting targeted therapy.* N Engl J Med, 2004. **350**(21): p. 2191-3.

152. Wikstrand, C.J., I. Cokgor, J.H. Sampson, and D.D. Bigner, *Monoclonal antibody therapy of human gliomas: current status and future approaches.* Cancer Metastasis Rev, 1999. **18**(4): p. 451-64.

153. Durrant, L.G., P. Noble, and I. Spendlove, *Immunology in the clinic review series; focus on cancer: glycolipids as targets for tumour immunotherapy.* Clin Exp Immunol, 2012. **167**(2): p. 206-15.

APPENDIX

Stage-specific embryonic antigen-4 as a potential therapeutic target in glioblastoma multiforme and other cancers

Yi-Wei Lou[a,b], Pao-Yuan Wang[b,c], Shih-Chi Yeh[b,d], Po-Kai Chuang[b,e], Shiou-Ting Li[b], Chung-Yi Wu[b], Kay-Hooi Khoo[f], Michael Hsiao[b], Tsui-Ling Hsu[b], and Chi-Huey Wong[b,1]

[a]Institute of Biochemical Sciences, National Taiwan University, Taipei 106, Taiwan; [b]Genomics Research Center, [c]Chemical Biology and Molecular Biophysics Program, Taiwan International Graduate Program, and [f]Institute of Biological Chemistry, Academia Sinica, Taipei 115, Taiwan; [d]Institute of Biochemistry and Molecular Biology, National Yang-Ming University, Taipei 112, Taiwan; and [e]Institute of Basic Medical Sciences, National Cheng-Kung University, Tainan 701, Taiwan

Contributed by Chi-Huey Wong, January 8, 2014 (sent for review November 18, 2013)

Glioblastoma multiforme (GBM), the grade IV astrocytoma, is the most common and aggressive brain tumor in adults. Despite advances in medical management, the survival rate of GBM patients remains poor, suggesting that identification of GBM-specific targets for therapeutic development is urgently needed. Analysis of several glycan antigens on GBM cell lines revealed that eight of 11 GBM cell lines are positive for stage-specific embryonic antigen-4 (SSEA-4), and immunohistochemical staining confirmed that 38/55 (69%) of human GBM specimens, but not normal brain tissue, were SSEA-4^{+} and correlated with high-grade astrocytoma. In addition, an SSEA-4–specific mAb was found to induce complement-dependent cytotoxicity against SSEA-4^{hi} GBM cell lines in vitro and suppressed GBM tumor growth in mice. Because SSEA-4 is expressed on GBM and many other types of cancers, but not on normal cells, it could be a target for development of therapeutic antibodies and vaccines.

glycosphingolipids | Globo H | SSEA-3 | gangliosides | targeted therapy

Glioblastoma multiforme (GBM), accounting for 60–70% of malignant gliomas, is the most aggressive form of glioma and the most common primary brain tumor in adults (1). Despite treatment, including surgery, and chemo- or radiotherapy, the prognosis for GBM patients is poor, with a median survival rate of 14–15 mo (2). GBM is notoriously resistant to most anticancer drugs and is extremely infiltrative, hampering complete surgical resection; therefore most patients develop tumor recurrence or progression even after multiple therapies. Because of the high mortality, new therapeutic approaches, such as immunotherapy and gene therapy, have been proposed for the treatment of GBM (3).

Altered glycosylation is a feature of cancer cells, and several glycan structures are well-known tumor markers (4, 5). These aberrant changes include the overall increase in the branching of N-linked glycans (6) and sialic acid content (7) and the overexpression of certain glycan epitopes, such as sialyl Lewis x (sLe^{x}), sialyl Tn (sTn), Lewis y (Le^{y}), fucosyl Gb5 (Globo H), and polysialic acid (8–10). Many tumors also exhibit increased expression of certain glycolipids, especially the gangliosides, glycosphingolipids (GSLs) with sialic acid(s) attached to the glycan chain. Gangliosides normally are observed in neural systems and are elevated in tumors, particularly the complex gangliosides associated with malignancy (11).

It has been reported that human glioma biopsies show elevation of monosialylated GM3 and GM2 and their disialylated derivatives GD3 and GD2 (12–14). The increase of GD3 was most significant, but the correlation between GD3 and malignancy remains obscure (15, 16). In addition, the lacto-series gangliosides 3′-isoLM1 and 3′,6′-isoLD1 are reported to be major gangliosides in human gliomas (16–18). Because some of these glioma-associated gangliosides are rarely expressed or even are absent in normal tissues (19), they are suitable for targeted therapy (20). Hence, discovering novel glioma-associated GSLs would provide new targets for development of new therapies against gliomas.

The GSLs of globo-series feature a Galα1–4Gal linkage to lactosylceramides, and this linkage is catalyzed by the lactosylceramide 4-alpha-galactosyltransferase, encoded by the *A4GALT* gene. Although globotriosylceramide (Gb3Cer) and globoside (Gb4Cer) constitute the basis of the P-blood group system (21), galactosyl globoside (Gb5Cer) and sialyl galactosyl globoside (sialyl Gb5Cer, SGG, MSGG), also known as "stage-specific embryonic antigen-3" (SSEA-3) and "stage-specific embryonic antigen-4" (SSEA-4) (22), respectively, are cell-surface markers widely used to define human embryonic stem cells (hESCs). Globo-series GSLs also have been observed in tumors: Globo H is overexpressed in many epithelial cancers [e.g., ovarian, gastric, prostate, lung, breast, and pancreatic cancers (23)]; SSEA-3, SSEA-4, and Globo H are expressed not only on breast cancer cells but also on breast cancer stem cells (24, 25). Moreover, high-level expression of SSEA-4 and disialosyl galactosyl globoside (disialosyl Gb5Cer) is observed in renal cell carcinoma (26), but whether globo-series GSLs are expressed in GBM is not known.

In the present study, we examined the expression levels of globo-series GSLs and several tumor-associated glycans in GBM cell lines by flow cytometry. The result showed that SSEA-4, a ganglioside rarely found in normal brain tissues, was highly expressed on GBM cells and GBM specimens, as confirmed by high-performance TLC (HPTLC) immunostaining and MS. We found that anti–SSEA-4 mAb (MC813-70) could induce complement-dependent cytotoxicity in vitro and inhibit the growth of GBM in nude mice. SSEA-4 is displayed on many other types of cancers and therefore can be a target for the development of therapeutic antibodies and vaccines against SSEA-4^{+} cancers.

Significance

Glioblastoma multiforme (GBM) is a deadly brain tumor. More than 50% of patients who suffer from GBM die within 15 mo even received all possible medical treatment. In this study we report that the glycolipid stage-specific embryonic antigen-4 (SSEA-4) is highly expressed on the surface of both GBM cells and GBM specimens. We further demonstrate that the growth of GBM tumor is inhibited when anti–SSEA-4 antibody is administered to experimental mice, suggesting a research proof of concept for the treatment GBM and other SSEA-4^{+} cancers.

Author contributions: Y.-W.L., C.-Y.W., K.-H.K., M.H., T.-L.H., and C.-H.W. designed research; Y.-W.L., P.-Y.W., S.-C.Y., P.-K.C., and S.-T.L. performed research; Y.-W.L., P.-Y.W., S.-C.Y., P.-K.C., and S.-T.L. analyzed data; and Y.-W.L., T.-L.H., and C.-H.W. wrote the paper.

The authors declare no conflict of interest.

[1]To whom correspondence should be addressed. E-mail: chwong@gate.sinica.edu.tw.

This article contains supporting information online at www.pnas.org/lookup/suppl/doi:10.1073/pnas.1400283111/-/DCSupplemental.

Results

Flow Cytometric Analysis of Glycan Epitopes on GBM Cell Lines. We analyzed the expression levels of various glycan epitopes by flow cytometry in four human GBM cell lines: G5T, LN-18, U-138, and U-251. The glycan epitopes examined include O-linked glycans [Tn, sTn, and Thomsen–Friedenreich (TF) antigens], Lewis antigens (Le^x, Le^y, and sLe^x), complex gangliosides [GM2, GM1, GD1a, GD2, GT1b, and A2B5 (c-series gangliosides)], and globo-series GSLs (SSEA-3, SSEA-4, and Globo H) (Fig. 1*A*). The results showed that most of these four GBM cell lines expressed high levels of Tn, TF, Le^x, and Le^y, a low level of sLe^x, and no sTn (Table 1 and Fig. S1 *A* and *B*). In addition, these four GBM cell lines were positive for all the gangliosides we examined, although the expression levels varied (Fig. S1*C*). U-251 showed weak MC813-70 (anti–SSEA-4) staining intensity, and G5T, U-138, and LN-18 displayed high MC813-70 staining intensity (Fig. 1*B*). Among these four cell lines, positive MC631 (anti–SSEA-3) staining was observed only on G5T, and none of the cell lines was positive for VK9 (anti-Globo H) staining (Table 1 and Fig. S1 *D* and *E*). After these findings, we looked further into the expression patterns of globo-series GSLs in additional GBM cell lines and found that of the nine of the 17 GBM cell lines showed strong MC813-70 staining signal (SSEA-4^{hi}); three were weakly stained (SSEA-4^{lo}), and five were not stained by MC813-70 (Fig. 1*A*). Nine of the 17 cell lines were positive for MC631 staining, and six were positive for VK9 staining (Fig. S1 *D* and *E*). SVG p12, an immortalized human fetal glia cell, showed a very weak MC813-70 staining signal and no MC631 nor VK-9 staining signal (Fig. 1 and Fig. S1). These results indicated that most of the GBM cell lines examined were positively stained by MC813-70.

Specificity of MC813-70. Previous studies indicate that mAb MC813-70 recognizes the NeuAcα2-3Galβ1-3GalNAc epitope in SSEA-4 glycolipid (sialyl Gb5Cer) and the glycoproteins with an extended core 1 O-glycan structure (22, 27). In addition, MC813-70 shows cross-reactivity toward GM1b and GD1a when these two gangliosides are immobilized at a very high concentration/density. We used a glycan microarray (28) to investigate the binding specificity of MC813-70. As shown in Fig. 2, we found that, among the 152 chemically synthesized glycans on the glycan microarray (Fig. S2), MC813-70 recognizes only the SSEA-4 hexasaccharide with Neu5Ac or Neu5Gc at the terminal position (glycan Nos. 12 and 49). Compared with previous ELISA results (22), MC813-70 did not show any binding to GM1b (glycan No. 104) or GD1a (glycan No. 106), both of which contain the terminal trisaccharide epitope of SSEA-4 (NeuAcα2-3Galβ1-3GalNAc) with a different linkage (β1–4) to lactose at the reducing end. We also used the glycan array to determine the dissociation constants of MC813-70 with SSEA-4 hexasaccharide on the surface. The K_d value for the interaction was 4.21 ± 0.26 nM (Fig. 2, *Inset*), showing that MC813-70 is highly specific for SSEA-4.

Table 1. Expression profiles of glycan-related epitopes in GBM cell lines LN-18, U-138, U-251, and G5T

Antigen	LN-18	U-138	U-251	G5T
TF	83.3 ± 3.4	76.1 ± 17.7	12.8 ± 11.7	5.8 ± 0.2
Tn	77.7 ± 4.3	49.9 ± 28.5	54.2 ± 18.2	20.7 ± 12.5
sTn	5.1 ± 0.3	10.9 ± 5.9	5.3 ± 0.5	4.9 ± 0.8
Le^x	6.2 ± 0.7	22.2 ± 17.7	74.2 ± 14.6	76.5 ± 10.6
Le^y	29.3 ± 9.9	46.0 ± 31.3	61.9 ± 21.8	8.8 ± 1.2
sLe^x	4.8 ± 0.5	32.8 ± 1.7	8.2 ± 5.2	5.4 ± 0.3
GM2	82.8 ± 23.9	97.2 ± 2.7	89.8 ± 14.1	38.4
GM1	98.5 ± 0.1	97.9 ± 1.6	74.6 ± 30.2	39.4
GD1a	96.9 ± 4.4	99.3 ± 1.0	88.0 ± 9.9	27.6
GD2	43.4 ± 11.6	23.4 ± 9.7	10.3 ± 4.2	15.4 ± 8.9
GT1b	97.6 ± 3.3	96.1 ± 0.9	88.8 ± 1.5	30.1 ± 7.1
A2B5	58.2 ± 41.1	59.2 ± 12.0	36.6 ± 18.0	21.1 ± 11.4
SSEA-3	75.9 ± 16.2	38.9 ± 26.0	27.1 ± 24.8	97.7 ± 3.0
SSEA-4	99.6 ± 0.2	90.5 ± 16.4	43.1 ± 10.8	99.9 ± 0.1
Globo H	22.5	11.8	9.3 ± 4.0	5.5 ± 0.1

Expression of glycan-related epitopes was determined by flow cytometry as described in *Materials and Methods*. Values are the percentage (mean ± SD) of positive cells in total cells.

Verification of SSEA-4 Expression on GBM Cell Lines. To exclude the possibility that MC813-70 may bind to the extended core 1 O-glycan on glycoproteins in GBM cells, we treated DBTRG cells with methanol to remove lipids before staining with MC813-70. Upon methanol treatment, the immunoreactivity of MC813-70 disappeared, as analyzed by flow cytometry (Fig. S3*A*) and immunofluorescence microscopy (Fig. S3*B*), suggesting that MC813-70 is immunoreactive toward glycolipids, not glycoproteins. To confirm the presence of the SSEA-4 epitope on the GBM cell surface, we performed further MC631 staining on α2,3-sialidase–treated DBTRG cells (Fig. S4). When treated with α2,3-sialidase, the cells became MC813-70^- and $MC631^+$, indicating that the GBM cells did express SSEA-4.

To verify the expression of SSEA-4 further, we next purified the gangliosides using anion-exchange chromatography, developed the purified gangliosides on HPTLC plates, and visualized them by orcinol-H_2SO_4 staining or immunoblotting. As shown in Fig. *S5A*, the purified gangliosides from three different GBM cell lines exhibited similar patterns (Fig. *S5A*, *Left*, lanes 1–3), with abundant GM3, GM2, Neu5Ac-(n)Lc4/Gg4Cer, and Neu5Ac2-(n)Lc4/Gg4Cer. Consistent with the results of flow cytometric analysis, MC813-70 recognized two gangliosides (because of a

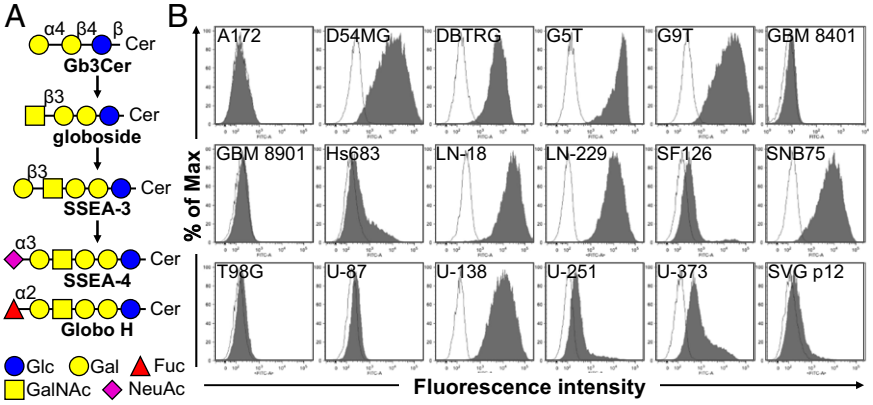

Fig. 1. The binding characteristics of mAb MC813-70 to GBM cell lines. (*A*) Schematic diagram of the biosynthesis of globo-series GSLs. SSEA-3, the precursor of SSEA-4 and Globo H, is synthesized from globoside. Glycosidic linkages and graphic notations are labeled. Glc, glucose; Gal, galactose; GalNAc, *N*-acetylgalactosamine; Fuc, fucose; NeuAc, *N*-acetylneuraminic acid. (*B*) GBM cells were stained with Alexa Fluor 488-conjugated MC813-70, and the staining intensity was analyzed with flow cytometry. All cells examined were GBM cell lines except for SVG p12, which is a normal human fetal glial cell line transformed with SV40 large T antigen. The histograms of the cells stained with MC813-70 and isotype control are shown in gray and white, respectively.

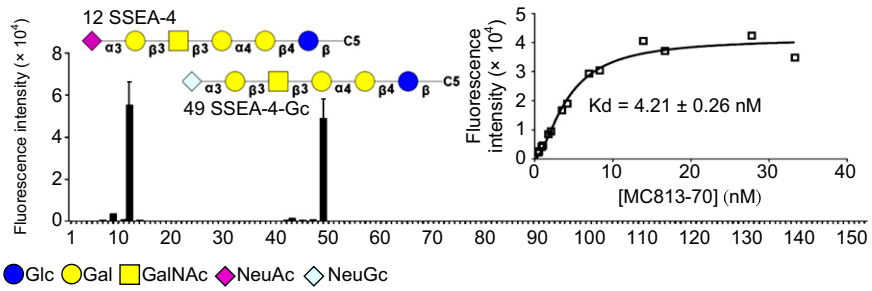

Fig. 2. The glycan-binding profile of mAb MC813-70. The glycan microarrays on glass slides were probed with Alexa Flour 647-conjugated MC813-70 (10 μg/mL) and were read in an array scanner at 635 nm. Data are presented as mean ± SD. C5, C5H10NH2. (*Inset*) The binding curve of MC813-70 to SSEA-4. The dissociation constant (K_d) of mAb MC813-70 toward SSEA-4 was detected on a glass slide printed with SSEA-4 glycan.

different chain length of fatty acids) on TLC from DBTRG and D54MG cells but not from GBM 8901 cells (Fig. 3*A*). The positions of the immunoreactive double bands in GBM gangliosides were the same as in the gangliosides purified from 2102Ep cells, which are embryonal carcinoma cells known to express a high level of SSEA-4 glycolipid (Fig. 3*A*, lane 4) (22). A double band that developed at a shorter distance than the MC813-70$^+$ glycolipid was detected by MC813-70 in YAC-1 cells (Fig. 3*A*, lane 5), in which GM1b is a major ganglioside (29), indicating that MC813-70 harbors a weak cross-reactivity toward GM1b. Immunoblotting with MC631 revealed that it also could recognize MC813-70$^+$ glycolipid but with a lower affinity than MC813-70 (Fig. S5*A*, *Right*). To examine the number of sialic acids on MC813-70$^+$ glycolipids, we eluted gangliosides in different salt conditions and performed immunoblotting with MC813-70. The result indicated that MC813-70–reactive gangliosides were monosialylated, because the two bands appeared at the fraction eluted in the low-salt condition (Fig. S5*B*). We next used sialidases to elucidate the linkage of the sialic acid on this MC813-70–reactive monosialoganglioside. Gangliosides developed on a TLC plate were treated with α2,3-sialidase, the sialidase that cleaves all linkages of sialic acids, and were blotted with MC813-70 and MC631. The results in Fig. S5*C* show that the immunoreactivity of MC813-70 disappeared after sialidase treatment (Fig. S5*C*, *Center*), whereas MC631 could detect strong signals (dashed rectangle in Fig. S5*C*, *Right*) at the positions resembling MC813-70–reactive doublets, indicating the presence of an α2,3-linked sialic acid.

We also analyzed the gangliosides from DBTRG cells by MALDI-MS profiling (Fig. 3*B*). The spectra were dominated by several major peaks that occurred in signal clusters because of the expected heterogeneity of the ceramide (Cer) portions. The respective gangliosides profiles were assigned based on the *m/z* values of major molecular ions, as fitted to permethylation of hexose (Hex), *N*-acetylhexosamine (HexNAc), or NeuAc residues, in combination with sphingosine and fatty acyl chains,. Consistent with the HPTLC results, MS profiling showed that the major species of gangliosides in DBTRG cells were GM3, GM2, Neu5Ac-(n)Lc4/Gg4Cer, and Neu5Ac2-(n)Lc4/Gg4Cer. The signal with Neu5Ac-Hex4-HexNAc-Cer (*m/z* = 2025.2) that represented SSEA-4 was detected also, although with low intensity, reflecting the existence of SSEA-4 in DBTRG cells. These data indicate that the MC813-70–reactive ganglioside was SSEA-4 and that, although it was a minor constituent of total gangliosides, SSEA-4 was expressed in GBM cells.

Expression of SSEA-4 in GBM Tissues. SSEA-4 is a widely used marker for stem cells, but information about the expression of SSEA-4 in GBM tissues as well as normal brain tissues has been limited. To understand if SSEA-4 is overexpressed in clinical GBM specimens, in addition to GBM cell lines, we analyzed the expression of SSEA-4 in grade I– IV astrocytomas and in normal brain tissues by immunohistochemistry (IHC) on human tissue microarrays (Fig. 4 and Fig. S6). We found that 38 of 55 GBM tissue specimens (69%) were positive for MC813-70 staining and around half of the GBM specimens were intensely stained, with a score of 2+ or higher (Fig. 4*C* and Fig. S6*A*). As shown in the positive specimens, SSEA-4 was situated on the plasma membrane of GBM cells (Fig. 4*B*, *Inset*). Furthermore, around 55% of low-grade astrocytoma specimens were weakly stained (scored as 1+) by MC813-70, and the SSEA-4 intensity scores correlated positively with astrocytoma grade (Fig. S6*B*). Most normal brain tissues were SSEA-4$^-$ (Fig. 4*A*). These results indicated SSEA-4 is highly expressed in GBM tumors.

MC813-70 Mediates Complement-Dependent Cytotoxicity Against GBM Cell Lines. To test if targeting SSEA-4 triggers complement-dependent cytotoxicity (CDC) in GBM cells, GBM cell lines were treated with MC813-70 and rabbit complement, and the degree of CDC was evaluated by detecting the level of released lactate dehydrogenase (LDH) caused by cell death. Fig. 5 shows that, in the presence of complement, mAb MC813-70 remarkably reduced the number of viable GBM cells. We observed a significant CDC in SSEA-4^{hi} GBM cell lines: 71.7% cytotoxicity of DBTRG, 46.6% of LN-229, 67% of G5T, and

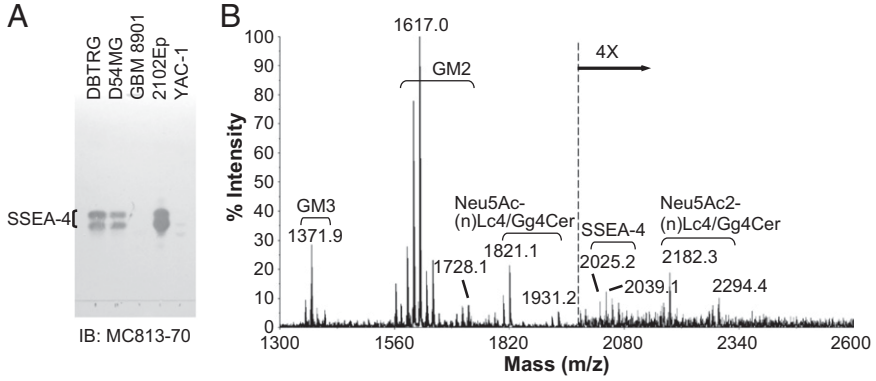

Fig. 3. HPTLC immunostaining and MALDI-MS profiles of gangliosides from GBM cell lines. (*A*) Gangliosides were separated on an HPTLC plate and detected with MC813-70 mAb. Gangliosides from 2012Ep (a human embryonal carcinoma cell line) and YAC-1 (a mouse lymphoma cell line) served as the positive controls for SSEA-4 and GM1b, respectively. SSEA-4 with different chain lengths of fatty acids migrated as two close bands. (*B*) The extracted gangliosides from DBTRG GBM cells were permethylated and analyzed by MALDI-MS. The major gangliosides in DBTRG cells were GM3 (*m/z* = 1,371.9), GM2 (*m/z* = 1,617.0), Neu5Ac-(n)Lc4/Gg4Cer (*m/z* = 1,821.1), and Neu5Ac2-(n)Lc4/Gg4Cer (*m/z* = 2,182.3). SSEA-4 (Neu5Ac-Hex4-HexNAc-Cer, *m/z* = 2025.2) was also observed, albeit in a relatively weak signal. Gangliosides with the same glycan moiety but with different fatty acyl contents are bracketed.

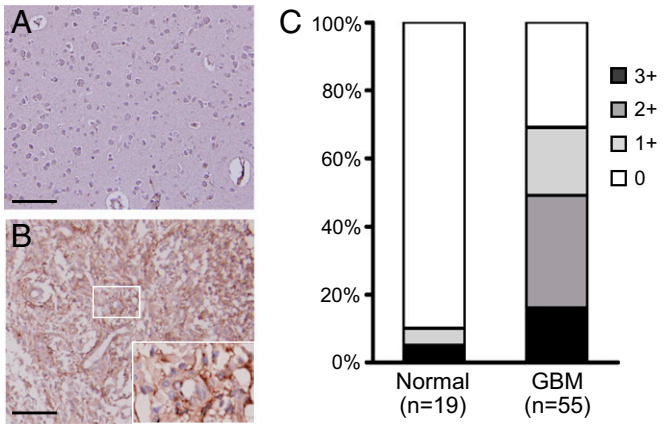

Fig. 4. Expression of SSEA-4 in GBM. (*A* and *B*) Representative images of normal brain tissues (*A*) and GBM (*B*) after immunohistochemical staining with MC-813–70. The inset in *B* shows a magnified picture of the small boxed area. (Scale bars, 100 μm.) (*C*) Statistical results of SSEA-4 IHC. GBM specimens (n = 55) and normal brain tissues (n = 19) were counterstained with hematoxylin after IHC. The staining intensity of the tissues was graded as 0 (negative), 1+ (weak), 2+ (moderate), and 3+ (strong).

65.4% of LN-18 cells. MC813-70–mediated CDC did not kill two GBM cell lines, Hs683 and U87, that expressed low or no SSEA-4. Therefore, the level of MC813-70–mediated CDC correlated positively with the level of SSEA-4expression in each GBM cell line.

MC813-70 Suppresses Brain Tumor Growth in Vivo. To check if MC813-70 was able to suppress GBM tumor growth in vivo, MC813-70 was administered to the nude mice injected s.c. with DBTRG cells when the tumors grew to palpable bumps (15–30 mm^3 at day 11 postinjection). MC813-70 (200 μg) was given i.p. to each mouse every 4 d for a total of three times; an irrelevant mouse IgG3 (isotype control) was injected in parallel for comparison. The experiment revealed that the administration of MC813-70 could inhibit tumor growth in DBTRG cells (Fig. 6). The growth of DBTRG tumors was completely suppressed in two of three mice treated with MC813-70; the third mouse developed tumor after the cessation of antibody treatment. As compared with mice receiving MC813-70 treatment, DBTRG tumors grew aggressively (with an average tumor volume of 184 mm^3 at day 31) in the control group injected with mouse IgG3. These results demonstrated that MC813-70 can inhibit the growth of SSEA-4–expressing GBM tumors, possibly through CDC and antibody-dependent cell-mediated cytotoxicity in vivo.

Expression of SSEA-4 in Various Cancer Cell Lines. SSEA-4 expression has been reported on renal carcinoma (26), basaloid lung cancer (30), epithelial ovarian carcinoma (31), breast cancer (25), and oral cancer (32) cells. Here, we analyzed the expression levels of SSEA-3, Globo H, and SSEA-4 on various cancer cell lines by flow cytometry. As shown in Table 2, we examined 134 cancer cell lines (17 brain cancer cell lines, 20 lung cancer cell lines, 23 breast cancer cell lines, 13 oral cancer cell lines, two esophageal cancer cell lines, six gastric cancer cell lines, 10 liver cancer cell lines, five bile duct cancer cell lines, eight pancreatic cancer cell lines, seven colon cancer cell lines, six renal cancer cell lines, four cervical cancer cell lines, nine ovarian cancer cell lines, and four prostate cancer cell lines). The names and the expressed GSLs of these cell lines are listed in Table S1. We found that SSEA-4 was expressed in every type of cancer cell line (in 96 of 134 cancer cell lines). Globo H was expressed in 88 of 134 cancer cell lines, preferentially in lung, breast, pancreas, colon, stomach, mouth, liver, and kidney cancer cell lines, and 70 of 134 cancer cell lines expressed SSEA-4 and Globo H simultaneously. On the other hand, SSEA-3 expression was always accompanied by a high level of SSEA-4 expression, indicating that SSEA-4 and Globo H are the major globo-series GSLs on the cancer cells. To validate the identity of SSEA-4, we purified the gangliosides from nine MC813-70$^+$ cell lines and from TF1a, an MC813-70$^-$ leukemia cell line, and performed immunostaining on HPTLC plates. As expected, SSEA-4 was detected in these nine cancer cell lines but not in TF1a (Fig. S7), and the intensity correlated well with the geometric mean fluorescence intensity as examined by flow cytometry. These results showed that SSEA-4 can be expressed in a variety of cancer cell lines and may serve as a potential target for multiple types of cancers.

Discussion

In the present study, we evaluated the expression of globo-series GSLs on human GBM cell lines and found that SSEA-4 is highly expressed in most GBM cell lines; SSEA-3 and Globo H also are expressed at lower levels.

SSEA-4, first identified in 1983 (22), often has been used as a pluripotency marker for hESCs and for the isolation and characterization of cells with stem cell properties. Nonetheless, information about the distribution of SSEA-4 in normal tissues is limited. SSEA-4 has been reported to be expressed as a minor GSL in erythrocytes (22) and on the epithelial cells of several glandular tissues [e.g., breast, colon, gastrointestinal tract, kidney, lung, ovary, pancreas, rectum, stomach, testes, thymus, and uterine cervix (24)]. In solid tumors, SSEA-4 expression was found on renal cell carcinomas in 1997 by Saito et al. (26) using IHC with RM1, another SSEA-4 mAb. In the last few years, SSEA-4 expression has been reported on breast cancer cells and breast cancer stem cells (25), basaloid lung cancer (30), epithelial ovarian carcinoma (31), and oral cancer (32). The relationship between the level of SSEA-4 expression and tumor malignancy differs in various types of cancers: The expression of SSEA-4 in basaloid lung cancer is associated with poor prognosis (30), whereas a reduction of SSEA-4 correlates with more advanced tumor stage and tumor cell differentiation in ovarian cancer (31). Here, we examined the expression of SSEA-4 in GBM and found that SSEA-4 is expressed not only in GBM/grade IV astrocytoma but also in ∼55% of grade I, ∼55% of grade II, and ∼60% of grade III astrocytoma. Nevertheless, there appears to be a trend for higher expression of SSEA-4 to be associated with higher grade of astrocytomas. We propose that SSEA-4 may play an active role during tumor progression of astrocytomas and may

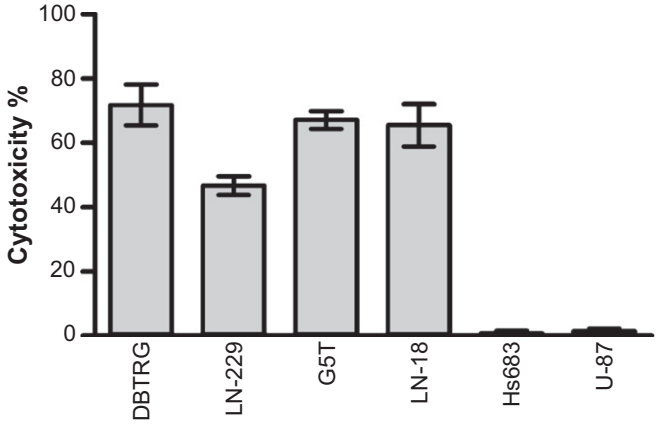

Fig. 5. MC813-70 triggered CDC in GBM cells. GBM cell lines were treated with 20 μg/mL MC813-70 and rabbit complement to observe MC813-70–induced cell lysis. The CDC activity of MC813-70 was measured by the LDH release assay as described in *Materials and Methods*. The data are shown as mean ± SD.

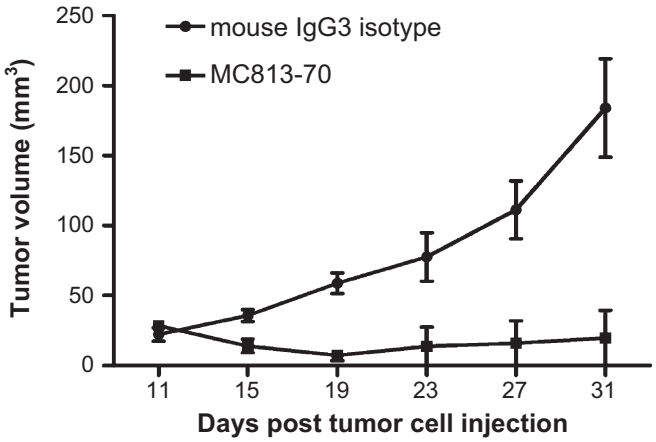

Fig. 6. Inhibition of DBTRG tumor growth by MC813-70. On day 0, male nude mice were inoculated with DBTRG cells in the right flank, and MC813-70 or mouse IgG3 isotype control (200 μg per dose) was administered i.p. at days 11, 15, and 19. Mice were killed at day 31. The tumor volume in each group ($n = 3$) was measured at different time points and is shown as mean ± SD. $P = 0.001$ was obtained by two-way ANOVA.

serve as a potential therapeutic target in patients with GBM as well as low-grade astrocytomas. Furthermore, we provide evidence that SSEA-4 is expressed in multiple cancer cell lines, including lung, breast, ovarian, prostate, colon, and pancreatic cancers.

Although SSEA-4 has been known for more than 20 y, the molecular function of SSEA-4 has not been tested experimentally. Brimble et al. (33) depleted SSEA-3 and -4 in hESCs with D-threo-1-phenyl-2-decanoylamino-3-morpholino-1-propanol (D-PDMP), an inhibitor for glucosylceramide synthase, and found that D-PDMP treatment did not alter the gene-expression profile of hESCs or alter their capacity to differentiate in vitro, suggesting that SSEA-4 is not essential for hESCs' pluripotency. On the other hand, Van Slambrouck et al. (34) demonstrated that clustering of monosialyl-Gb5 induces the invasion of MCF-7 breast cancer cells by activating the FAK/c-Src signaling pathway. Recently, SSEA-4 was reported to bind to FK-506–binding protein 4, which may affect the transportation of SSEA-4 to the cell surface and the downstream signaling pathway (35).

In addition to SSEA-4, we examined the expression of two other globo-series GSLs, SSEA-3 and Globo H. SSEA-3 was expressed mainly in cell lines with high SSEA-4 expression. This result, together with the observation of Globo H expression in only six of the GBM cell lines we tested, indicates that SSEA-4 is the major globo-series GSL in GBM and that, once SSEA-3 is synthesized, it is converted efficiently to SSEA-4 (24). It has been suggested that an α2,3-sialyltransferase, encoded by *ST3GAL2* gene, is the major SSEA-4 synthase that is closely related to renal carcinogenesis (36) and that the mRNA level of *ST3GAL2* is increased in renal and colorectal carcinomas (37). We also observed that the mRNA level of *ST3GAL2*, but not of *fucosyltransferase (FUT) 1* and *2*, is abundant in GBM cell lines (Fig. S8), perhaps explaining why SSEA-4 is the predominant globo-series GSL in GBM cells. It is also interesting to establish the correlation of *A4GALT*, *ST3GAL2*, *FUT1*, and *FUT2* mRNA levels with the expression of globo-series GSLs in GBM specimens, to help detect globo-series GSLs in small amounts of tumor samples.

Targeted therapy, which blocks tumor growth by using small molecules or mAbs to interfere with specific molecules, is a growing part of many cancer treatment regimens (38); for example, a series of anti-EGFRvIII mAbs has been generated for GBM therapy (39, 40). Moreover, anti-glycolipid–targeted therapy is showing great promise in the treatment of several cancers (41) [e.g., anti-GD2 in neuroblastoma (42)]. In addition, a recent report indicates that a Globo H-DT vaccine can elicit specific IgG not only against Globo H but also against SSEA-3 and SSEA-4 (25). The expression profile of these three glycolipids in different types of cancer cell lines, as shown in Table 2, provides a direction in cancer vaccine therapy. In addition, our finding of high-level SSEA-4 expression in GBM provides a potential target for GBM diagnosis and therapy.

Materials and Methods

For additional details, see *SI Materials and Methods*.

Flow Cytometry. Cells (1×10^5) were stained with 0.5 μg Alexa Flour 488-conjugated anti–SSEA-3 mAb (MC-631), anti–SSEA-4 mAb (MC813-70), or allophycocyanin (APC)-conjugated anti-Globo H mAb (VK9, a gift from Philip O. Livingston, Memorial Sloan–Kettering Cancer Center, New York) in 50 μL FACS buffer (PBS solution with 1% FBS) on ice for 30 min. For lectin staining, cells were incubated for 30 min on ice in lectin-binding buffer [1% BSA, 0.5× Carbo-Free Blocking buffer (Vector Laboratories), 2 mM $MgCl_2$, 2 mM $CaCl_2$] containing biotinylated lectin. After being washed twice with lectin-binding buffer, cells were incubated with streptavidin-APC (1:500 diluted in FACS buffer; Biolegend). After being washed twice with 200 μL FACS buffer, cells were resuspended in 200 μL FACS buffer containing 1 μg/mL propidium iodide (PI) and subjected to analysis. Data acquisition was performed on a FACSCanto (BD Biosciences) with FACSDiva software (BD Biosciences), and data analyses were performed using FlowJo software (TreeStar). Live PI^- cells were gated for analysis. For methanol washing, cells were washed and fixed

Table 2. Expression of globo-series GSLs in cancer cell lines

Tumor origin	SSEA-4$^+$	SSEA-3$^+$	Globo H$^+$	SSEA4$^+$ or SSEA3$^+$ or Globo H$^+$	SSEA-4$^+$ SSEA-3$^+$	SSEA-4$^+$ Globo H$^+$	SSEA-4$^+$ SSEA-3$^+$ Globo H$^+$
Brain	12/17	9/17	6/17	12/17	9/17	6/17	5/17
Lung	13/20	5/20	13/20	16/20	5/20	10/20	5/20
Breast	17/23	6/23	14/23	18/23	6/23	13/23	6/23
Mouth	8/13	2/13	11/13	12/13	2/13	7/13	2/13
Esophagus	1/2	0/2	2/2	2/2	0/2	1/2	0/2
Stomach	4/6	3/6	6/6	6/6	3/6	4/6	3/6
Liver	6/10	4/10	9/10	9/10	4/10	6/10	4/10
Bile duct	2/5	1/5	3/5	3/5	1/5	2/5	1/5
Pancreas	8/8	3/8	6/8	8/8	3/8	6/8	3/8
Colon	5/7	0/7	6/7	7/7	0/7	4/7	0/7
Kidney	5/6	0/6	5/6	6/6	0/6	4/6	0/6
Cervix	3/4	2/4	1/4	3/4	2/4	1/4	0/4
Ovary	8/9	2/9	5/9	8/9	2/9	5/9	2/9
Prostate	4/4	1/4	1/4	4/4	1/4	1/4	0/4

Expression of globo-series GSLs was determined by flow cytometry. Cell lines in which more than 15% of total cells were positive in flow cytometry are labeled positive.

with 4% (wt/vol) paraformaldehyde in PBS for 15 min at room temperature, followed by incubation in methanol for 10 min before staining with specific antibodies.

TLC Immunostaining. GSLs were separated on HPTLC plates as described above. After chromatography, the TLC plate was air-dried, immersed three times in 2.1% (wt/vol) poly(isobutyl-methacrylate) (Sigma) in hexane/chloroform (42:8, vol/vol), and soaked overnight in PBS at 37 °C. The plate was dried, blocked with in PBS for 30 min at room temperature, and reacted with MC813-70 or MC-631 (5 μg/mL) for 2 h at room temperature. After being gently washed three times with PBS and 0.05% Tween-20 (PBST), the plate was incubated with biotinylated secondary antibody (1 μg/mL) for 1 h, followed by incubation with streptavidin-alkaline phosphatase (1:1,000; Millipore). After washing with PBST, the TLC plate was developed with nitro blue tetrazolium/(5-bromo-4-chloro-1H-indol-3-yl) dihydrogen phosphate (Thermo Scientific).

In Vivo Tumor Growth. BALB/cAnN.Cg-Foxn1nu/CrlNarl mice were purchased from the National Laboratory Animal Center (Taiwan) and maintained under specific pathogen-free conditions. The animals' health status was monitored daily. Procedures involving animals and their care were conducted according to the guidelines of the Academia Sinica Institutional Animal Care and Utilization Committee in compliance with national and international laws and policies. DBTRG cells (1×10^7/250 μL PBS) were s.c. injected into the flank regions of 8- to 10-wk-old mice to generate the xenograft model. On days 11, 15, and 19, each mouse was i.p. injected with 200 μg of MC813-70 (purified from the ascites) or with mouse IgG3 isotype as the control antibody. Tumor size was determined by Vernier caliper by measuring the length (L) and width (W), and the tumor volume (in mm^3) was calculated as $1/2 \times LW^2$.

ACKNOWLEDGMENTS. We thank Drs. Jin-Yuh Shew, Hua-Chien Chen, Chia-Ning Shen, and Shih-Hwa Chiou for providing various cancer cell lines and the Genomics Research Center MS Core Facilities, Academia Sinica, for glycolipid analysis. We are also grateful to the experimental assistance from Dr. Chien-Yu Chen and Tsung-Ching Lai. This research was supported by the Genomics Research Center, Academia Sinica, Taiwan.

1. Louis DN, et al. (2007) The 2007 WHO classification of tumours of the central nervous system. *Acta Neuropathol* 114(2):97–109.
2. Van Meir EG, et al. (2010) Exciting new advances in neuro-oncology: The avenue to a cure for malignant glioma. *CA Cancer J Clin* 60(3):166–193.
3. Meyer MA (2008) Malignant gliomas in adults. *N Engl J Med* 359(17):1850, author reply 1850.
4. Meezan E, Wu HC, Black PH, Robbins PW (1969) Comparative studies on the carbohydrate-containing membrane components of normal and virus-transformed mouse fibroblasts. II. Separation of glycoproteins and glycopeptides by sephadex chromatography. *Biochemistry* 8(6):2518–2524.
5. Hakomori S (2002) Glycosylation defining cancer malignancy: New wine in an old bottle. *Proc Natl Acad Sci USA* 99(16):10231–10233.
6. Lau KS, Dennis JW (2008) N-Glycans in cancer progression. *Glycobiology* 18(10): 750–760.
7. van Beek WP, Smets LA, Emmelot P (1973) Increased sialic acid density in surface glycoprotein of transformed and malignant cells—a general phenomenon? *Cancer Res* 33(11):2913–2922.
8. Sell S (1990) Cancer-associated carbohydrates identified by monoclonal antibodies. *Hum Pathol* 21(10):1003–1019.
9. Hakomori S, Zhang Y (1997) Glycosphingolipid antigens and cancer therapy. *Chem Biol* 4(2):97–104.
10. Taylor-Papadimitriou J, Epenetos AA (1994) Exploiting altered glycosylation patterns in cancer: Progress and challenges in diagnosis and therapy. *Trends Biotechnol* 12(6): 227–233.
11. Birklé S, Zeng G, Gao L, Yu RK, Aubry J (2003) Role of tumor-associated gangliosides in cancer progression. *Biochimie* 85(3-4):455–463.
12. Fredman P, et al. (1986) Potential ganglioside antigens associated with human gliomas. *Neurol Res* 8(2):123–126.
13. Yates AJ, Becker LE, Sachs LA (1979) Brain tumors in childhood. *Childs Brain* 5(1): 31–39.
14. Traylor TD, Hogan EL (1980) Gangliosides of human cerebral astrocytomas. *J Neurochem* 34(1):126–131.
15. Berra B, Gaini SM, Riboni L (1985) Correlation between ganglioside distribution and histological grading of human astrocytomas. *Int J Cancer* 36(3):363–366.
16. Fredman P, von Holst H, Collins VP, Granholm L, Svennerholm L (1988) Sialyllactotetraosylceramide, a ganglioside marker for human malignant gliomas. *J Neurochem* 50(3):912–919.
17. Månsson JE, et al. (1986) Characterization of new gangliosides of the lactotetraose series in murine xenografts of a human glioma cell line. *FEBS Lett* 201(1):109–113.
18. Fredman P, von Holst H, Collins VP, Dellheden B, Svennerholm L (1993) Expression of gangliosides GD3 and 3′-isoLM1 in autopsy brains from patients with malignant tumors. *J Neurochem* 60(1):99–105.
19. Svennerholm L, et al. (1989) Human brain gangliosides: Developmental changes from early fetal stage to advanced age. *Biochim Biophys Acta* 1005(2):109–117.
20. Kato Y, et al. (2010) GMab-1, a high-affinity anti-3′-isoLM1/3′,6′-isoLD1 IgG monoclonal antibody, raised in lacto-series ganglioside-defective knockout mice. *Biochem Biophys Res Commun* 391(1):750–755.
21. Schenkel-Brunner H (1995) *P System. Human Blood Groups* (Springer Vienna), pp 211–234.
22. Kannagi R, et al. (1983) Stage-specific embryonic antigens (SSEA-3 and -4) are epitopes of a unique globo-series ganglioside isolated from human teratocarcinoma cells. *EMBO J* 2(12):2355–2361.
23. Zhang S, et al. (1997) Selection of tumor antigens as targets for immune attack using immunohistochemistry: I. Focus on gangliosides. *Int J Cancer* 73(1):42–49.
24. Chang WW, et al. (2008) Expression of Globo H and SSEA3 in breast cancer stem cells and the involvement of fucosyl transferases 1 and 2 in Globo H synthesis. *Proc Natl Acad Sci USA* 105(33):11667–11672.
25. Huang YL, et al. (2013) Carbohydrate-based vaccines with a glycolipid adjuvant for breast cancer. *Proc Natl Acad Sci USA* 110(7):2517–2522.
26. Saito S, et al. (1997) Expression of globo-series gangliosides in human renal cell carcinoma. *Jpn J Cancer Res* 88(7):652–659.
27. Kannagi R, et al. (1983) New globoseries glycosphingolipids in human teratocarcinoma reactive with the monoclonal antibody directed to a developmentally regulated antigen, stage-specific embryonic antigen 3. *J Biol Chem* 258(14):8934–8942.
28. Wang CC, et al. (2008) Glycan microarray of Globo H and related structures for quantitative analysis of breast cancer. *Proc Natl Acad Sci USA* 105(33):11661–11666.
29. Zarei M, Müthing J, Peter-Katalinić J, Bindila L (2010) Separation and identification of GM1b pathway Neu5Ac- and Neu5Gc gangliosides by on-line nanoHPLC-QToF MS and tandem MS: Toward glycolipidomics screening of animal cell lines. *Glycobiology* 20(1): 118–126.
30. Gottschling S, et al. (2013) Stage-specific embryonic antigen-4 is expressed in basaloid lung cancer and associated with poor prognosis. *Eur Respir J* 41(3):656–663.
31. Ye F, et al. (2010) Stage-specific embryonic antigen 4 expression in epithelial ovarian carcinoma. *Int J Gynecol Cancer* 20(6):958–964.
32. Noto Z, et al. (2013) CD44 and SSEA-4 positive cells in an oral cancer cell line HSC-4 possess cancer stem-like cell characteristics. *Oral Oncol* 49(8):787–795.
33. Brimble SN, et al. (2007) The cell surface glycosphingolipids SSEA-3 and SSEA-4 are not essential for human ESC pluripotency. *Stem Cells* 25(1):54–62.
34. Van Slambrouck S, Steelant WF (2007) Clustering of monosialyl-Gb5 initiates downstream signalling events leading to invasion of MCF-7 breast cancer cells. *Biochem J* 401(3):689–699.
35. Hung TC, Lin CW, Hsu TL, Wu CY, Wong CH (2013) Investigation of SSEA-4 binding protein in breast cancer cells. *J Am Chem Soc* 135(16):5934–5937.
36. Saito S, et al. (2003) Human alpha2,3-sialyltransferase (ST3Gal II) is a stage-specific embryonic antigen-4 synthase. *J Biol Chem* 278(29):26474–26479.
37. Kudo T, et al. (1998) Up-regulation of a set of glycosyltransferase genes in human colorectal cancer. *Lab Invest* 78(7):797–811.
38. Green MR (2004) Targeting targeted therapy. *N Engl J Med* 350(21):2191–2193.
39. Mishima K, et al. (2001) Growth suppression of intracranial xenografted glioblastomas overexpressing mutant epidermal growth factor receptors by systemic administration of monoclonal antibody (mAb) 806, a novel monoclonal antibody directed to the receptor. *Cancer Res* 61(14):5349–5354.
40. Wikstrand CJ, Cokgor I, Sampson JH, Bigner DD (1999) Monoclonal antibody therapy of human gliomas: Current status and future approaches. *Cancer Metastasis Rev* 18(4):451–464.
41. Durrant LG, Noble P, Spendlove I (2012) Immunology in the clinic review series; focus on cancer: Glycolipids as targets for tumour immunotherapy. *Clin Exp Immunol* 167(2):206–215.
42. Yu AL, et al.; Children's Oncology Group (2010) Anti-GD2 antibody with GM-CSF, interleukin-2, and isotretinoin for neuroblastoma. *N Engl J Med* 363(14):1324–1334.

Supporting Information

Lou et al. 10.1073/pnas.1400283111

SI Materials and Methods

Reagents. Anti-Lewis x (anti-Le^x), anti-sialyl Lewis x (anti-sLe^x), and anti-GD2 antibodies were purchased from BD Biosciences. Anti-GD1a, anti-GT1b, and Alexa Fluor 488 anti-A2B5 antibodies were purchased from Millipore. Antibodies against complex gangliosides GM1 and GM2 (anti-GM1 and anti-GM2, respectively) were purchased from Calbiochem. Anti-Lewis y (anti-Le^y) and anti-sialyl Tn (anti-sTn) antibodies were purchased from Abcam. Anti-Thomsen–Friedenreich (TF) antigen antibody was purchased from Thermo Scientific. Anti-Tn antibody was purchased from DakoCytomation. Fluorescence-labeled or purified MC813-70 (anti–SSEA-4 mAb) and MC631 were purchased from Biolegend. MC813-70 ascites was purchased from the Developmental Studies Hybridoma Bank at the University of Iowa. The use of these antibodies in individual experiments is described in the following paragraphs.

Cell Culture. U-251, U-138, LN-18, T98, LN-229, U87, U-373, Hs683, D54MG, GBM 8401, GBM 8901, G5T, G9T, SNB75, A172, and SF126 cells were routinely maintained in high-glucose DMEM (Life Technologies) supplemented with 10% (vol/vol) FBS (Biological Industries). DBTRG cells were maintained in RPMI 1640 (Life Technologies) with 10% (vol/vol) FBS.

Immunofluorescent Staining. Cells were plated on plastic tissue-culture chamber slides (Nunc) overnight to allow sufficient attachment, fixed with 4% (wt/vol) paraformaldehyde for 15 min at room temperature, washed three times with PBS, and then blocked with 3% (wt/vol) BSA in PBS. Cells then were incubated overnight with 10 μg/mL of mAb MC813-70 (Biolegend), washed three times with PBS, and incubated for 2 h at room temperature with 5 μg/mL FITC-conjugated anti-mouse IgG (eBioscience). Nuclei were counterstained with Hoechst 33342 (2 μg/mL) (Life Technologies). All images were acquired by an Olympus IX71 microscope.

Immunohistochemistry. For MC813-70 staining on normal brain and glioblastoma multiforme (GBM) specimens, three different tissue microarray slides (Biomax), comprising a total of 19 normal brain sections and 55 GBM sections, were tested. The slides were dried at 56 °C for 1 h, deparaffinized in xylene, and rehydrated in graded alcohols, followed by treatment with blocking buffer [2% (wt/vol) Blocking Reagent (Roche) in PBS with 0.1% Triton X-100] for 30 min at room temperature. The slides then were incubated overnight at 4 °C with mAb MC813-70 (10 μg/mL) in blocking buffer. After gentle washing with PBS and Tween-20 (PBST), the immunoreactivity on specimens was detected with the SuperSensitive Polymer-HRP IHC Detection System (BioGenex), and the slides were counterstained with hematoxylin and prepared for mounting.

Glycan Array Fabrication. Microarrays were printed (BioDot; Cartesian Technologies) by robotic pin (SMP3; TeleChem International Inc.) with the deposition of ∼0.6 nL per spot. Amine-containing glycans in printing buffer [300 mM sodium phosphate (pH 8.5), 0.01% Triton X-100] were spotted onto *N*-Hydroxysuccinimide (NHS)-activated glass slides. Each glycan was printed at 100 μM in a replicate of four or at 50 μM in a replicate of six for K_d determination. Printed slides were allowed to incubate in 80% humidity for 30 min, followed by desiccation overnight. Remaining NHS groups were blocked by immersing the slides for 1 h in SuperBlock (PBS) Blocking Buffer (Pierce).

Antibody-Binding Assay. mAb MC813-70 (Alexa Fluor 647; Biolegend) was prepared in 100 μL of PBS-BSA-Tween (pH 7.4, with 3% (wt/vol) BSA and 0.05% Tween-20) and applied to cover the grid. After incubation in a moist chamber for 30 min, the slides were rinsed with PBST and deionized water and were blow-dried. The slides were scanned at 635 nm in GenePix 4300A (Molecular Devices). Data were analyzed by GenePix Pro-6.0 (Molecular Devices).

Sialidase Treatment. Cells were washed and resuspended in PBS buffer at 1×10^7 cells/mL. Cells (10^6 cells/100 μL) were incubated with or without 500 mU α2,3 sialidase (New England BioLabs) for 1 h at 37 °C and were washed twice with FACS buffer followed by surface staining and flow cytometry. The efficiency of sialidase treatment was measured by biotinylated *Maackia amurensis* lectin II (MAL II; Vector Laboratories), which recognizes α2,3-linked sialic acids.

Extraction of Glycosphingolipids. Cells (4×10^7) were harvested, washed, with PBS, and homogenized in water. Methanol and chloroform were added to the homogenate at a ratio of 8:4:3 (vol/vol/vol), and the sample was incubated in a bath sonicator for 30 min. After centrifugation at 3,000 × *g* for 15 min, the pellet was repeatedly extracted with 4:8:3 (vol/vol/vol) chloroform/methanol/water, and the combined supernatant was dried under a stream of nitrogen. The total lipid extract then was dissolved in chloroform/methanol/water (30:60:8, vol/vol/vol), and gangliosides were purified by DEAE-Sephadex A-25 (GE Healthcare)-based anion-exchange chromatography. Unbound flow-through containing neutral glycolipids was collected and dried. After washing with chloroform/methanol/water (30:60:8, vol/vol/vol), gangliosides were eluted with chloroform/methanol/aqueous NaCl (0.02, 0.2, and 0.8 M stepwise) (30:60:8, vol/vol/vol), followed by desalting with Sep-Pak C18 Cartridges (Waters). The extracts were dried under nitrogen, and the ganglioside residues and neutral glycolipid residues were redissolved in 100 μL chloroform/methanol (2:1, vol/vol).

High-Performance TLC. Glycosphingolipids (GSLs) were separated on high-performance TLC (HPTLC) plates precoated with glass-packed silica gel 60 (Merck). Gangliosides were chromatographed in chloroform/methanol/water (120:85:20, vol/vol/vol). and neutral GSLs were chromatographed in chloroform/methanol/water (120:70:17, vol/vol/vol), each supplemented with 2 mM $CaCl_2$. For analytic purposes, GSLs were stained with 0.3% orcinol in 3 M H_2SO_4 and then were transferred to a preheated heating plate (110 °C) until blue/purple spots appeared.

MALDI-MS Profiling and MS/MS Analysis. MALDI-MS analysis of permethylated glycans was conducted in an ABI 4700 Proteomics Analyzer (Applied Biosystems) using 2,5-dihydroxybenzoic acid (DHB) as the matrix (10 mg/mL). MALDI-MS/MS sequencing with low- and high-energy collision-induced dissociation was performed in a Q/TOF Ultima MALDI (Waters Micromass) and a 4700 Proteomics Analyzer using the DHB matrix as described above.

Complement-Dependent Cytotoxicity Assay. The complement-dependent cytotoxicity activity of anti–stage-specific embryonic antigen-4 (anti–SSEA-4) (MC813-70) mAb was measured by lactate dehydrogenase (LDH)-release assay using the CytoTox 96 Non-Radioactive Cytotoxicity Assay kit (Promega). Cells (1×10^4) were plated in each well of 96-well plates and were washed with PBS twice after overnight growth. The cells then

were incubated with 1 μg MC813-70 or mouse IgG3 isotype (control) in 50 μL phenol red-free DMEM or RPMI with rabbit complement (1:5 dilution) (Life Technologies). After incubation in a 5% CO_2 incubator at 37 °C for 1 h, the degree of cell lysis was determined by measuring the amount of LDH released into the culture supernatant. Maximum LDH release was determined by lysing the cells with the LYSIS Solution provided with the kit. Percentage of specific lysis was calculated according to the equation: % lysis = (experimental release − spontaneous release)/(maximum release − spontaneous release) × 100.

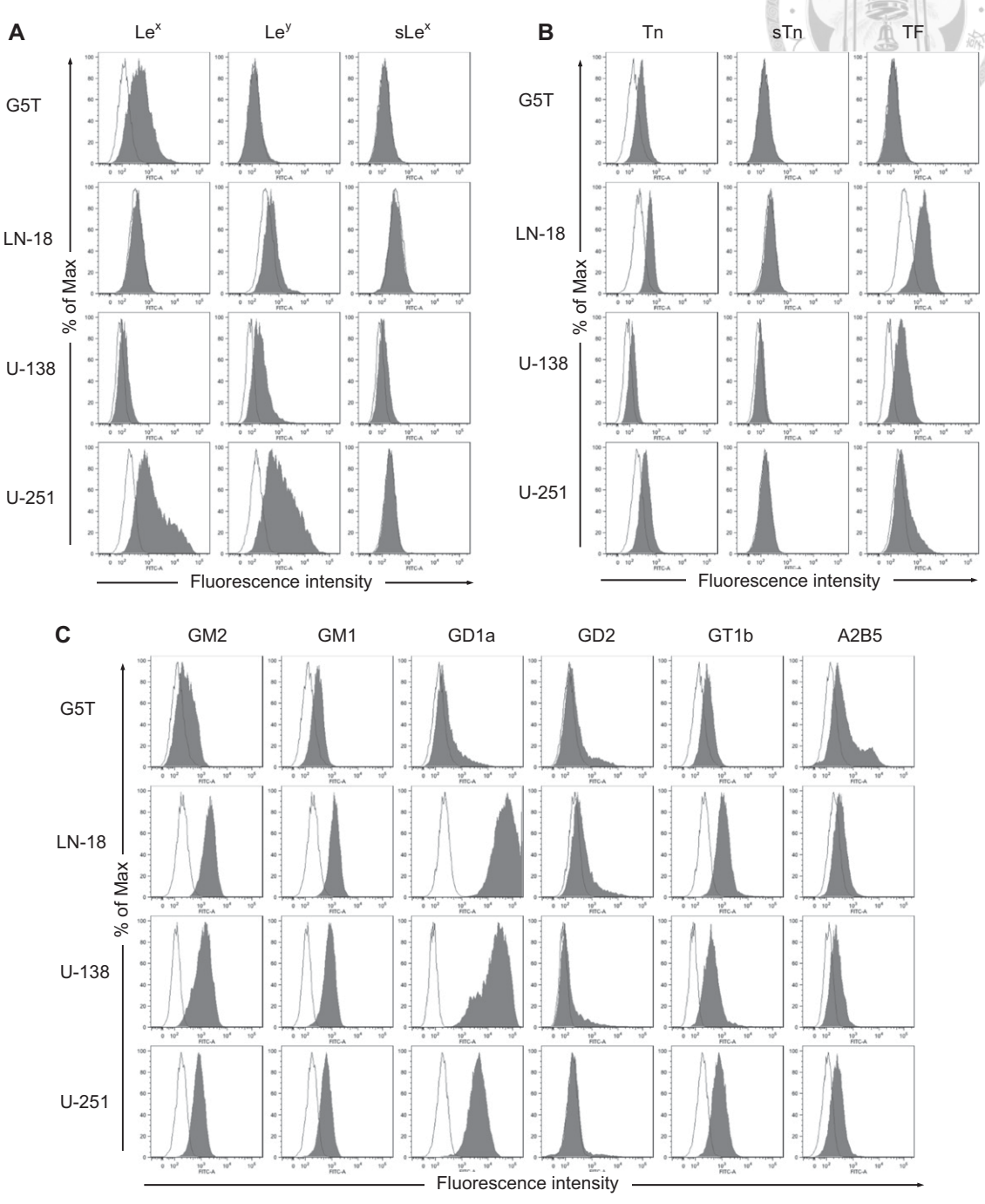

Fig. S1. (Continued)

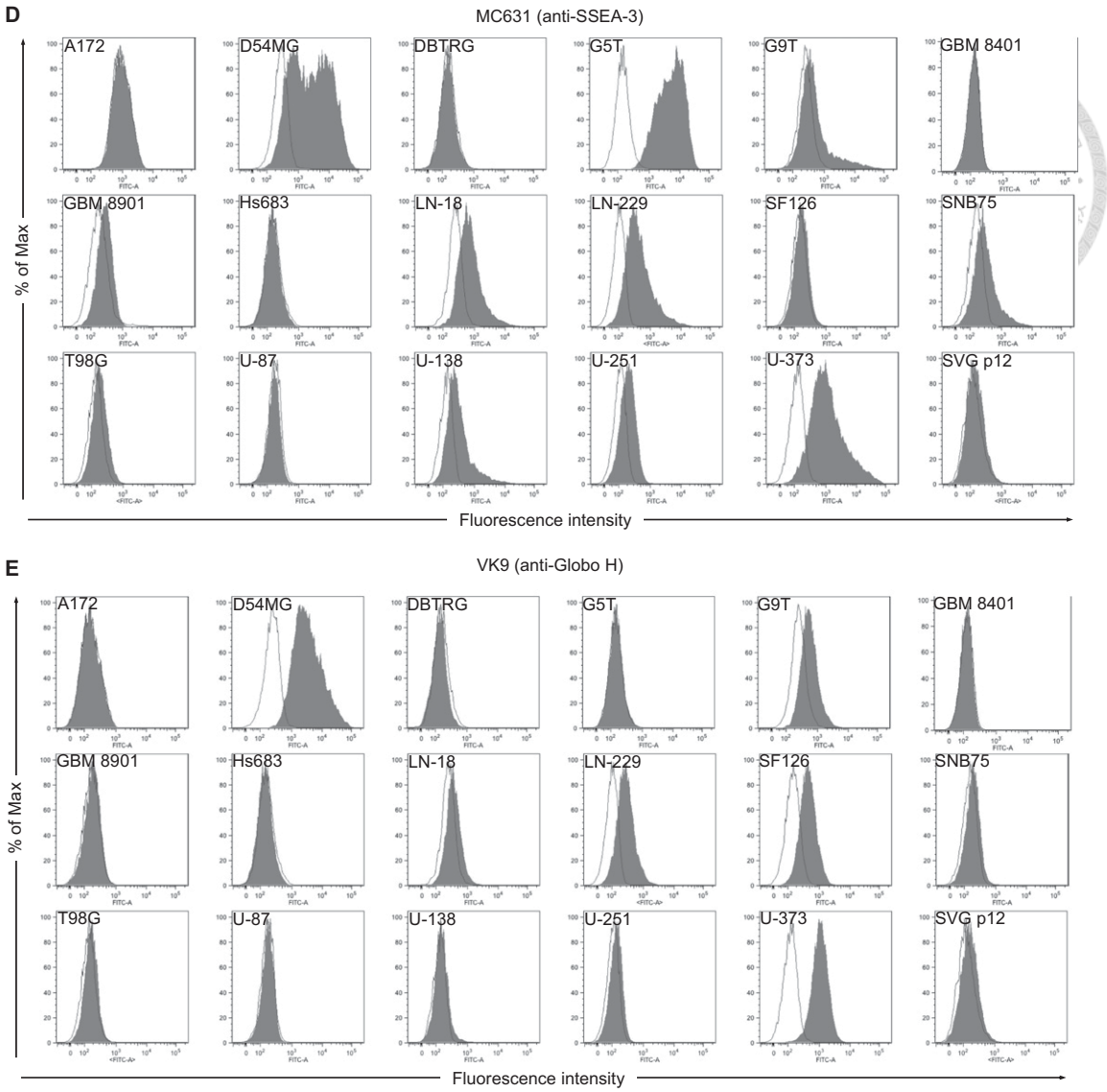

Fig. S1. Flow cytometric analyses of glycan-related molecules on GBM cell lines. Expression of Lewis antigens Le^x, Le^y, and sLe^x (*A*), O-linked glycans Tn, sTn, and TF (*B*), complex gangliosides GM2, GM1, GD1a, GD3, GD2, GT1b, and A2B5 (c-series gangliosides) (*C*), stage-specific embryo antigen 3 (SSEA-3) (*D*), and fucosyl Gb5Cer (Globo H) (*E*) were analyzed. Cells were incubated with optimal concentrations of the primary antibodies and fluorescent-labeled secondary antibodies or Alexa Fluor 488-conjugated MC631 or allophycocyanin-conjugated VK9 and were analyzed by a FACSCanto flow cytometer. All cells examined were GBM cell lines, except for SVG p12, which is a normal human fetal glial cell line transformed with SV40 large T antigen. The histograms of the cells stained with specific antibodies and isotype control are shown in gray and white, respectively.

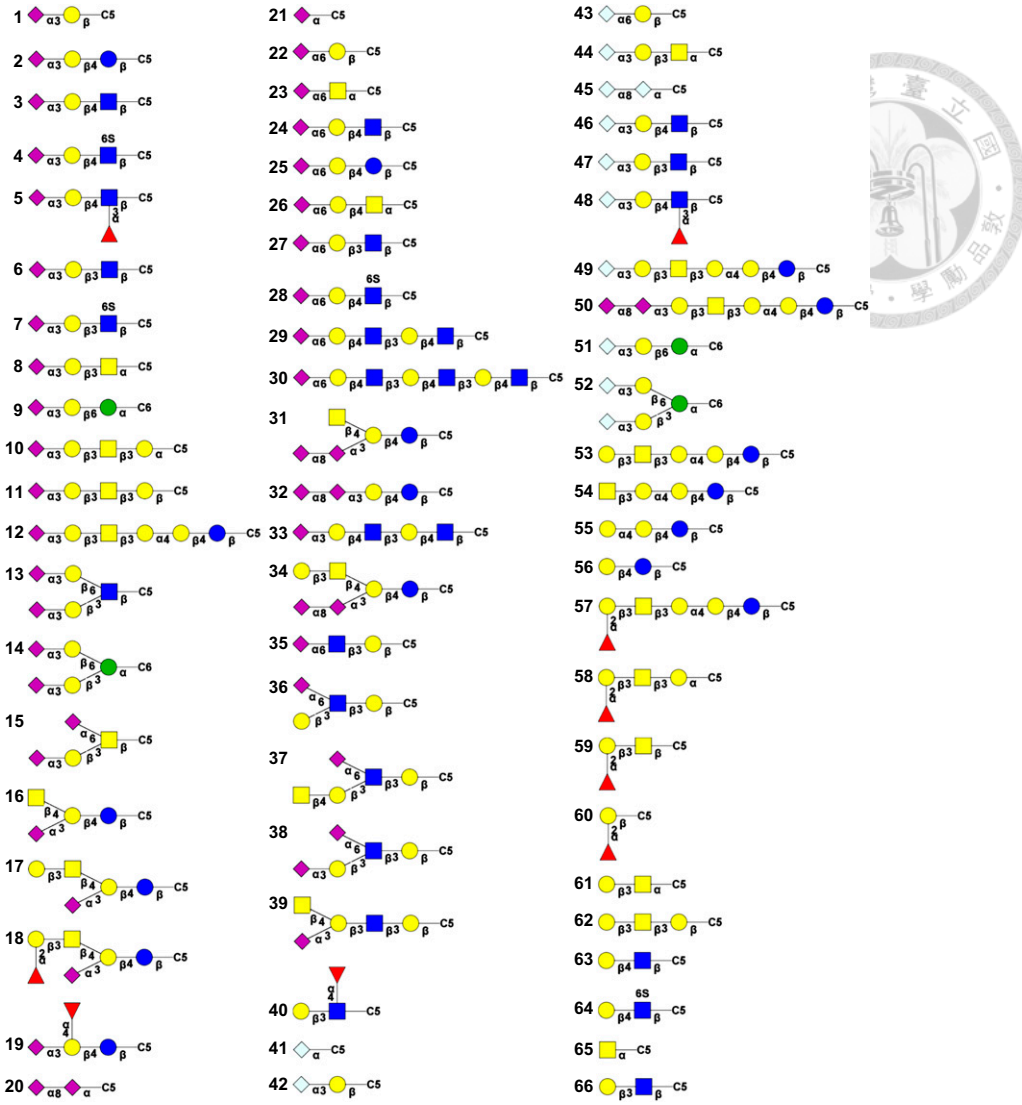

Fig. S2. (Continued)

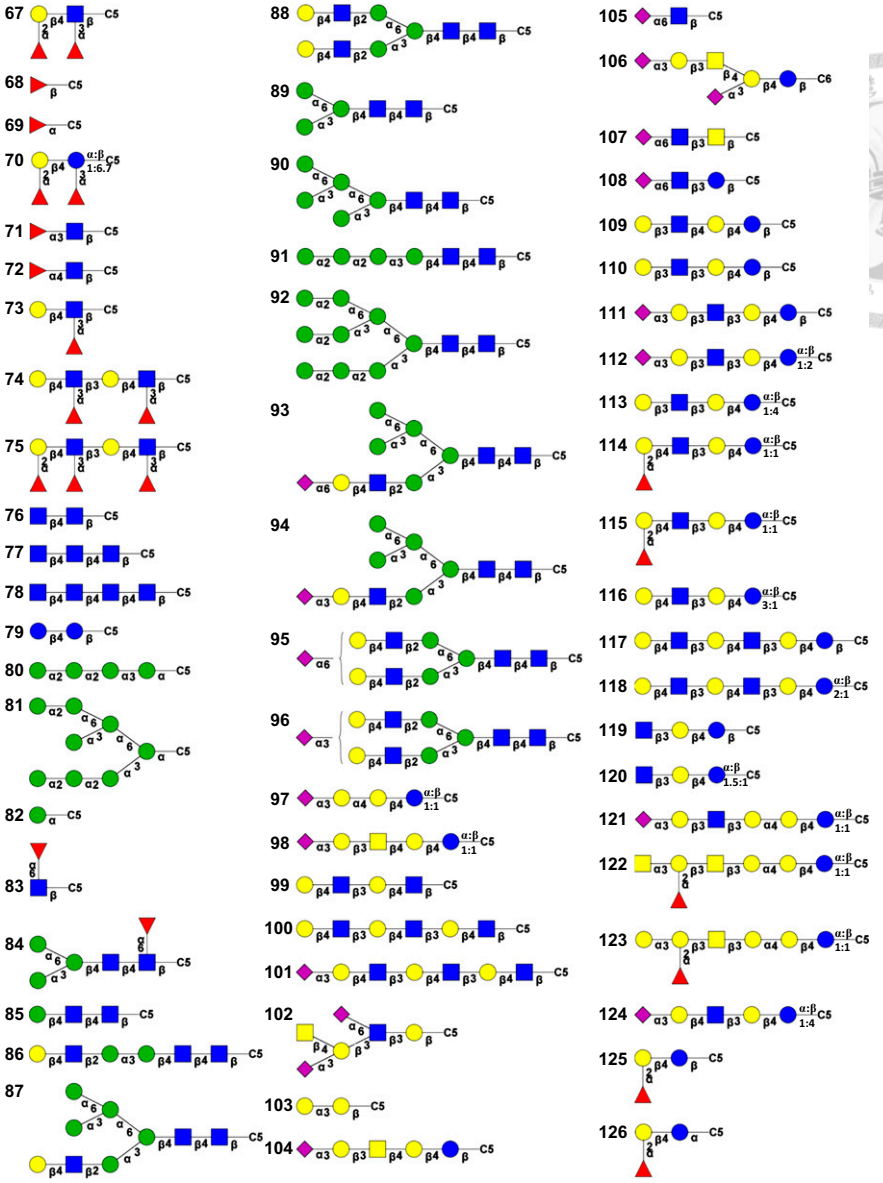

Fig. S2. (Continued)

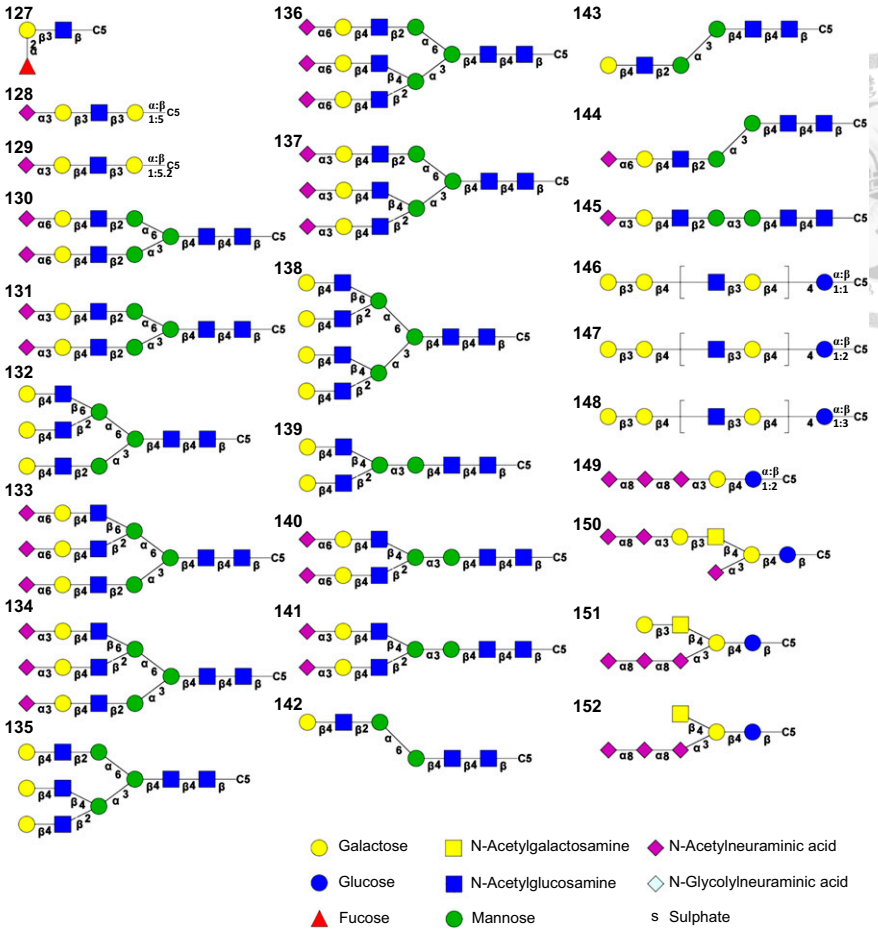

Fig. S2. Chemical structures of 152 oligosaccharides on glycan microarray glass slides. The graphical notation of glycan structures in this figure is based on the symbols proposed by the Consortium for Functional Glycomics. Enantiomeric ratios are indicated for the glycans containing enantiomers. C5, C5H10NH2; C6, C6H12NH2.

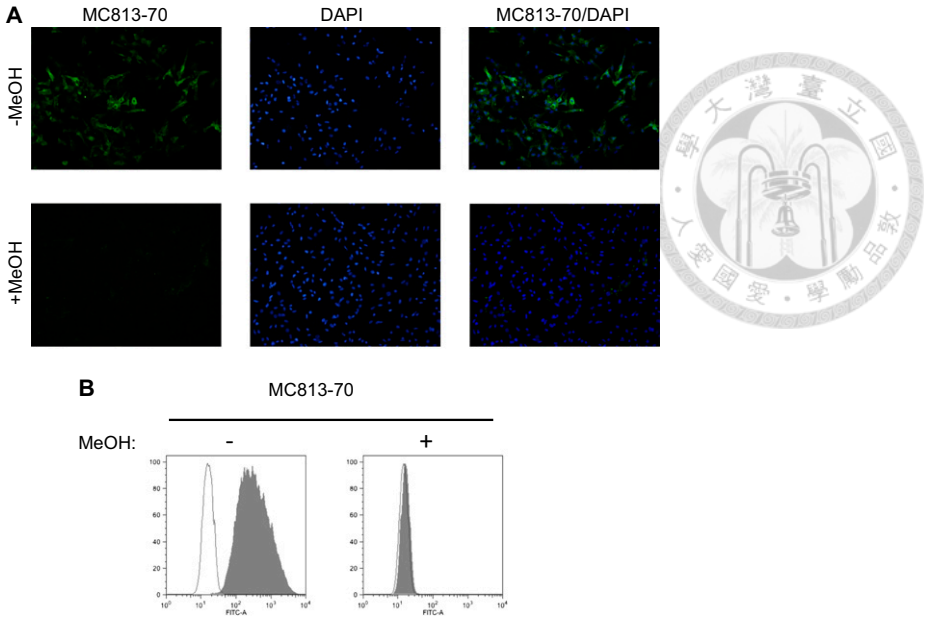

Fig. S3. Effect of methanol on MC813-70 immunoreactivity toward GBM cells. DBTRG cells with or without methanol (MeOH) treatment were stained with MC813-70 and subjected to immunofluorescent microscopy (*A*) and flow cytometry (*B*). DBTRG cells showed positive immunofluorescent staining (green in *A*, gray histogram in *B*), which disappeared after treatment with MeOH. For immunofluorescent microscopy, nuclei were stained with DAPI (blue); for flow cytometry, staining with isotype control is shown as a white histogram.

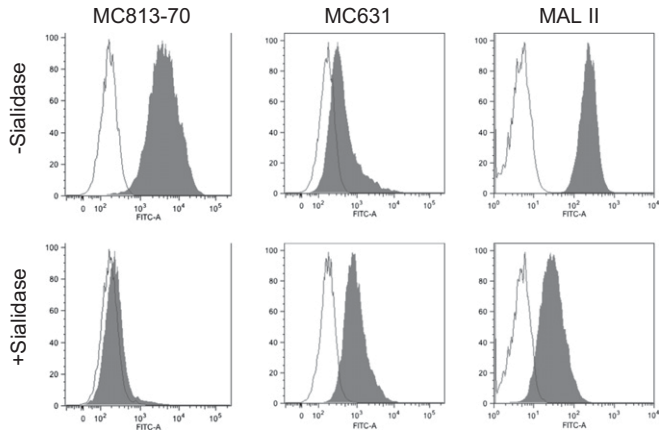

Fig. S4. Desialylation of GBM cells affected MC813-70 and MC631 staining. DBTRG cells were treated with α2,3-sialidase before staining with MC813-70 and MC631. Flow cytometric analysis showed that the intensity of MC631 staining increased and MC813-70 staining disappeared after sialidase treatment. The efficiency of sialidase treatment was monitored by staining with MAL II, which recognizes α2,3-linked sialic acids. The histograms of the cells stained with mAb and MAL II are shown in gray, and the histograms representing isotype control staining are shown in white.

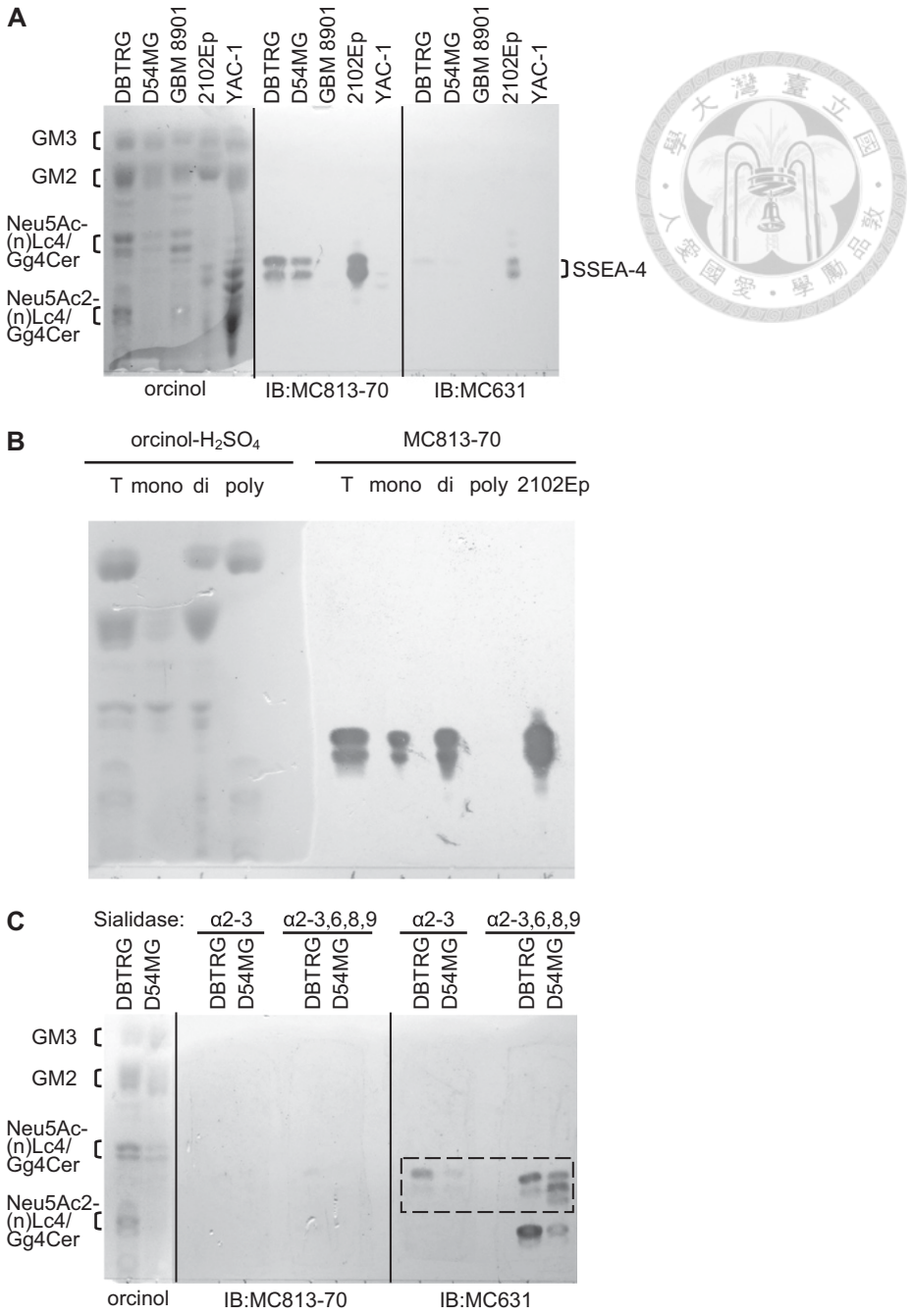

Fig. S5. HPTLC profiles and immunostaining of gangliosides from GBM cell lines. (*A*) Gangliosides were separated on an HPTLC plate and detected with orcinol (*Left*), MC813-70 mAb (*Center*), or MC631 mAb (*Right*). Gangliosides from 2012Ep (a human embryonal carcinoma cell line) and YAC-1 (a mouse lymphoma cell line) were applied to serve as the positive controls for SSEA-4 and GM1b, respectively. (*B*) Gangliosides from DBTRG cells were eluted by 0.8 M NaCl at once (T) or were fractionated into mono-, di-, and polysialylated gangliosides by stepwise elution with 0.02 M, 0.2 M, and 0.8 M NaCl. Gangliosides were separated on an HPTLC plate and detected by orcinol staining (*Left*) or MC813-70 immunostaining (*Right*). MC813-70^{+} signals were detected in the monosialylated ganglioside fraction. The gangliosides extracted from 2012Ep cells, which are known to express SSEA-4, were used as a positive control. (*C*) Detection of desialylated gangliosides on an HPTLC plate with orcinol (*Left*), MC813-70 mAb (*Center*), or MC631 mAb (*Right*). The GBM-associated ganglioside originally recognized by MC813-70 showed MC813-70 (–) and MC631 (+) after sialidase treatment, as marked in the dashed rectangle.

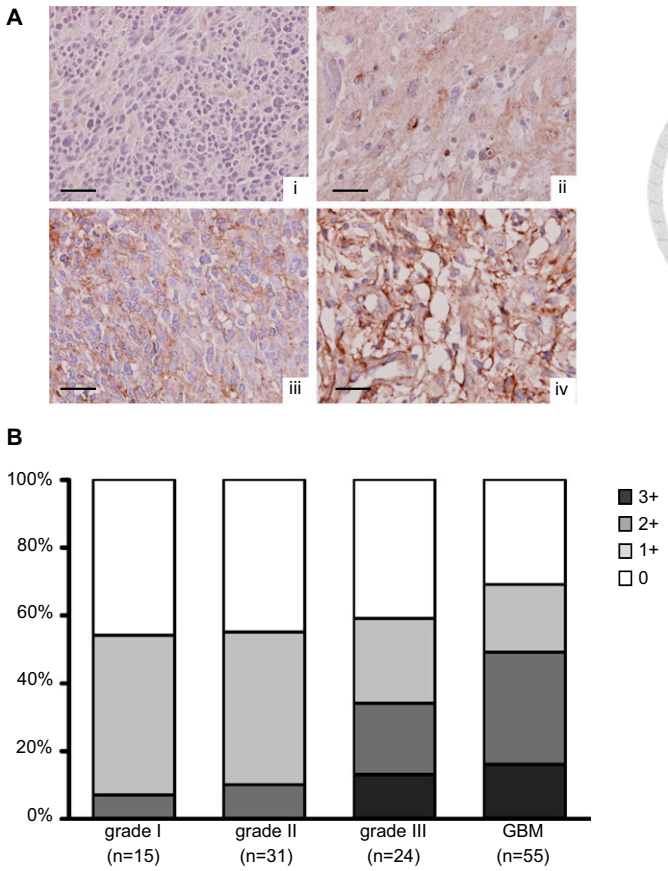

Fig. S6. Expression of SSEA-4 in grade I–IV astrocytoma. (*A*) GBM tissues were immunohistochemically stained with MC813-70. The staining intensity of GBM specimens was graded as 0 (negative, i), 1+ (weak, ii), 2+ (moderate, iii), and 3+ (strong, iv). (Scale bars, 100 μm.) (*B*) Statistical results of SSEA-4 immunohistochemistry (IHC). Grade I ($n = 15$), grade II ($n = 31$), grade III ($n = 24$), and grade IV (GBM, $n = 55$) specimens were counterstained with hematoxylin after IHC. The staining intensity of the tissues was graded as 0 (negative), 1+ (weak), 2+ (moderate), and 3+ (strong).

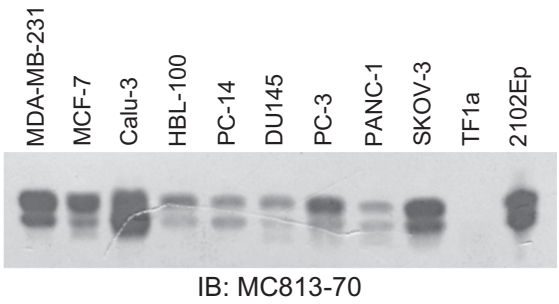

Fig. S7. Immunostaining of SSEA-4 on HPTLC-separated gangliosides from cancer cells. Representative breast (MDA-MB-231, MCF-7, and HBL-100), lung (Calu-3 and PC-14), prostate (DU145 and PC-3), pancreatic (PANC-1), ovarian (SKOV-3), erythroleukemia (TF1a), and embryonal carcinoma (2012Ep) cell lines are shown.

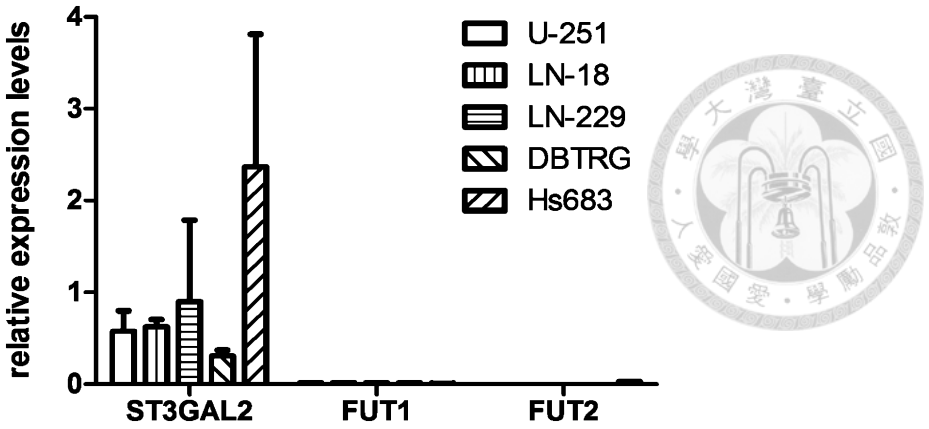

Fig. S8. Human GBM cell lines express a higher level of *ST3GAL2* than *FUT1* and *FUT2*. Total RNA was extracted from GBM cell lines and reverse-transcribed to cDNA. The expression levels of *ST3GAL2*, *FUT1*, and *FUT2* were determined by real-time PCR and normalized against the expression level of *GAPDH*.

Table S1. Expression of globo-series GSLs on various cancer cell lines

Tumor origin	Cell line	Antigen
Brain	A172	
Brain	D54MG	3, 4, H
Brain	DBTRG	4
Brain	G5T	3, 4
Brain	G9T	3, 4, H
Brain	GBM 8401	
Brain	GBM 8901	
Brain	Hs683	4
Brain	LN-18	3, 4, H
Brain	LN-229	3, 4, H
Brain	SF126	4, H
Brain	SNB75	3, 4
Brain	T95G	
Brain	U-138 MG	3, 4
Brain	U-251 MG	3, 4
Brain	U-373 MG	3, 4, H
Brain	U-87 MG	
Lung	A549	4, H
Lung	Calu-3	4
Lung	CL1	4
Lung	CL1-0	4, H
Lung	CL1-5	4, H
Lung	CL2	H
Lung	CL3	
Lung	H1299	
Lung	H1355	4, H
Lung	H157	3, 4, H
Lung	H441	4, H
Lung	H460	
Lung	H480	3, 4, H
Lung	H520	H
Lung	H661	3, 4, H
Lung	H928	3, 4, H
Lung	NuLi-1	3, 4, H
Lung	PC-13	H
Lung	PC-14	
Lung	PC-9	4
Breast	Au565	
Breast	BT-20	
Breast	BT-474	
Breast	BT-483	
Breast	BT-549	4
Breast	DU4475	4, H
Breast	HBL-100	4, H
Breast	HBL-435	
Breast	HCC1395	3, 4, H
Breast	HCC1599	4, H
Breast	HCC1806	3, 4, H
Breast	HCC1937	4
Breast	HCC38	4, H
Breast	Hs578T	3, 4, H
Breast	MCF-7	3, 4, H
Breast	MDA-MB-157	3, 4, H
Breast	MDA-MB-231	3, 4, H
Breast	MDA-MB-361	4, H
Breast	MDA-MB-453	4, H
Breast	MDA-MB-468	4
Breast	SK-BR-3	H
Breast	T47D	3, 4, H
Breast	ZR75	4, H
Colon	CX-1	4, H
Colon	DLD-1	H

Table S1. Cont.

Tumor origin	Cell line	Antigen
Colon	H3347	4, H
Colon	HCT1116	4
Colon	HT-29	H
Colon	SW480	4, H
Colon	SW620	4, H
Mouth	Ca922	4, H
Mouth	Cal27	4, H
Mouth	HSC3	4, H
Mouth	OC3	H
Mouth	OECM1	H
Mouth	SAS	H
Mouth	SCC25	4
Mouth	SCC4	3, 4, H
Mouth	Tu-183	H
Mouth	Tw1.5	4, H
Mouth	Tw2.6	4, H
Mouth	UMSCC-1	3, 4, H
Mouth	YD-15	3, 4, H
Esophagus	CE81T	H
Esophagus	KYSE70	4, H
Stomach	AGS	H
Stomach	AZ521	3, 4, H
Stomach	KATO III	3, 4, H
Stomach	NCI-N87	H
Stomach	SCM-1	3, 4, H
Stomach	SNU-1	4, H
Liver	59T	3, 4, H
Liver	Changliver	H
Liver	HA22T	H
Liver	Hep3b	3, 4, H
Liver	HepG2	4, H
Liver	Huh-7	4, H
Liver	J5	H
Liver	Mahlavu	
Liver	NTU-BL	3, 4, H
Liver	SK-HEP-1	3, 4, H
Bile duct	HuccT1	3, 4, H
Bile duct	SNU-1079	
Bile duct	SNU-1196	H
Bile duct	SNU-245	4, H
Bile duct	SNU-308	
Pancreas	AsPC1	4
Pancreas	BxPC3	4, H
Pancreas	HPAC	4, H
Pancreas	KP-4	3, 4, H
Pancreas	MIA PaCa-2	3, 4, H
Pancreas	Panc0203	4, H
Pancreas	PANC1	4
Pancreas	PL45	3, 4, H
Kidney	769-P	3, 4, H
Kidney	A498	4
Kidney	A704	H
Kidney	ACHN	3, 4, H
Kidney	Caki-1	3, 4, H
Kidney	Caki-2	3, 4, H
Cervix	HeLa	3, 4
Cervix	HeLa 229	3, 4
Cervix	HeLa S3	
Cervix	ME-180	4, H
Ovary	C33A	4
Ovary	CAOV3	4
Ovary	ES-2	4, H
Ovary	NUGCC	3, 4, H

Table S1. Cont.

Tumor origin	Cell line	Antigen
Ovary	OVCAR-3	4, H
Ovary	SiHa	
Ovary	SKOV3	4
Ovary	TOV-112D	4, H
Ovary	TOV-21G	3, 4, H
Prostate	22Rr1	4, H
Prostate	Du145	4
Prostate	hTERT-HPNE	3, 4
Prostate	PC-3	4

Antigen: 3, SSEA-3; 4, SSEA-4; H, Globo H.